QR – Issue

QR – Article

Denis Chemezov
Vladimir Industrial College
M.Sc.Eng., Corresponding Member of International Academy of
Theoretical and Applied Sciences, Lecturer, Russian Federation
https://orcid.org/0000-0002-2747-552X
vic-science@yandex.ru

Anzhelika Bayakina
Vladimir Industrial College
Lecturer, Russian Federation

Egor Prozorov
Vladimir Industrial College
Student, Russian Federation

Elena Stepanova
Vladimir Industrial College
Lecturer, Russian Federation

Aleksey Fetisov
Vladimir Industrial College
Student, Russian Federation

Andrey Karasyov
Vladimir Industrial College
Student, Russian Federation

Anton Ilin
Vladimir Industrial College
Student, Russian Federation

Georgiy Karatun
Vladimir Industrial College
Student, Russian Federation

Vyacheslav Matveev
«Security Navigator» LLC
Mechanic, Vladimir, Russian Federation

REFERENCE DATA OF PRESSURE DISTRIBUTION ON THE SURFACES OF AIRFOILS HAVING THE NAMES BEGINNING WITH THE LETTER G (THE SECOND PART)

Abstract: The results of the computer calculation of air flow around the airfoils having the names beginning with the letter G (continuation) are presented in the article. The contours of pressure distribution on the surfaces of

Clarivate
Analytics indexed

the airfoils at the angles of attack of 0, 15 and -15 degrees in conditions of the subsonic airplane flight speed were obtained.

Key words*: the airfoil, the angle of attack, pressure, the surface.*
Language*: English*
Citation*: Chemezov, D., et al. (2022). Reference data of pressure distribution on the surfaces of airfoils having the names beginning with the letter G (the second part). ISJ Theoretical & Applied Science, 03 (107), 901-984.*
Soi*: http://s-o-i.org/1.1/TAS-03-107-70*   ***Doi****: crossref https://dx.doi.org/10.15863/TAS.2022.03.107.70*
Scopus ASCC*: 1507.*

Introduction

Creating reference materials that determine the most accurate pressure distribution on the airfoils surfaces is an actual task of the airplane aerodynamics.

Materials and methods

The study of air flow around the airfoils was carried out in a two-dimensional formulation by means of the computer calculation in the *Comsol Multiphysics* program. The airfoils in the cross section were taken as objects of research [1-19]. In this work,

the airfoils having the names beginning with the letter *G* were adopted. Air flow around the airfoils was carried out at the angles of attack (α) of 0, 15 and -15 degrees. The flight speed of the airplane in each case was subsonic. The airplane flight in the atmosphere was carried out under normal weather conditions. The geometric characteristics of the studied airfoils are presented in the Table 1. The geometric shapes of the airfoils in the cross section are presented in the Table 2.

Table 1. The geometric characteristics of the airfoils.

Airfoil name	Max. thickness	Max. camber	Leading edge radius	Trailing edge thickness
GOE 344 (PFALZ 71)	7.2% at 20.0% of the chord	2.71% at 40.0% of the chord	0.9858%	0.65%
GOE 346 (FRIEDRICHSHAFEN-STAAKEN)	5.74% at 40.0% of the chord	3.79% at 40.0% of the chord	0.8336%	0.35%
GOE 358	10.87% at 20.0% of the chord	5.69% at 50.0% of the chord	1.7859%	0.32%
GOE 359	7.8% at 30.0% of the chord	5.88% at 40.0% of the chord	0.7637%	0.15%
GOE 360	9.68% at 30.0% of the chord	5.86% at 30.0% of the chord	1.0559%	0.21%
GOE 361	6.8% at 20.0% of the chord	5.53% at 40.0% of the chord	0.7836%	0.0%
GOE 362	6.6% at 20.0% of the chord	5.29% at 40.0% of the chord	0.817%	0.0%
GOE 363	11.07% at 20.0% of the chord	5.71% at 40.0% of the chord	1.1665%	0.11%
GOE 364	10.8% at 30.0% of the chord	6.51% at 30.0% of the chord	1.4952%	0.0%
GOE 365	11.7% at 30.0% of the chord	5.14% at 40.0% of the chord	1.2843%	0.0%
GOE 366	13.14% at 30.0% of the chord	7.24% at 40.0% of the chord	2.0949%	0.3%
GOE 367	16.28% at 30.1% of the chord	4.59% at 40.1% of the chord	2.2776%	0.32%
GOE 368	7.71% at 15.0% of the chord	3.81% at 30.0% of the chord	0.6519%	0.0%
GOE 369	5.85% at 30.0% of the chord	5.45% at 40.0% of the chord	1.0264%	0.0%
GOE 370	4.65% at 20.0% of the chord	5.74% at 40.0% of the chord	0.5893%	0.0%
GOE 371	6.95% at 30.0% of the chord	4.61% at 40.0% of the chord	0.7646%	0.0%
GOE 372	6.2% at 30.0% of the chord	4.31% at 40.0% of the chord	0.7036%	0.0%
GOE 373	6.5% at 30.0% of the chord	5.07% at 40.0% of the chord	0.8293%	0.0%
GOE 374	6.45% at 30.0% of the chord	4.52% at 30.0% of the chord	0.6862%	0.0%
GOE 375	6.5% at 20.0% of the chord	4.48% at 30.0% of the chord	0.8317%	0.0%
GOE 376	6.6% at 30.0% of the chord	4.95% at 30.0% of the chord	0.8085%	0.0%
GOE 377	6.45% at 30.0% of the chord	3.89% at 40.0% of the chord	0.6471%	0.0%
GOE 379	6.45% at 30.0% of the chord	5.24% at 40.0% of the chord	0.5995%	0.0%
GOE 380	6.55% at 30.0% of the chord	5.6% at 30.0% of the chord	0.7142%	0.0%
GOE 381	6.38% at 30.0% of the chord	5.76% at 30.0% of the chord	0.6607%	0.16%
GOE 382	20.0% at 30.3% of the chord	5.98% at 40.2% of the chord	2.7117%	0.21%
GOE 383	20.14% at 30.5% of the chord	4.91% at 40.4% of the chord	4.1176%	0.32%
GOE 384	19.53% at 30.1% of the chord	6.83% at 40.1% of the chord	2.7606%	0.43%
GOE 385	9.89% at 30.0% of the chord	4.14% at 30.0% of the chord	0.9339%	0.42%
GOE 386	20.17% at 30.3% of the chord	5.4% at 40.3% of the chord	4.2208%	0.32%
GOE 387	14.85% at 30.0% of the chord	5.52% at 40.0% of the chord	2.3316%	0.0%
GOE 388	10.19% at 30.0% of the chord	5.43% at 40.0% of the chord	1.2692%	0.21%
GOE 389	10.31% at 30.0% of the chord	3.97% at 40.0% of the chord	0.9723%	0.21%
GOE 390	20.24% at 30.2% of the chord	6.88% at 40.1% of the chord	3.8427%	0.21%
GOE 391	5.1% at 40.0% of the chord	3.21% at 40.0% of the chord	0.5818%	0.0%
GOE 392	10.15% at 30.0% of the chord	4.84% at 40.0% of the chord	0.5911%	0.0%
GOE 393	6.07% at 20.0% of the chord	4.21% at 30.0% of the chord	0.9021%	0.13%
GOE 394	6.1% at 20.0% of the chord	5.88% at 40.0% of the chord	0.8856%	0.15%
GOE 395	6.11% at 20.0% of the chord	6.97% at 50.0% of the chord	0.9048%	0.15%

Impact Factor:

ISRA (India) = **6.317**	**SIS** (USA) = **0.912**	**ICV** (Poland) = **6.630**
ISI (Dubai, UAE) = **1.582**	**РИНЦ** (Russia) = **3.939**	**PIF** (India) = **1.940**
GIF (Australia) = **0.564**	**ESJI** (KZ) = **9.035**	**IBI** (India) = **4.260**
JIF = **1.500**	**SJIF** (Morocco) = **7.184**	**OAJI** (USA) = **0.350**

GOE 396	4.7% at 30.0% of the chord	5.77% at 40.0% of the chord	0.549%	0.0%
GOE 397	5.1% at 30.0% of the chord	3.96% at 40.0% of the chord	0.6581%	0.0%
GOE 398	13.85% at 30.0% of the chord	4.85% at 40.0% of the chord	1.9588%	0.0%
GOE 399	6.9% at 30.0% of the chord	4.22% at 40.0% of the chord	0.7201%	0.0%
GOE 400	6.12% at 20.0% of the chord	4.89% at 40.0% of the chord	0.8905%	0.08%
GOE 401	7.1% at 30.0% of the chord	4.86% at 30.0% of the chord	1.0286%	0.0%
GOE 402	6.8% at 20.0% of the chord	5.73% at 30.0% of the chord	0.7958%	0.0%
GOE 403	6.65% at 30.0% of the chord	4.32% at 40.0% of the chord	0.6692%	0.0%
GOE 404	13.16% at 30.0% of the chord	4.96% at 30.0% of the chord	2.6535%	0.16%
GOE 405	11.1% at 30.0% of the chord	6.54% at 40.0% of the chord	1.0156%	0.0%
GOE 406	11.69% at 30.0% of the chord	5.53% at 40.0% of the chord	1.6491%	0.0%
GOE 407	9.46% at 30.0% of the chord	4.78% at 40.0% of the chord	1.2507%	0.0%
GOE 408	7.75% at 30.0% of the chord	4.14% at 30.0% of the chord	0.8406%	0.0%
GOE 409	12.7% at 30.0% of the chord	0.0% at 0.0% of the chord	1.3835%	0.0%
GOE 410	16.1% at 30.0% of the chord	0.0% at 0.0% of the chord	2.5997%	0.0%
GOE 411	13.2% at 30.0% of the chord	0.0% at 0.0% of the chord	0.791%	0.0%
GOE 412	13.12% at 30.1% of the chord	5.1% at 40.0% of the chord	1.4844%	0.32%
GOE 413	16.35% at 30.1% of the chord	4.65% at 40.0% of the chord	3.0868%	0.16%
GOE 414	13.59% at 30.1% of the chord	5.25% at 40.0% of the chord	1.0621%	0.21%
GOE 415	8.47% at 20.0% of the chord	3.66% at 30.0% of the chord	0.664%	0.11%
GOE 416A	11.67% at 30.4% of the chord	1.33% at 60.2% of the chord	0.7305%	0.27%
GOE 417	6.0% at 20.0% of the chord	6.13% at 40.0% of the chord	0.7947%	0.0%
GOE 417A (GEW, PLATTE)	3.2% at 2.5% of the chord	5.9% at 40.0% of the chord	0.9824%	0.0%
GOE 418	12.7% at 20.0% of the chord	5.08% at 40.0% of the chord	2.7416%	0.0%
GOE 419	5.3% at 30.0% of the chord	4.4% at 40.0% of the chord	0.6142%	0.0%
GOE 420	18.75% at 30.0% of the chord	4.3% at 50.0% of the chord	2.9101%	0.0%
GOE 421	18.96% at 30.1% of the chord	8.08% at 50.0% of the chord	2.2439%	0.21%
GOE 422	17.04% at 30.1% of the chord	6.5% at 40.1% of the chord	2.9849%	0.21%
GOE 423	16.89% at 40.1% of the chord	5.05% at 40.1% of the chord	2.3626%	0.16%
GOE 424	19.99% at 30.5% of the chord	4.68% at 40.5% of the chord	2.022%	0.16%
GOE 425	16.01% at 30.2% of the chord	4.51% at 40.2% of the chord	1.8749%	0.11%
GOE 426	13.6% at 30.0% of the chord	4.55% at 40.0% of the chord	1.4758%	0.0%
GOE 427	4.6% at 20.0% of the chord	5.7% at 40.0% of the chord	0.5948%	0.0%
GOE 428	7.9% at 30.0% of the chord	5.22% at 40.0% of the chord	0.7011%	0.0%
GOE 429	11.38% at 30.0% of the chord	0.19% at 10.0% of the chord	1.3587%	0.32%
GOE 430	13.33% at 30.1% of the chord	4.82% at 50.0% of the chord	1.6524%	0.22%
GOE 431	11.8% at 20.0% of the chord	7.22% at 60.0% of the chord	1.1685%	0.0%
GOE 432	7.7% at 20.0% of the chord	4.34% at 40.0% of the chord	0.8878%	0.0%
GOE 433	17.32% at 30.3% of the chord	4.84% at 50.1% of the chord	2.8801%	0.16%
GOE 434	22.58% at 30.7% of the chord	5.15% at 50.4% of the chord	6.2006%	0.16%
GOE 435	25.88% at 31.2% of the chord	4.65% at 50.7% of the chord	6.1986%	0.27%
GOE 436	11.0% at 30.0% of the chord	3.75% at 30.0% of the chord	1.3684%	0.0%
GOE 437	7.05% at 30.0% of the chord	4.8% at 40.0% of the chord	0.6184%	0.0%
GOE 438	10.99% at 30.0% of the chord	3.76% at 40.0% of the chord	1.3846%	0.0%
GOE 439	7.9% at 30.0% of the chord	5.22% at 40.0% of the chord	0.7011%	0.0%
GOE 440	15.25% at 30.0% of the chord	9.7% at 40.0% of the chord	0.6807%	0.26%
GOE 441	15.92% at 30.0% of the chord	7.72% at 40.0% of the chord	2.5029%	0.27%
GOE 442	7.7% at 20.0% of the chord	4.33% at 40.0% of the chord	0.8907%	0.0%
GOE 443	5.0% at 30.0% of the chord	0.0% at 0.0% of the chord	0.7187%	0.0%
GOE 444	5.6% at 30.0% of the chord	0.0% at 0.0% of the chord	0.7187%	0.0%
GOE 445	6.4% at 40.0% of the chord	0.0% at 0.0% of the chord	0.7139%	0.0%
GOE 446	12.87% at 30.0% of the chord	6.33% at 40.0% of the chord	1.6709%	0.32%
GOE 447	12.67% at 30.0% of the chord	8.01% at 40.0% of the chord	1.6979%	0.32%
GOE 448	12.88% at 30.0% of the chord	10.51% at 39.9% of the chord	1.4524%	0.26%
GOE 449	16.95% at 30.0% of the chord	5.39% at 40.0% of the chord	2.2757%	0.0%
GOE 450	8.9% at 30.0% of the chord	5.18% at 40.0% of the chord	0.9927%	0.21%
GOE 456	7.2% at 30.0% of the chord	5.2% at 40.0% of the chord	0.5726%	0.0%
GOE 457	7.83% at 20.0% of the chord	4.22% at 40.0% of the chord	0.8864%	0.0%
GOE 458	7.2% at 30.0% of the chord	5.2% at 40.0% of the chord	0.5644%	0.0%
GOE 459	12.7% at 30.0% of the chord	0.0% at 0.0% of the chord	1.3224%	0.0%
GOE 460	20.5% at 30.0% of the chord	0.0% at 0.0% of the chord	2.9061%	0.0%
GOE 462	10.99% at 10.0% of the chord	13.37% at 29.9% of the chord	1.1379%	0.0%
GOE 464	7.72% at 7.5% of the chord	9.91% at 29.9% of the chord	1.4907%	0.0%
GOE 474	6.95% at 30.0% of the chord	2.9% at 40.0% of the chord	0.7757%	0.0%
GOE 476	14.43% at 30.1% of the chord	5.2% at 40.1% of the chord	2.5605%	0.0%
GOE 477	10.05% at 30.0% of the chord	4.88% at 40.0% of the chord	1.5475%	0.0%
GOE 478	13.33% at 30.1% of the chord	4.29% at 40.1% of the chord	2.4149%	0.0%

GOE 479	11.6% at 30.0% of the chord	4.0% at 40.0% of the chord	1.5902%	0.0%
GOE 480	11.75% at 30.0% of the chord	5.5% at 40.0% of the chord	2.1319%	0.0%
GOE 481	13.57% at 10.2% of the chord	8.8% at 39.8% of the chord	3.3044%	0.0%
GOE 481A	15.27% at 30.1% of the chord	5.49% at 40.1% of the chord	3.1629%	0.0%
GOE 482	16.49% at 30.0% of the chord	8.8% at 40.0% of the chord	2.0245%	0.0%
GOE 483	5.45% at 15.0% of the chord	5.82% at 40.0% of the chord	0.595%	0.0%
GOE 484	6.25% at 30.0% of the chord	4.95% at 50.0% of the chord	0.9239%	0.0%
GOE 488	6.8% at 20.0% of the chord	3.04% at 40.0% of the chord	0.8526%	0.0%
GOE 490	8.81% at 20.0% of the chord	3.83% at 40.0% of the chord	0.8796%	0.0%
GOE 491	4.85% at 20.0% of the chord	2.95% at 30.0% of the chord	0.6235%	0.0%
GOE 492	6.2% at 30.0% of the chord	3.37% at 50.0% of the chord	0.6641%	0.0%
GOE 493	14.97% at 30.3% of the chord	3.36% at 50.2% of the chord	1.4106%	0.0%
GOE 494	4.95% at 20.0% of the chord	5.1% at 50.0% of the chord	0.6508%	0.0%
GOE 495	6.9% at 30.0% of the chord	5.0% at 50.0% of the chord	0.7483%	0.0%
GOE 496	9.95% at 30.0% of the chord	5.0% at 50.0% of the chord	1.1611%	0.0%
GOE 497	12.7% at 30.0% of the chord	5.33% at 50.0% of the chord	1.6033%	0.0%
GOE 498	15.86% at 30.2% of the chord	5.49% at 50.0% of the chord	2.8845%	0.0%
GOE 499	6.8% at 30.0% of the chord	5.85% at 50.0% of the chord	0.7529%	0.0%
GOE 500	10.0% at 30.0% of the chord	6.0% at 50.0% of the chord	1.1234%	0.0%
GOE 501	12.8% at 30.0% of the chord	6.3% at 50.0% of the chord	1.6978%	0.0%
GOE 502	15.83% at 30.1% of the chord	6.09% at 50.0% of the chord	2.9382%	0.0%
GOE 503	15.59% at 30.0% of the chord	6.97% at 40.0% of the chord	1.4831%	0.0%
GOE 504	17.95% at 30.2% of the chord	5.39% at 40.2% of the chord	1.4327%	0.0%
GOE 505	13.97% at 20.1% of the chord	5.88% at 40.0% of the chord	1.4547%	0.0%
GOE 506	16.45% at 30.2% of the chord	4.66% at 40.2% of the chord	1.3907%	0.0%
GOE 507	8.65% at 30.0% of the chord	2.92% at 40.0% of the chord	1.6554%	0.0%
GOE 508	16.5% at 30.0% of the chord	5.64% at 40.0% of the chord	2.5874%	0.0%
GOE 509	11.05% at 20.0% of the chord	5.17% at 30.0% of the chord	1.2246%	0.0%
GOE 510	13.72% at 20.0% of the chord	5.84% at 40.0% of the chord	1.7965%	0.0%
GOE 511	16.61% at 20.0% of the chord	7.98% at 30.0% of the chord	2.5638%	0.0%
GOE 512	13.91% at 20.0% of the chord	5.62% at 30.0% of the chord	1.555%	0.0%
GOE 513	16.62% at 20.1% of the chord	5.22% at 30.1% of the chord	2.3329%	0.0%
GOE 514	16.58% at 20.1% of the chord	6.44% at 40.0% of the chord	1.8094%	0.0%
GOE 515	8.45% at 30.0% of the chord	2.79% at 40.0% of the chord	0.9365%	0.0%
GOE 517	7.0% at 30.0% of the chord	4.65% at 40.0% of the chord	1.3226%	0.0%
GOE 518	17.99% at 30.0% of the chord	7.29% at 30.0% of the chord	2.6353%	0.0%
GOE 522	21.72% at 30.5% of the chord	5.18% at 50.3% of the chord	4.2335%	0.0%
GOE 523	16.45% at 30.0% of the chord	9.7% at 49.9% of the chord	2.2978%	0.0%
GOE 525	16.45% at 30.0% of the chord	9.7% at 49.9% of the chord	2.2978%	0.0%
GOE 526	12.29% at 30.1% of the chord	4.13% at 40.1% of the chord	1.9446%	0.0%
GOE 527	16.52% at 30.1% of the chord	5.81% at 40.1% of the chord	2.3719%	0.0%
GOE 528	12.44% at 30.0% of the chord	6.19% at 40.0% of the chord	1.595%	0.0%

Table 2. The geometric shapes of the airfoils in the cross section.

Impact Factor:

ISRA (India) = **6.317**	**SIS** (USA) = **0.912**	**ICV** (Poland) = **6.630**
ISI (Dubai, UAE) = **1.582**	**РИНЦ** (Russia) = **3.939**	**PIF** (India) = **1.940**
GIF (Australia) = **0.564**	**ESJI** (KZ) = **9.035**	**IBI** (India) = **4.260**
JIF = **1.500**	**SJIF** (Morocco) = **7.184**	**OAJI** (USA) = **0.350**

GOE 372

GOE 373

GOE 374

GOE 375

GOE 376

GOE 377

GOE 379

GOE 380

GOE 381

GOE 382

GOE 383

GOE 384

GOE 385

GOE 386

GOE 387

GOE 388

GOE 389

GOE 390

GOE 391

GOE 392

GOE 393

GOE 394

GOE 395

GOE 396

GOE 397

GOE 398

GOE 399

GOE 400

GOE 401

GOE 402

GOE 403

GOE 404

GOE 405

GOE 406

GOE 407

GOE 408

GOE 409

GOE 410

GOE 411

GOE 412

GOE 413

GOE 414

GOE 415

GOE 416A

GOE 417

GOE 417A (GEW, PLATTE)

GOE 418

GOE 419

GOE 420

GOE 421

GOE 422

GOE 423

GOE 424

GOE 425

GOE 426

GOE 427

GOE 428

GOE 429

GOE 430

GOE 431

GOE 432

GOE 433

GOE 434

GOE 435

GOE 436

GOE 437

GOE 438

GOE 439

GOE 440

GOE 441

GOE 442

GOE 443

GOE 444

GOE 445

GOE 446

GOE 447

GOE 448

GOE 449

GOE 450

GOE 456

GOE 457

GOE 458

GOE 459

GOE 460

GOE 462

GOE 464

GOE 474

GOE 476

GOE 477

GOE 478

GOE 479

GOE 480

GOE 481

GOE 481A

GOE 482

GOE 483

GOE 484

GOE 488

GOE 490

GOE 491

GOE 492

GOE 493

GOE 494

GOE 495

GOE 496

GOE 497

GOE 498

GOE 499

GOE 500

GOE 501

GOE 502

GOE 503

GOE 504

GOE 505

GOE 506

GOE 507

GOE 508

GOE 509

GOE 510

GOE 511

GOE 512

GOE 513

GOE 514

GOE 515

GOE 517

GOE 518

GOE 522

GOE 523

GOE 525

GOE 526

GOE 527

GOE 528

Results and discussion

The calculated pressure contours on the surfaces of the airfoils at the different angles of attack are presented in the Figs. 1-148. The calculated values on the scale can be represented as the basic values when comparing the pressure drop under conditions of changing the angle of attack of the airfoils. In this work, 148 airfoils of the GOE series were studied, both symmetrical and asymmetrical geometric shapes in the cross section of the airplane wing.

The biconvex airfoils of the subsonic airplanes (GOE 409 – GOE 411, GOE 459 – GOE 460) and the arc airfoils of the supersonic airplanes (GOE 443 – GOE 445) are symmetrical. The other airfoils are asymmetrical.

The following airfoils of the airplanes wings were selected for consideration among them:

1. Subsonic airplane.

- convex-concave: GOE 358, GOE 431, GOE 482, GOE 523, GOE 525;

- flat-convex: GOE 422, GOE 518;

- biconvex asymmetrical: GOE 382, GOE 424, GOE 449, GOE 493.

2. Transonic airplane.

- biconvex asymmetrical: GOE 415, GOE 426, GOE 479.

For the asymmetrical airfoils selected above (from each type of the wing profile) used at the subsonic airplane flight speed, the calculated values of the pressure change at the leading edge (drag) were analyzed. The calculated values of positive and negative pressures arising at the different angles of attack of the airfoil are (at α = 0/15/-15 degrees):

GOE 358 – 6.58/-54/-19.9 kPa;

GOE 431 – 6.63/-50.8/-45.1 kPa;

GOE 482 – 6.7/-23.1/-30.4 kPa;

GOE 523 – 6.76/-23.8/-22.7 kPa;

GOE 525 – 6.76/-23.8/-22.7 kPa.

The GOE 523 and GOE 525 have the best aerodynamic characteristics of the considered airfoils in conditions of maneuvers. The surface area of the leading edge and the thickness of the airfoil affect the value of drag in conditions of horizontal flight of the airplane. Therefore, the GOE 358 airfoil has the optimal geometric shape.

The pressures values were obtained for the following airfoils:

GOE 422 – 6.65/-27/-57.1 kPa;

GOE 518 – 6.63/-22.4/-11.5 kPa.

The GOE 518 airfoil has less drag than the GOE 422 airfoil.

GOE 382 – 6.68/-21.1/-53.1 kPa;

GOE 424 – 6.65/-22.9/-57.9 kPa;
GOE 449 – 6.63/-28.5/-54.3 kPa;
GOE 493 – 6.64/-46.7/-64.4 kPa.

Minimum drag is observed in the GOE 382 (the analysis was performed on the basis of the considered biconvex asymmetrical airfoils).

The similar analysis of the aerodynamic characteristics was performed for the airfoils of the wings used for the transonic airplanes. The calculated values of pressures arising at the different angles of attack of the airfoil are (at α = 0/15/-15 degrees):

GOE 415 – 6.49/-94.4/-15.8 kPa;
GOE 426 – 6.6/-44.2/-56.1 kPa;
GOE 479 – 6.55/-47.2/-72.9 kPa.

Considering the numerical values, it was found that the pressures difference in conditions of the airplane maneuvers is maximum for the GOE 415 airfoil, and minimum for the GOE 426 airfoil.

The analysis of the aerodynamic characteristics showed that an increase in the thickness of the subsonic symmetrical airfoils and a decrease in the radius of the leading edge and the thickness of the supersonic symmetrical airfoils contribute to a decrease in the drag difference.

The GOE 440 airfoil during horizontal flight and descent of the airplane is affected by almost the same positive pressure at the leading edge. Drag of the GOE 440 airfoil during climb of the airplane is comparable to drag of the supersonic airfoils.

The GOE 462 airfoil is curved. The areas of positive and negative pressures are formed at the leading edge at all positions of the airplane wing. The drag coefficient of the given airfoil when the airplane climb is twice as high as when the airplane descent.

A maximum increase in pressure at the leading edge occurs at the angle of attack of -15 degrees for the following airfoils: GOE 367, GOE 382, GOE 383, GOE 384, GOE 386, GOE 390, GOE 398, GOE 404, GOE 411, GOE 412, GOE 413, GOE 414, GOE 418, GOE 420, GOE 421, GOE 422, GOE 423, GOE 424, GOE 425, GOE 426, GOE 429, GOE 430, GOE 433, GOE 434, GOE 435, GOE 436, GOE 438, GOE 441, GOE 445, GOE 449, GOE 459, GOE 476, GOE 478, GOE 479, GOE 481, GOE 481A, GOE 482, GOE 493, GOE 497, GOE 498, GOE 501, GOE 502, GOE 503, GOE 504, GOE 505, GOE 506, GOE 508, GOE 510, GOE 512, GOE 513, GOE 514, GOE 522, GOE 526 and GOE 527. A maximum increase in pressure at the leading edge occurs at the angle of attack of 15 degrees for the other airfoils.
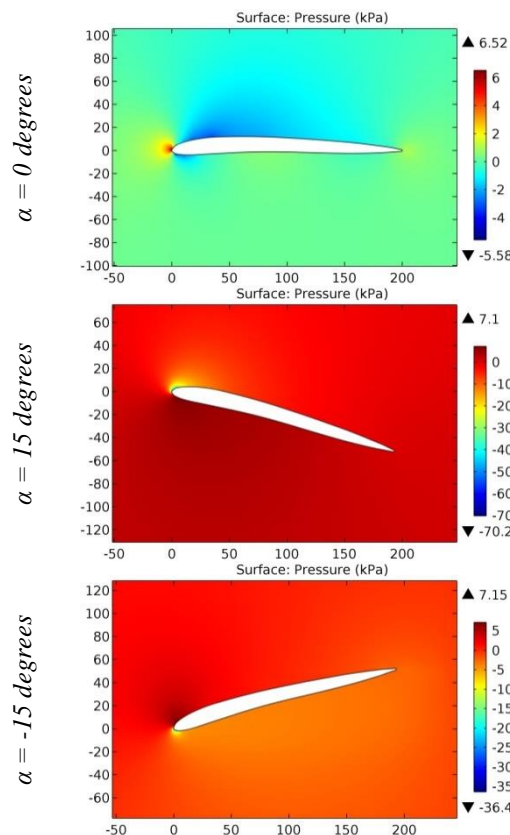
Figure 1. The pressure contours on the surfaces of the GOE 344 (PFALZ 71) airfoil.

Clarivate Analytics **indexed**
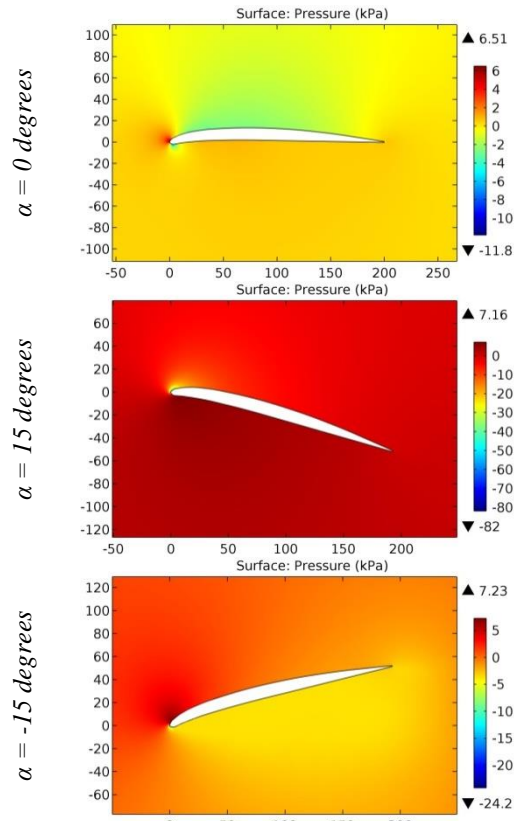
Figure 2. The pressure contours on the surfaces of the GOE 346 (FRIEDRICHSHAFEN-STAAKEN) airfoil.
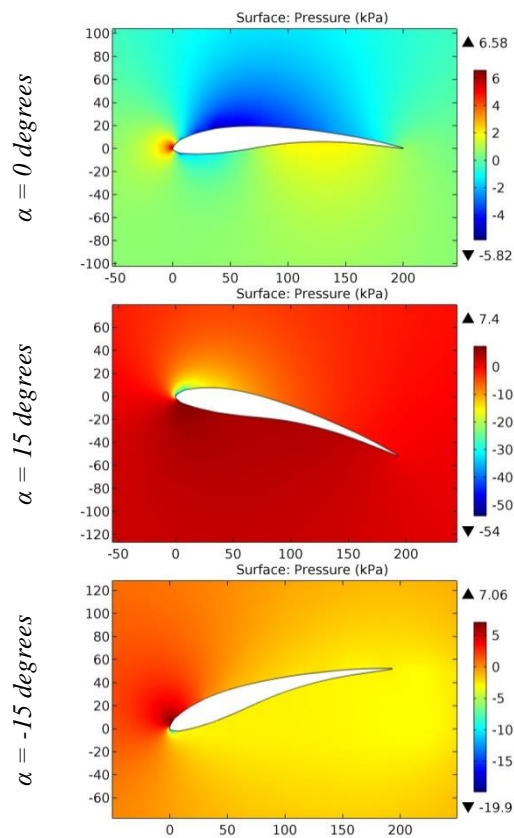
Figure 3. The pressure contours on the surfaces of the GOE 358 airfoil.
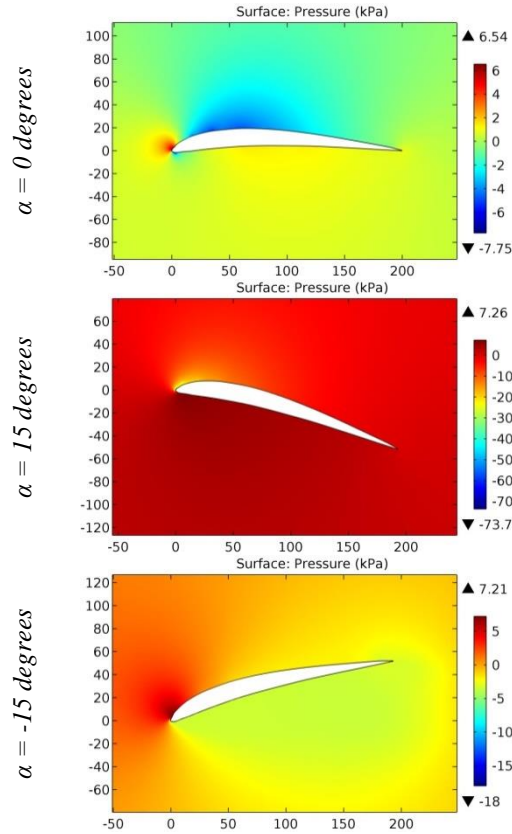
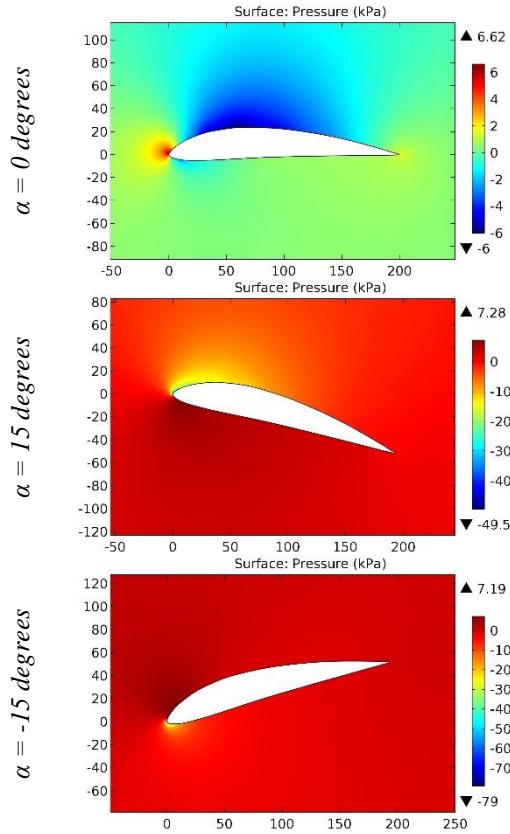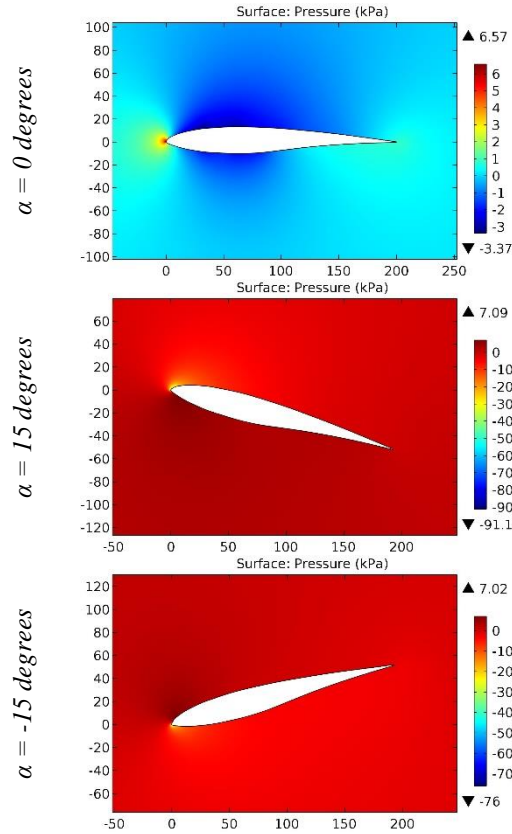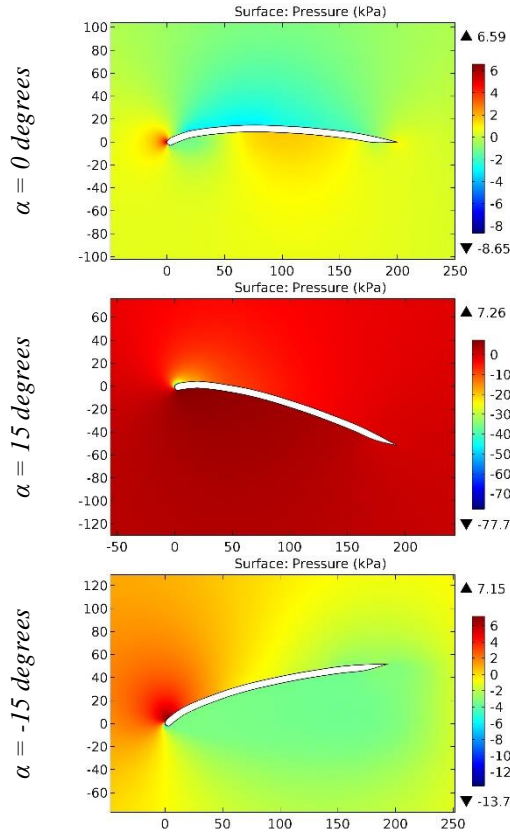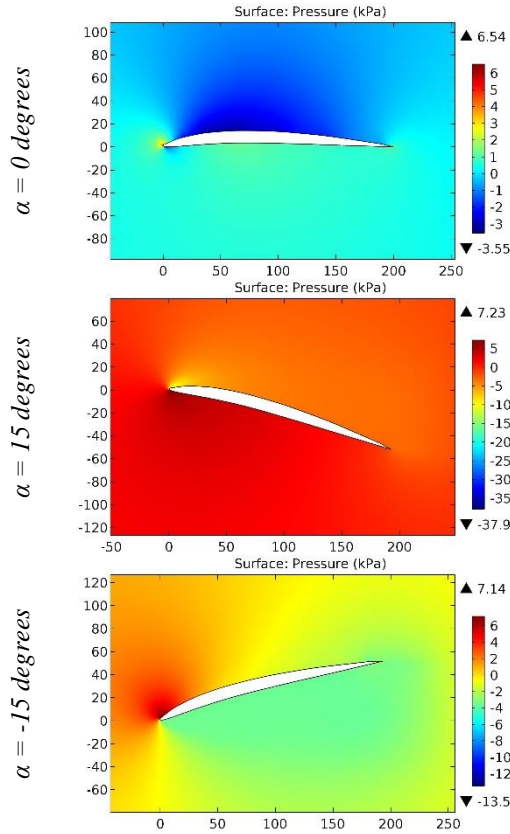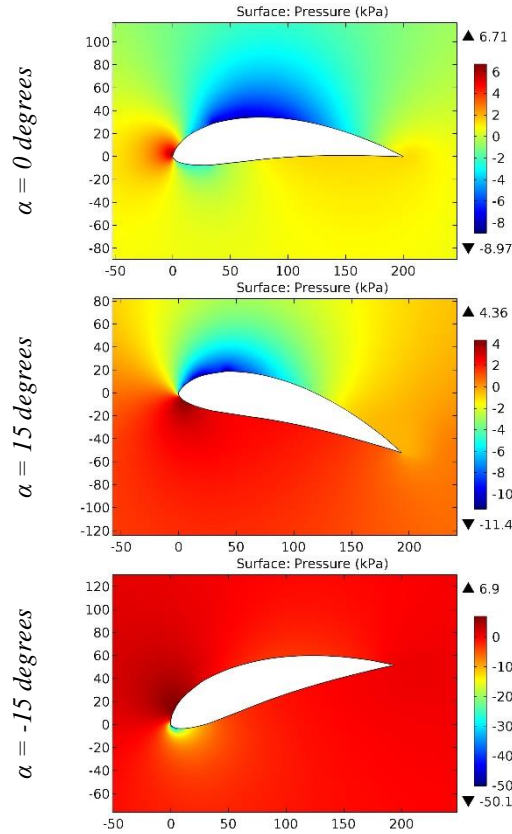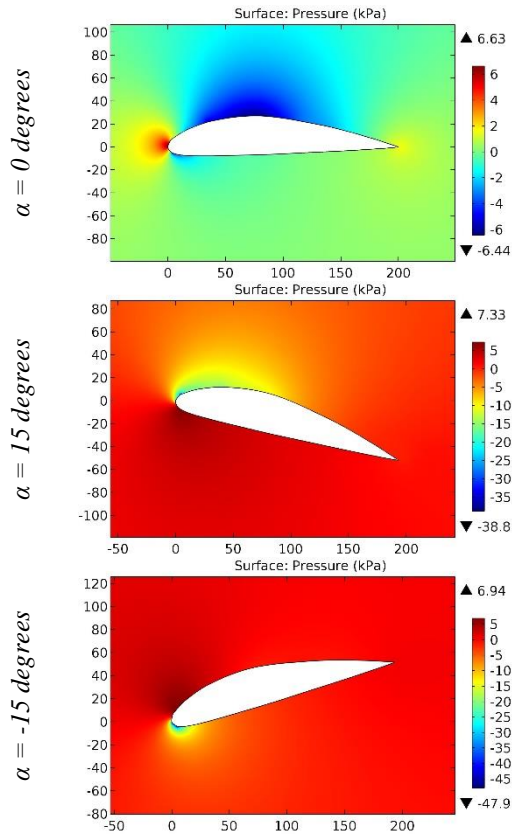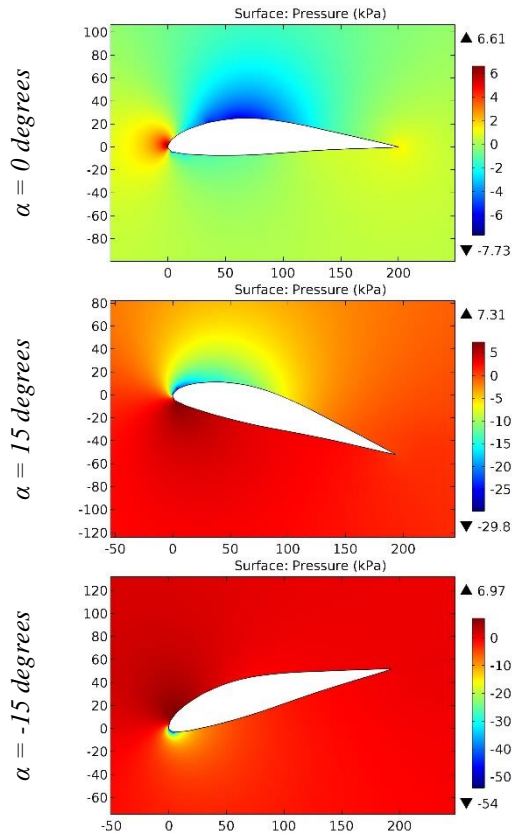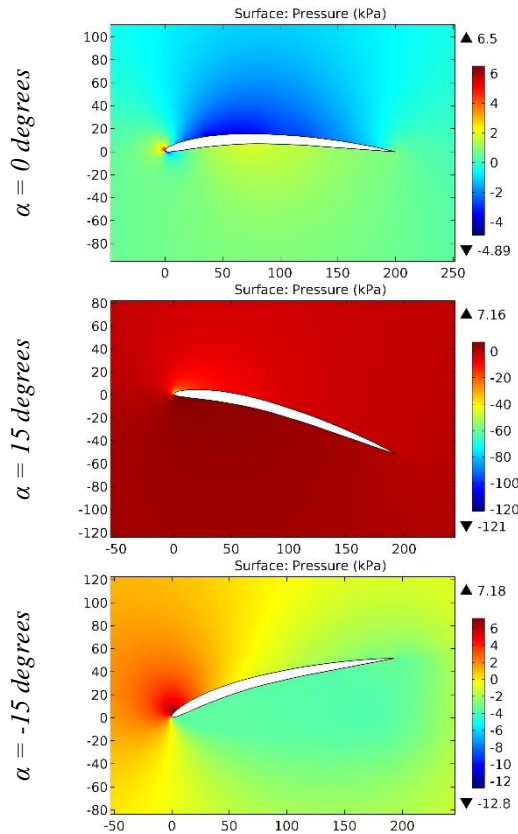**Figure 4. The pressure contours on the surfaces of the GOE 359 airfoil.**
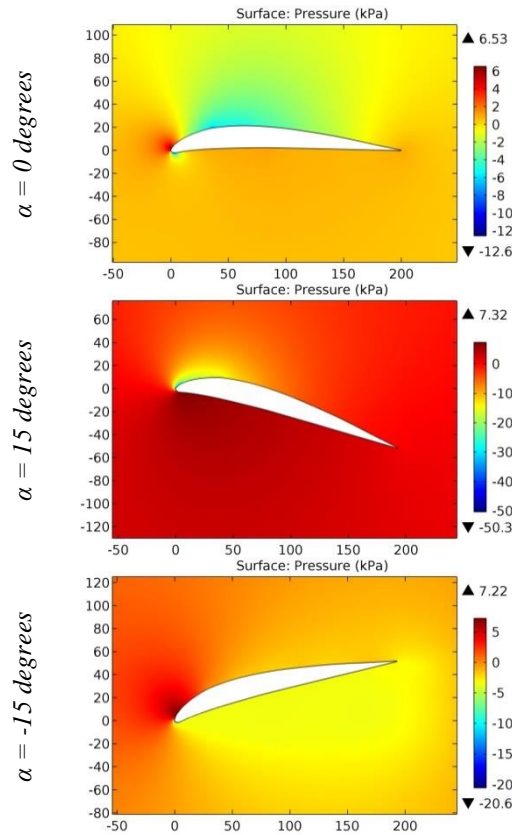
Figure 5. The pressure contours on the surfaces of the GOE 360 airfoil.
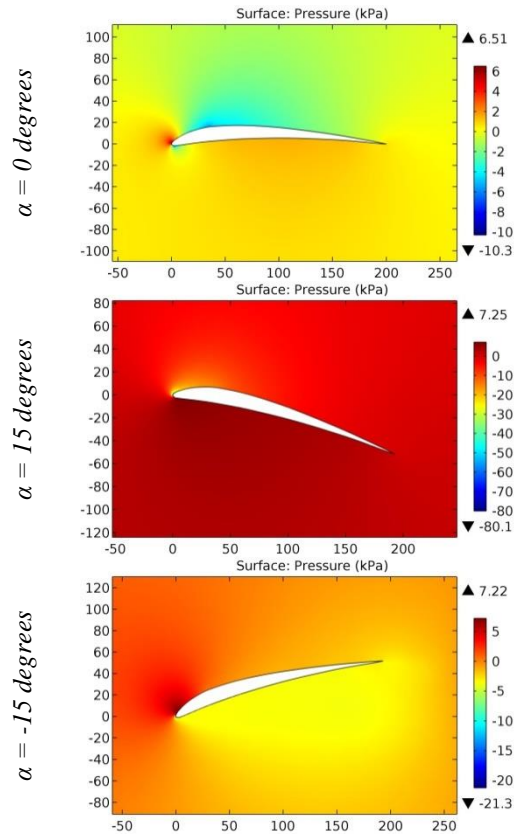
Figure 6. The pressure contours on the surfaces of the GOE 361 airfoil.
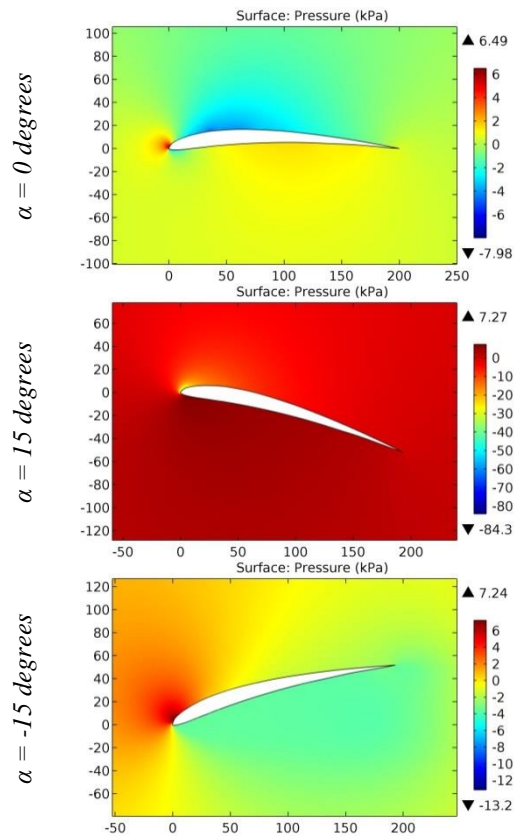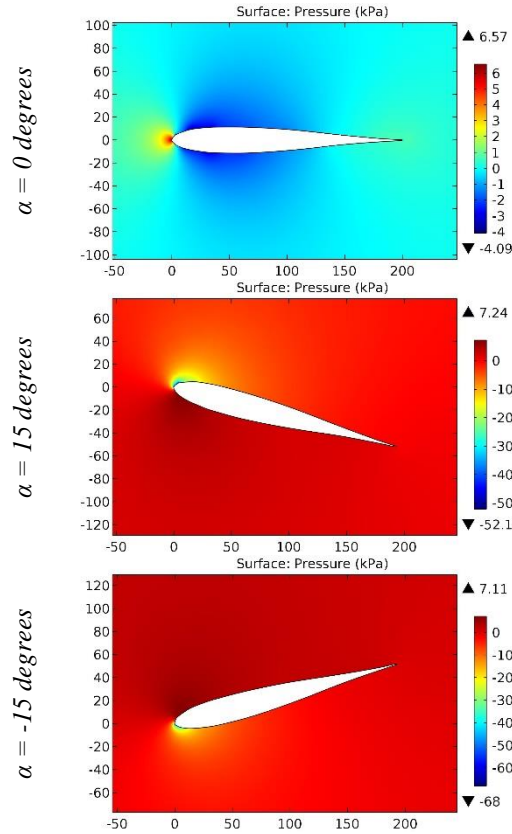

Figure 7. The pressure contours on the surfaces of the GOE 362 airfoil.
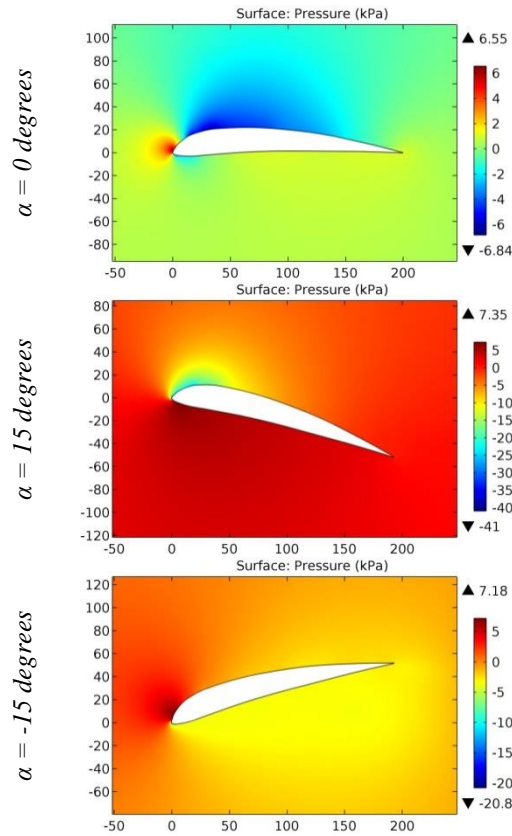
Figure 8. The pressure contours on the surfaces of the GOE 363 airfoil.
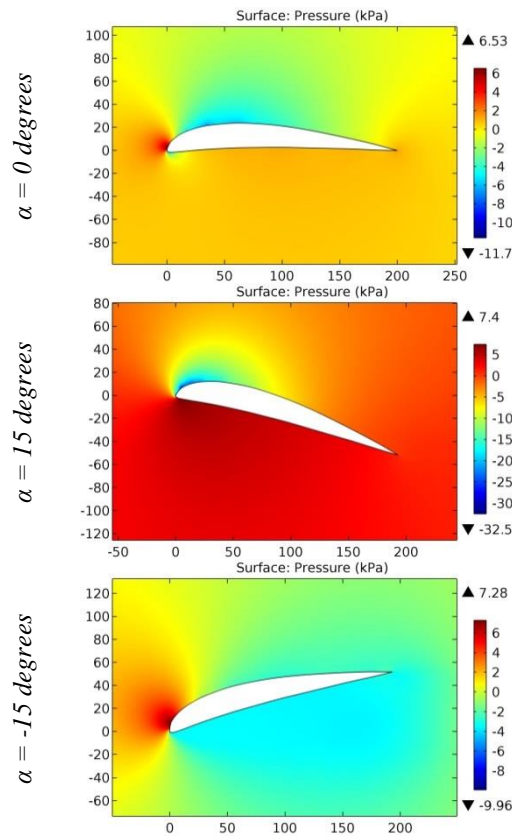
Figure 9. The pressure contours on the surfaces of the GOE 364 airfoil.
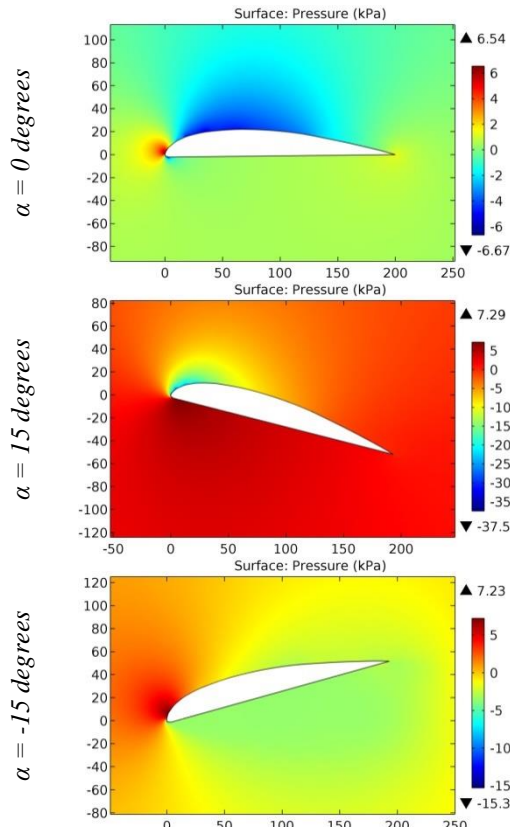
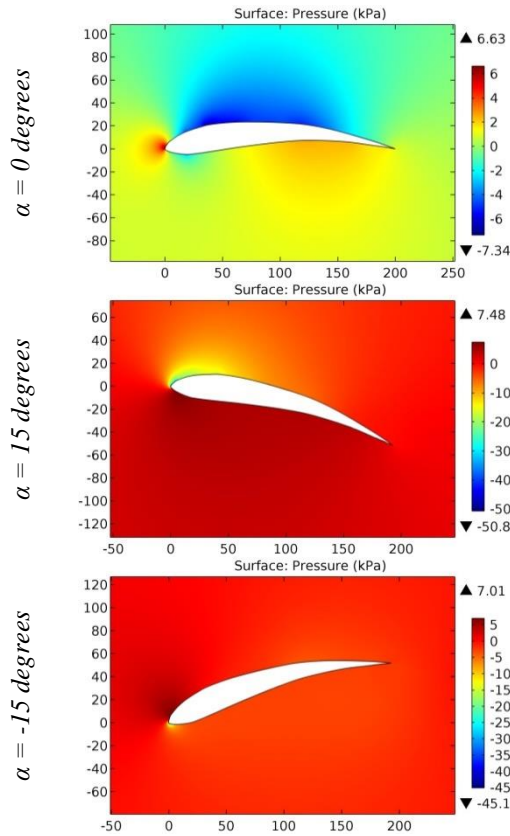**Figure 10. The pressure contours on the surfaces of the GOE 365 airfoil.**
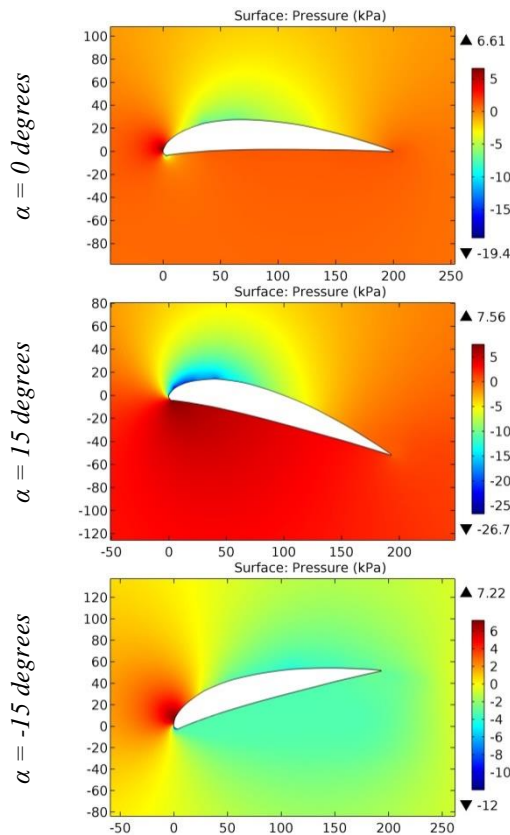
Figure 11. The pressure contours on the surfaces of the GOE 366 airfoil.
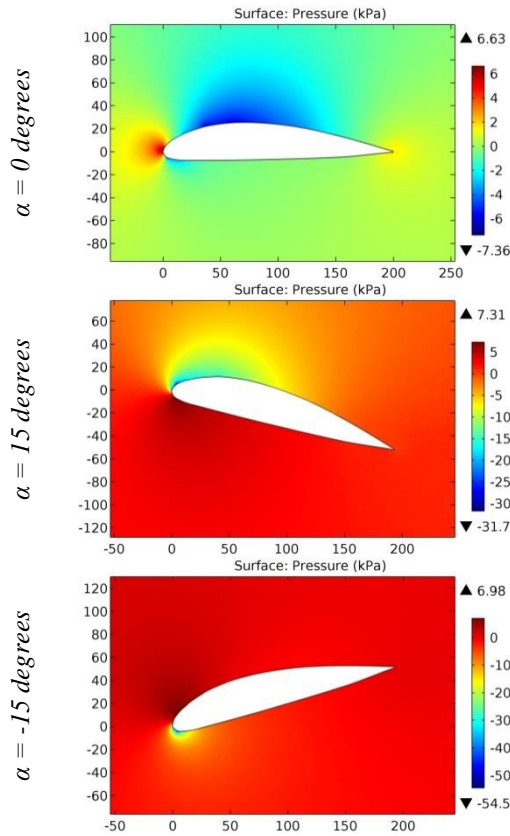
Figure 12. The pressure contours on the surfaces of the GOE 367 airfoil.
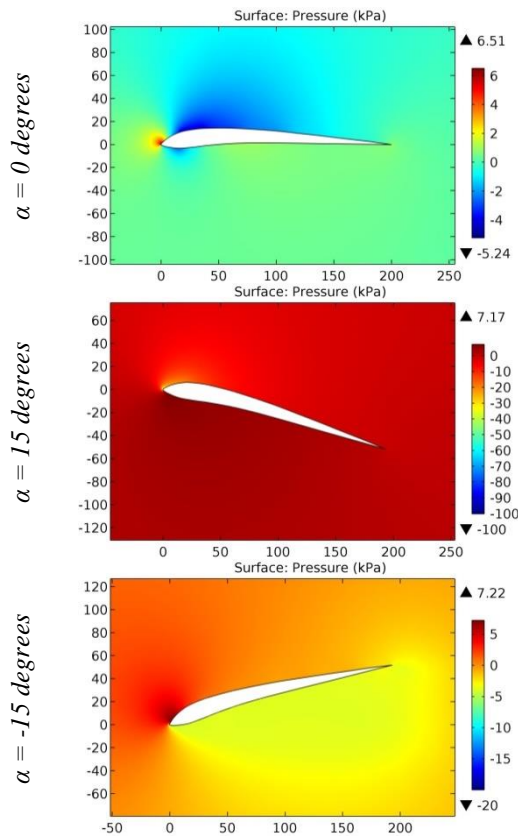
Figure 13. The pressure contours on the surfaces of the GOE 368 airfoil.
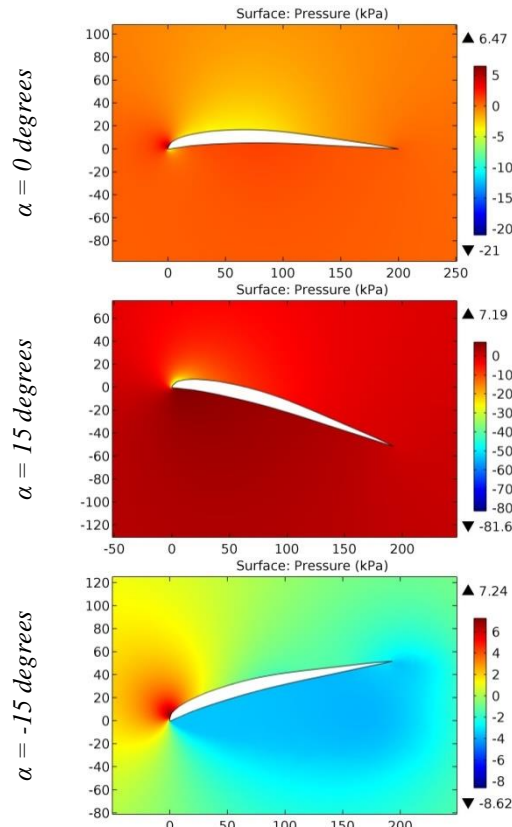
Figure 14. The pressure contours on the surfaces of the GOE 369 airfoil.
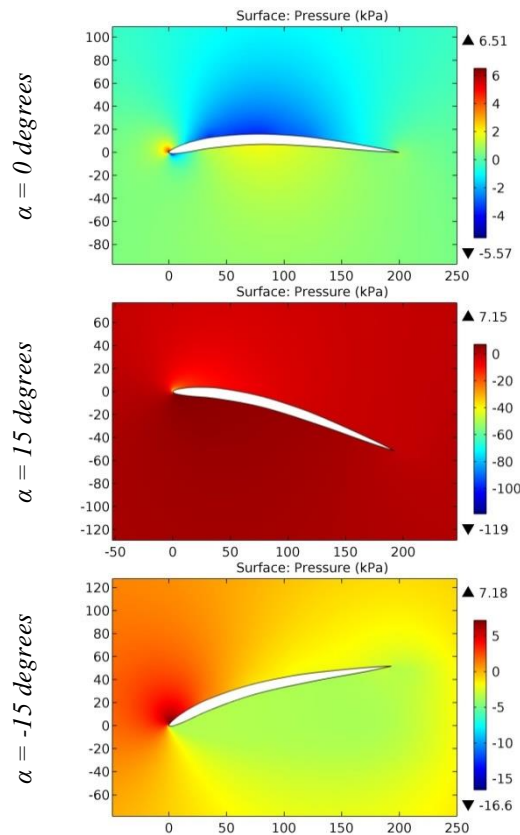
Figure 15. The pressure contours on the surfaces of the GOE 370 airfoil.
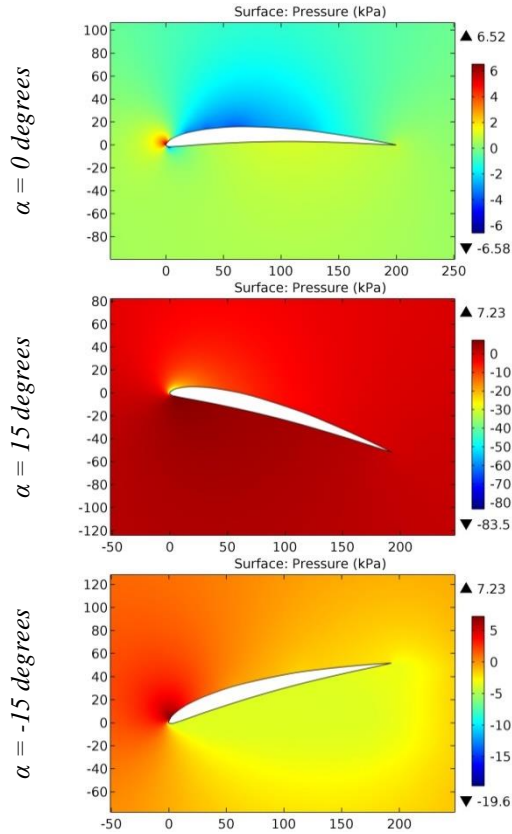
Figure 16. The pressure contours on the surfaces of the GOE 371 airfoil.
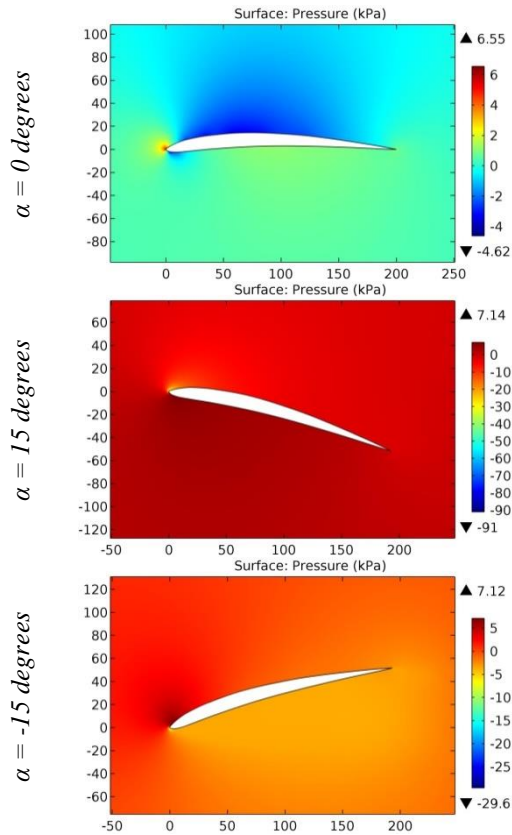
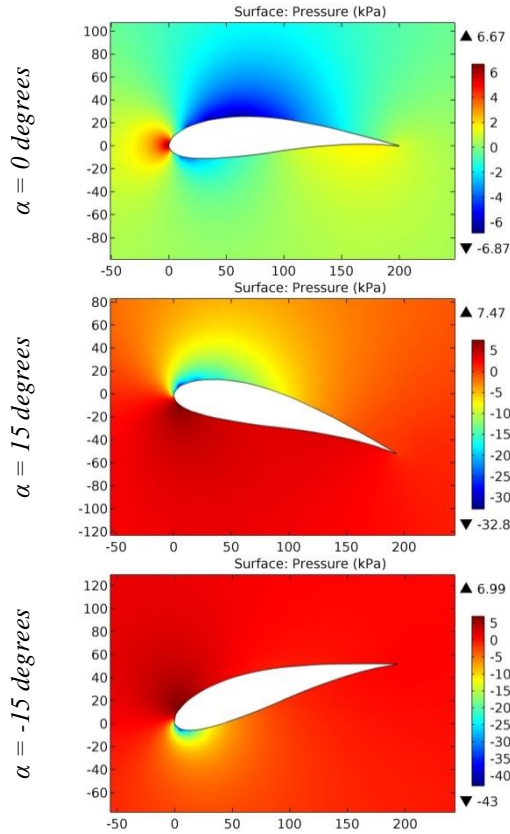**Figure 17. The pressure contours on the surfaces of the GOE 372 airfoil.**
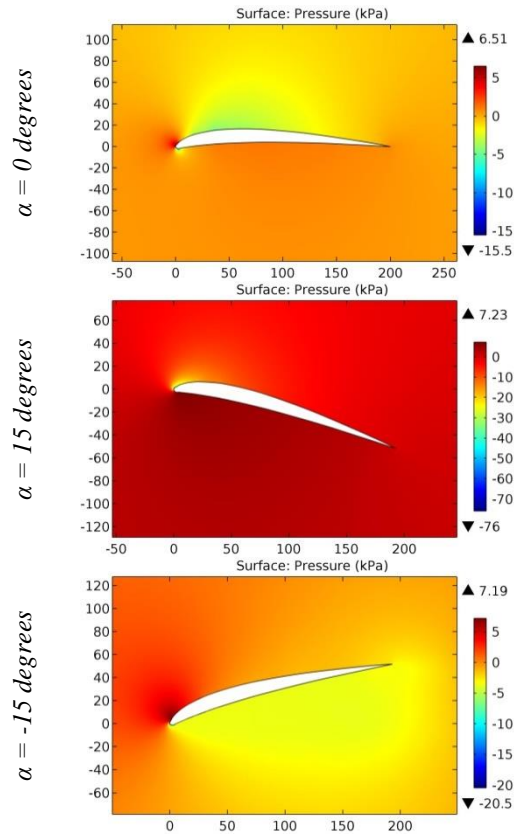
Figure 18. The pressure contours on the surfaces of the GOE 373 airfoil.
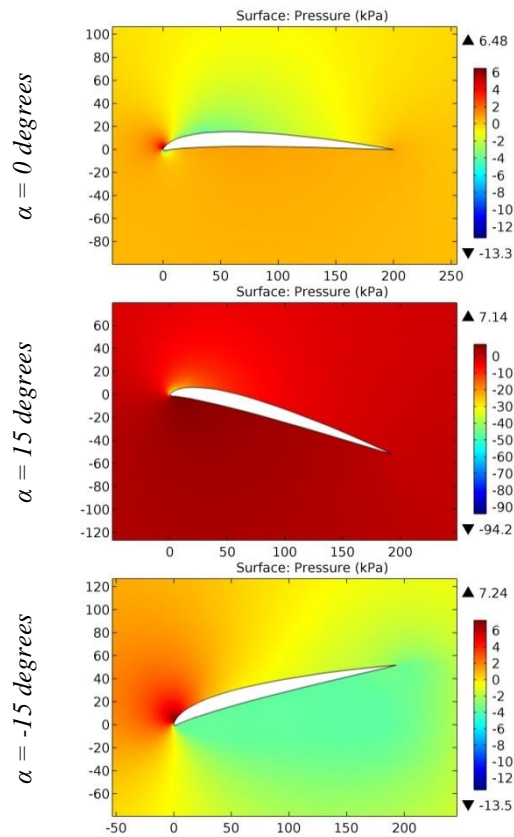
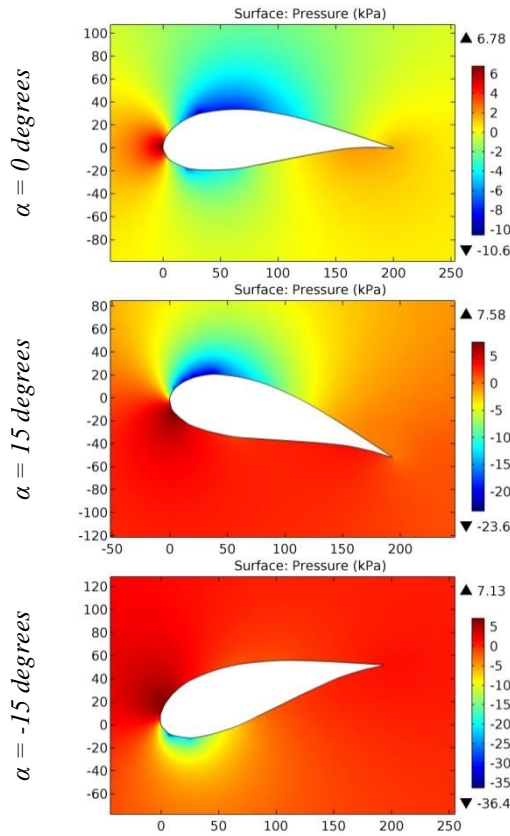**Figure 19. The pressure contours on the surfaces of the GOE 374 airfoil.**
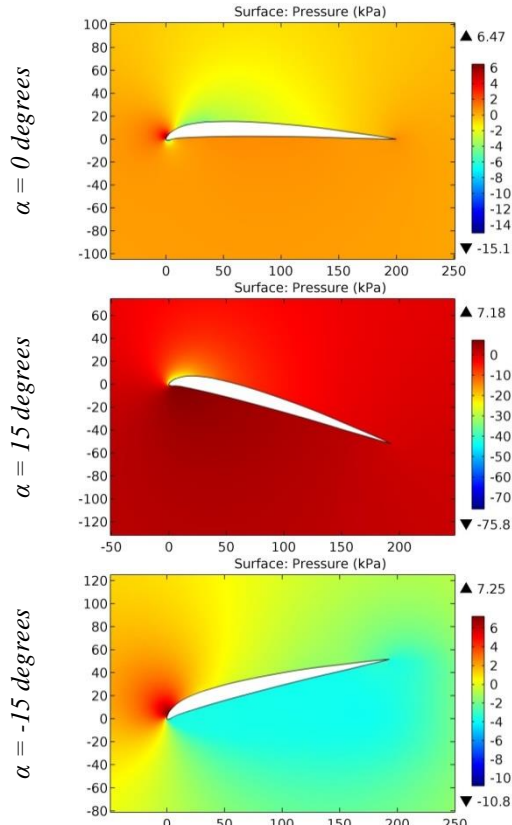
Figure 20. The pressure contours on the surfaces of the GOE 375 airfoil.
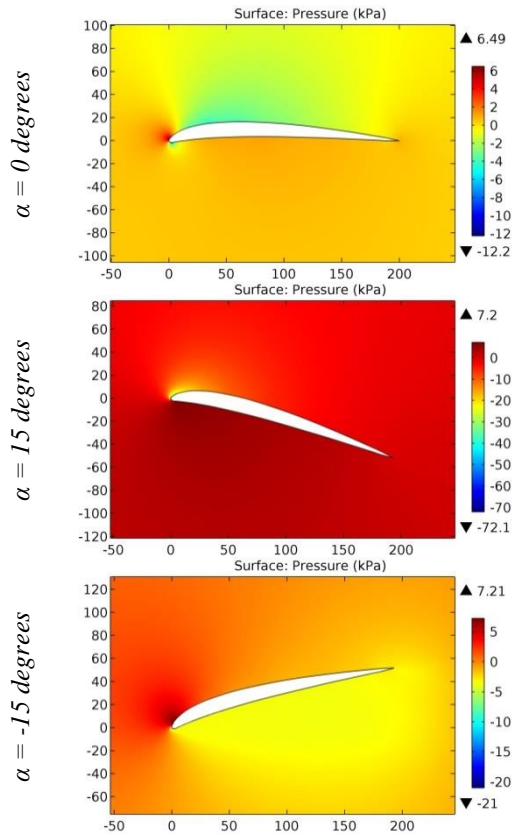
Figure 21. The pressure contours on the surfaces of the GOE 376 airfoil.
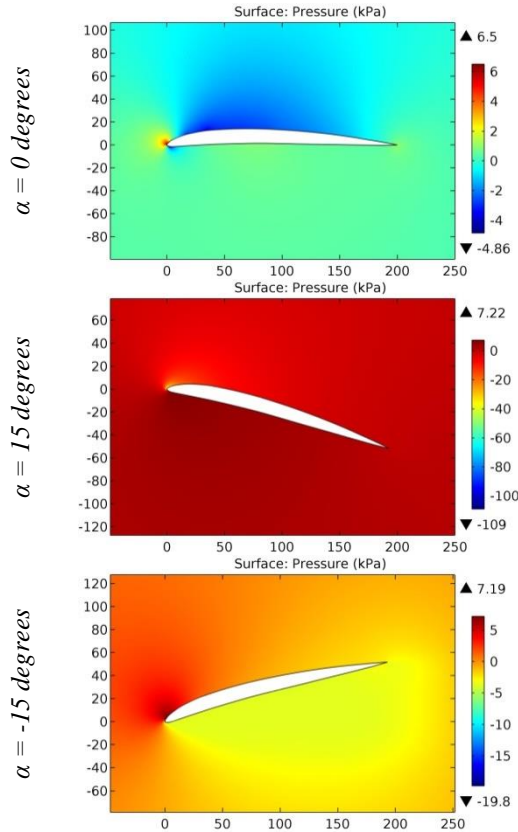
Figure 22. The pressure contours on the surfaces of the GOE 377 airfoil.
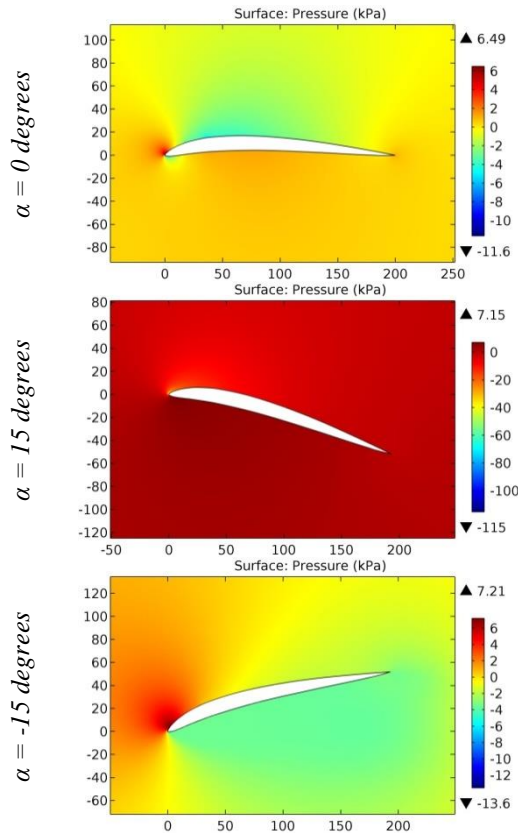
Figure 23. The pressure contours on the surfaces of the GOE 379 airfoil.

Clarivate Analytics **indexed**

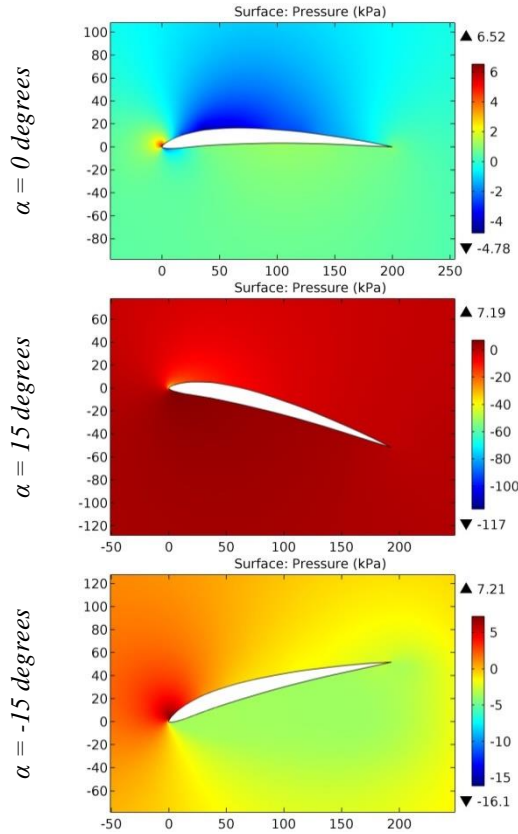**Figure 24. The pressure contours on the surfaces of the GOE 380 airfoil.**
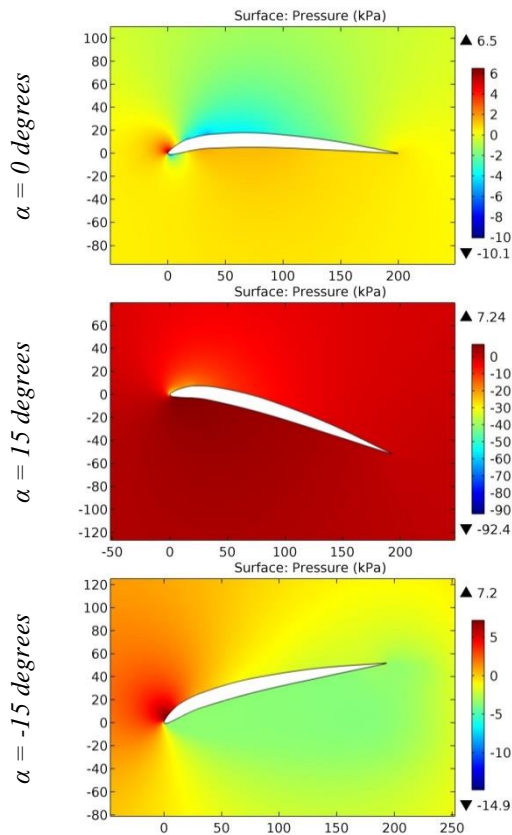
Figure 25. The pressure contours on the surfaces of the GOE 381 airfoil.
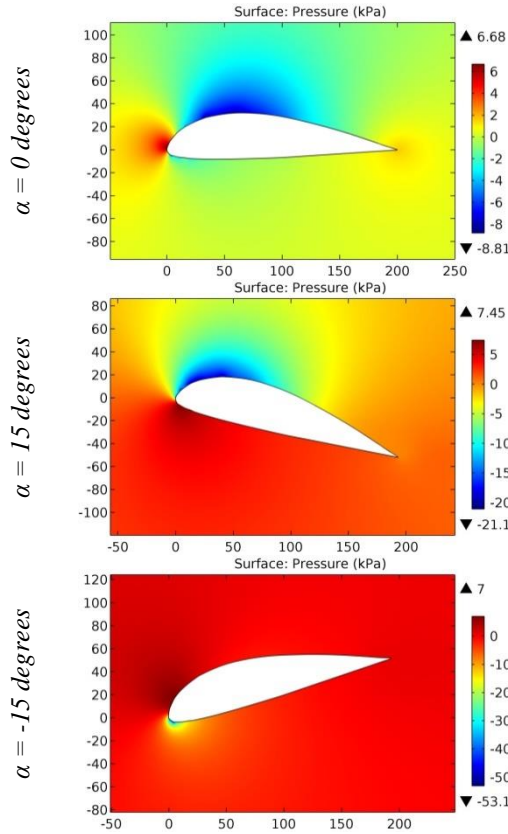
Figure 26. The pressure contours on the surfaces of the GOE 382 airfoil.
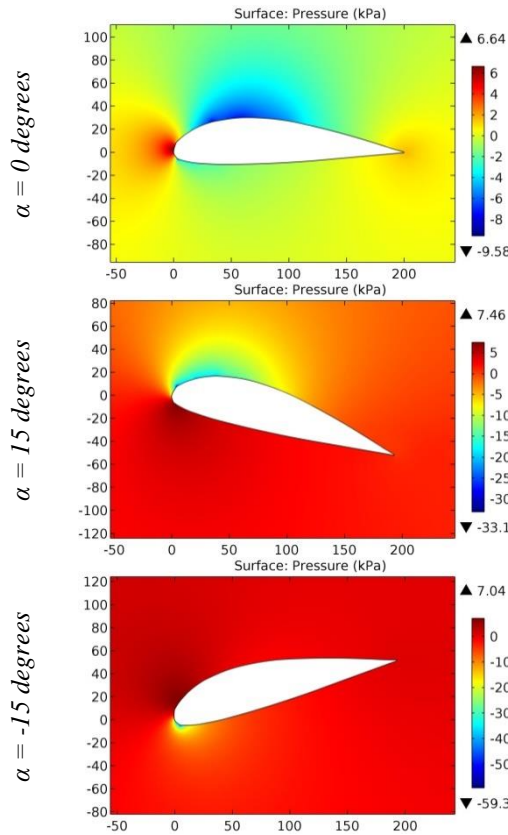
Figure 27. The pressure contours on the surfaces of the GOE 383 airfoil.
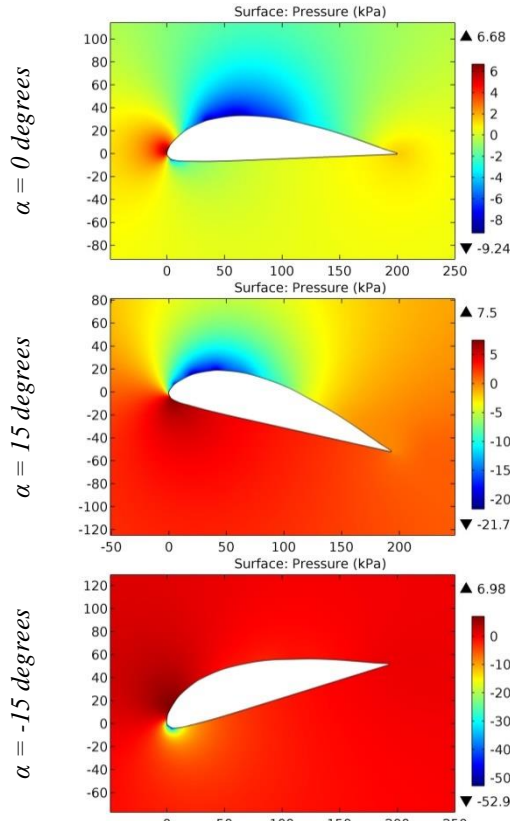
Figure 28. The pressure contours on the surfaces of the GOE 384 airfoil.
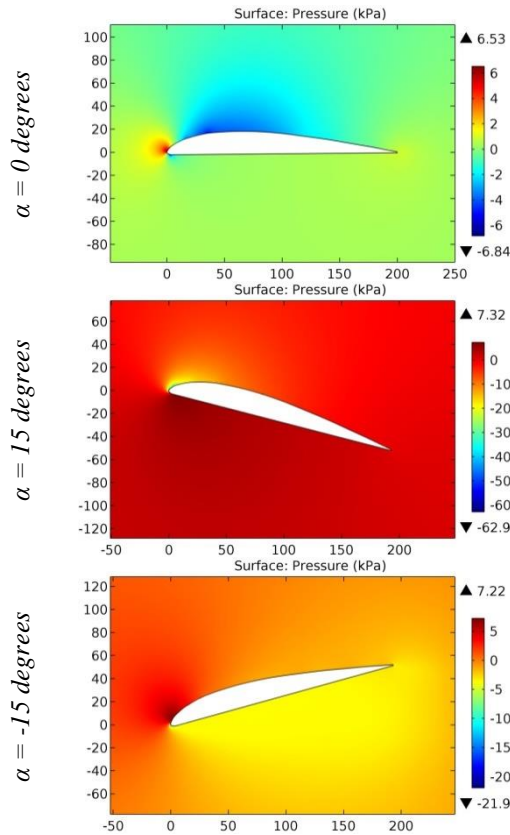
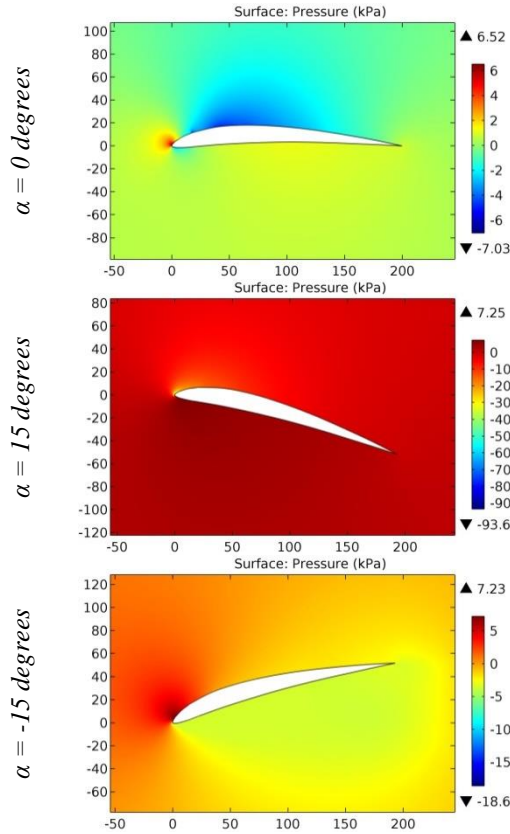**Figure 29. The pressure contours on the surfaces of the GOE 385 airfoil.**
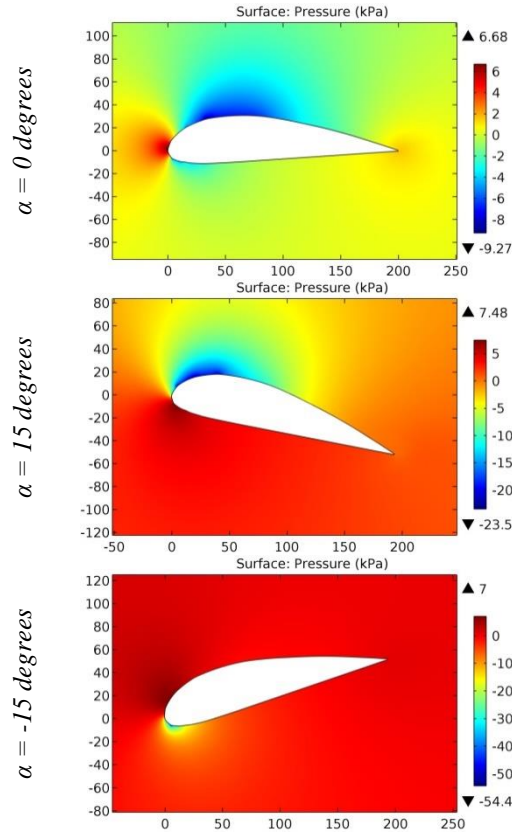
Figure 30. The pressure contours on the surfaces of the GOE 386 airfoil.
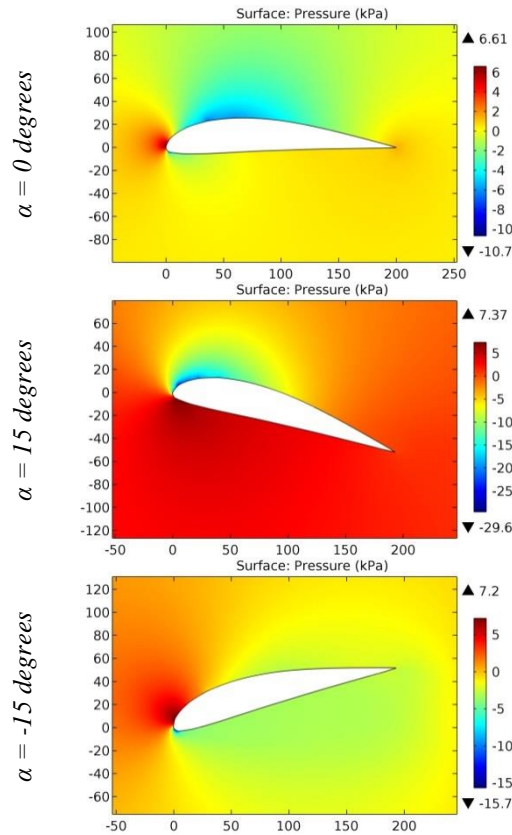
Figure 31. The pressure contours on the surfaces of the GOE 387 airfoil.

Figure 32. The pressure contours on the surfaces of the GOE 388 airfoil.
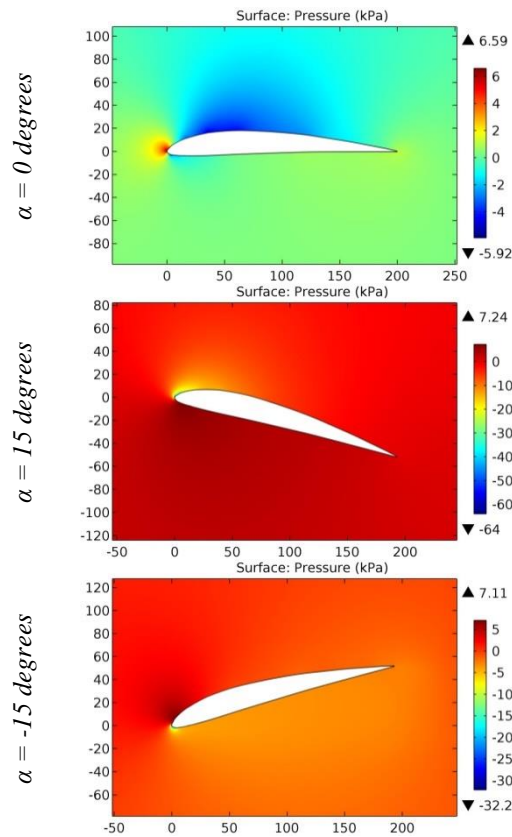
Figure 33. The pressure contours on the surfaces of the GOE 389 airfoil.
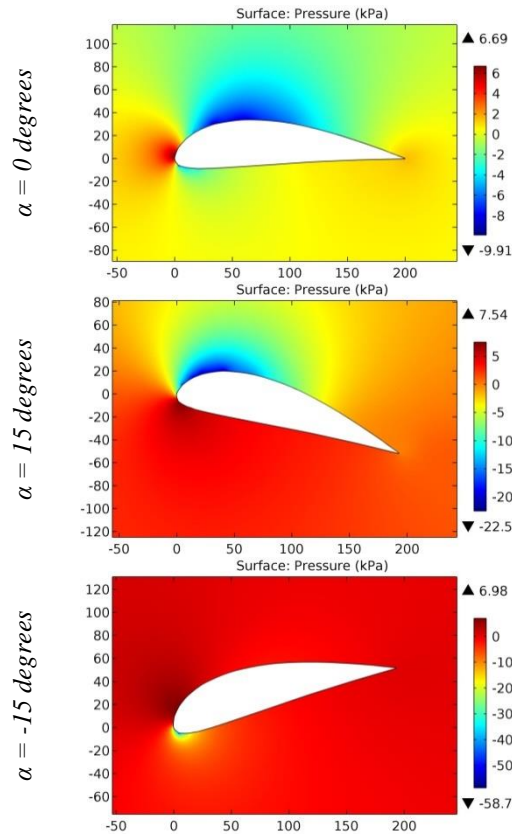
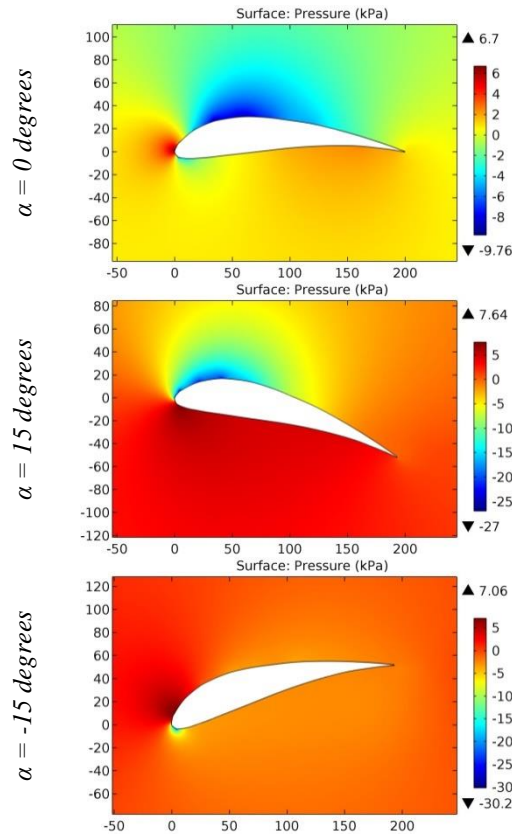**Figure 34. The pressure contours on the surfaces of the GOE 390 airfoil.**
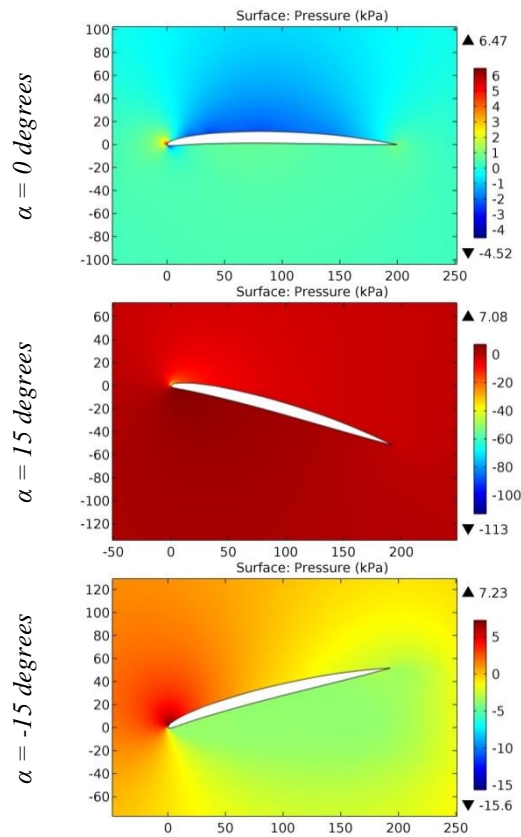
Figure 35. The pressure contours on the surfaces of the GOE 391 airfoil.
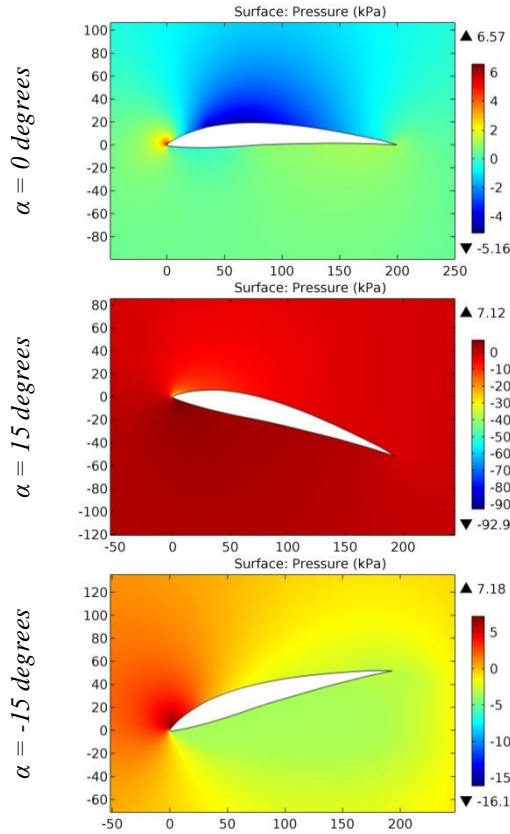
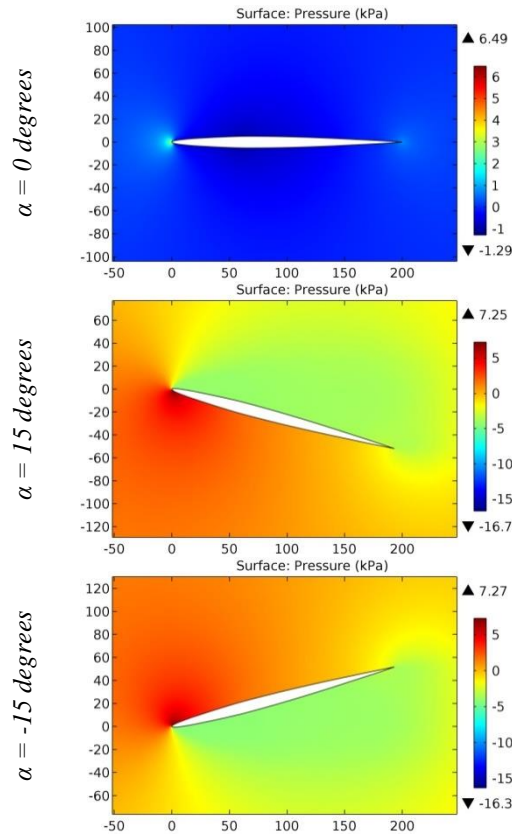**Figure 36. The pressure contours on the surfaces of the GOE 392 airfoil.**
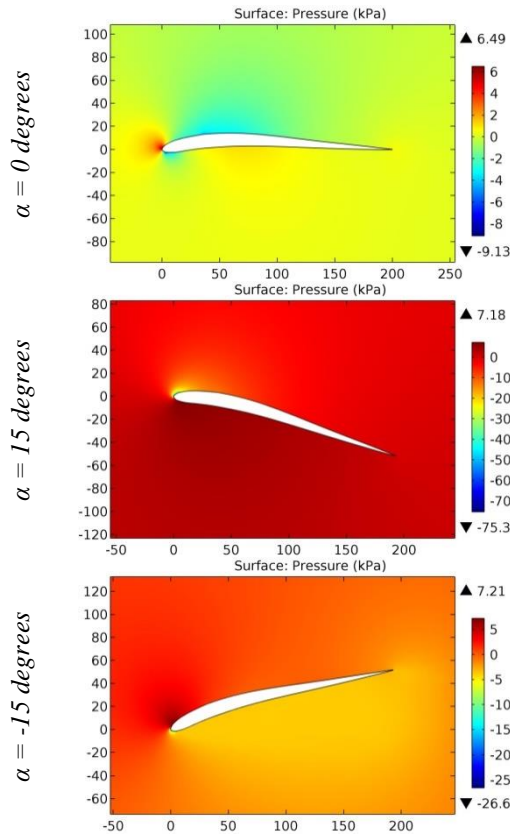
Figure 37. The pressure contours on the surfaces of the GOE 393 airfoil.
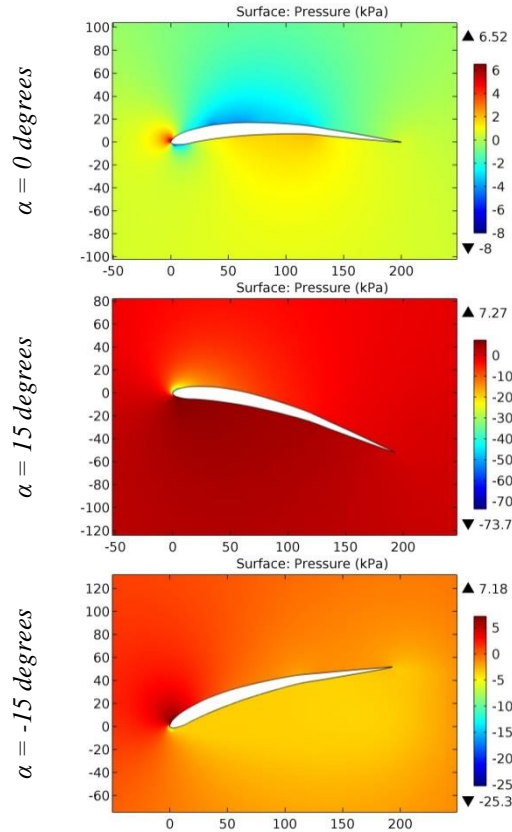
Figure 38. The pressure contours on the surfaces of the GOE 394 airfoil.
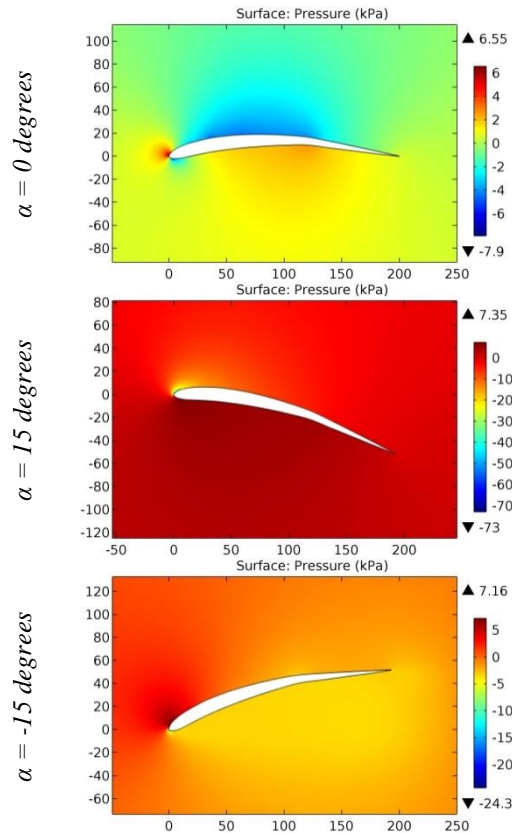
Figure 39. The pressure contours on the surfaces of the GOE 395 airfoil.

Figure 40. The pressure contours on the surfaces of the GOE 396 airfoil.
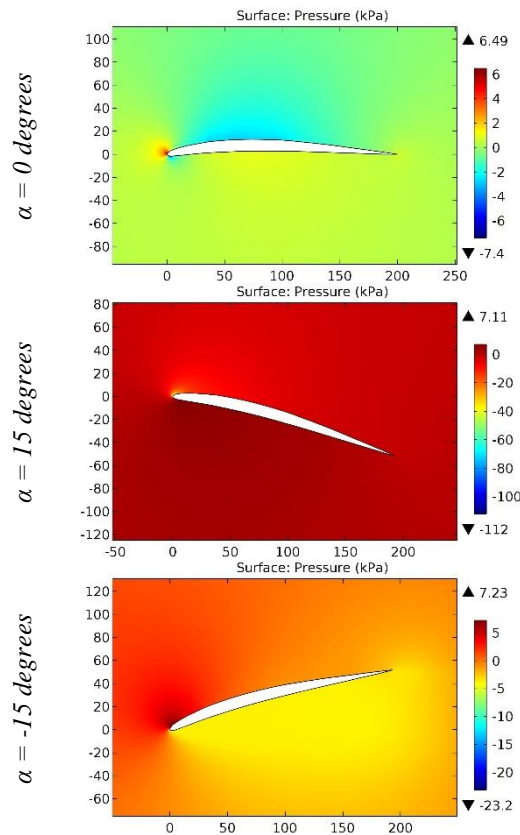
Figure 41. The pressure contours on the surfaces of the GOE 397 airfoil.

Figure 42. The pressure contours on the surfaces of the GOE 398 airfoil.
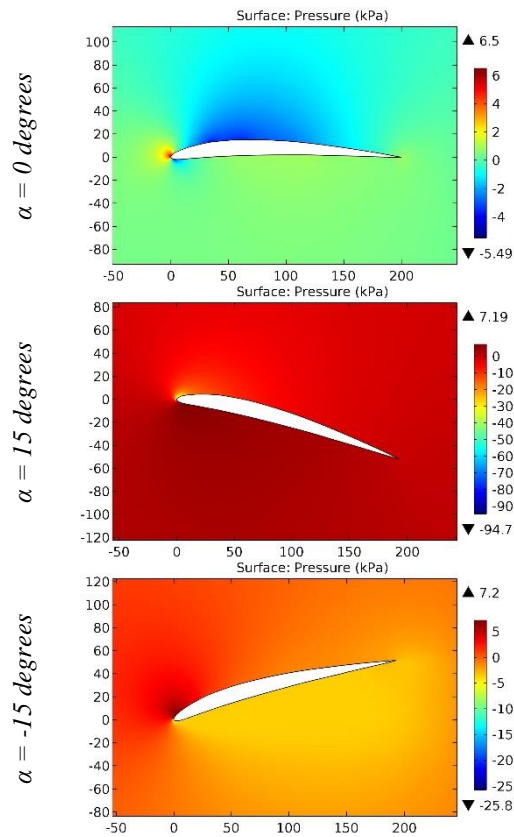
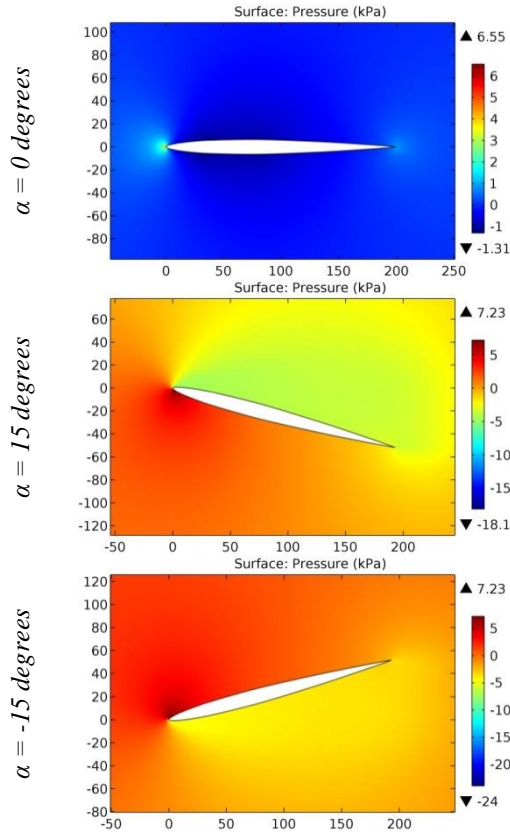Figure 43. The pressure contours on the surfaces of the GOE 399 airfoil.

Figure 44. The pressure contours on the surfaces of the GOE 400 airfoil.
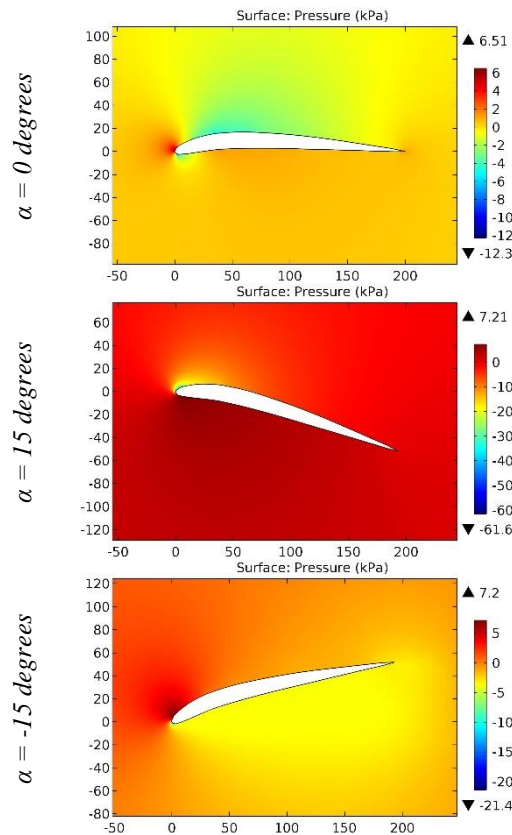
Figure 45. The pressure contours on the surfaces of the GOE 401 airfoil.
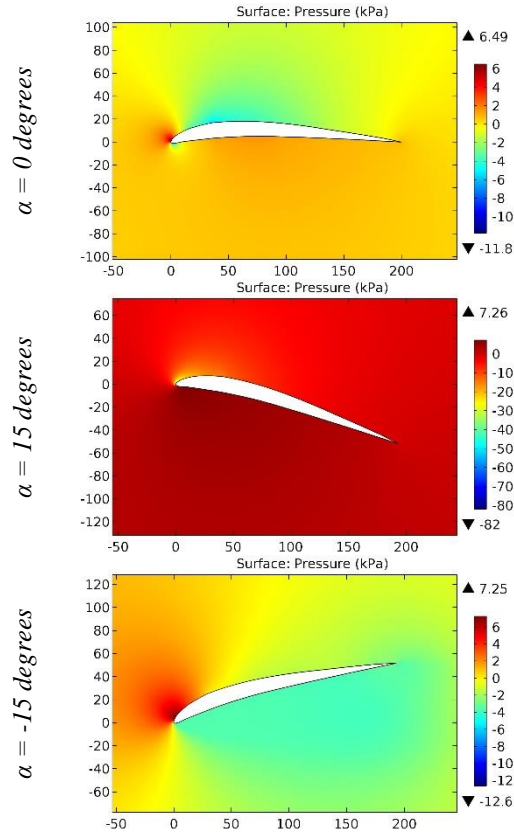
Figure 46. The pressure contours on the surfaces of the GOE 402 airfoil.
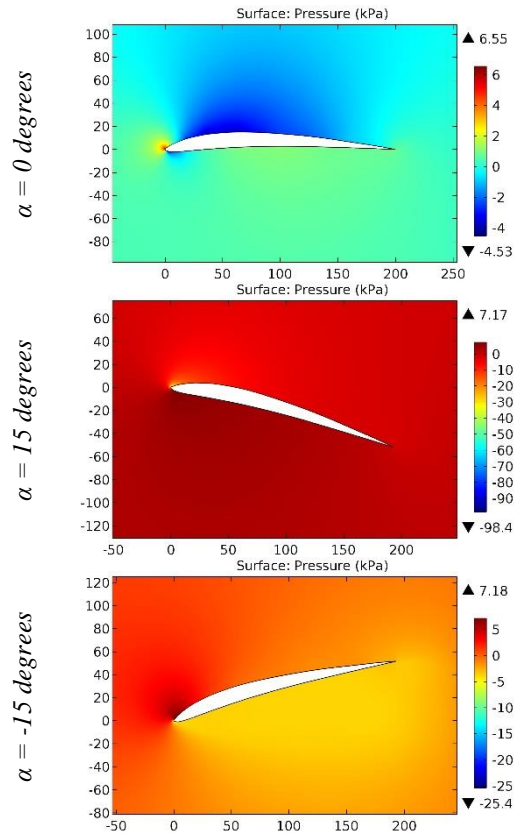
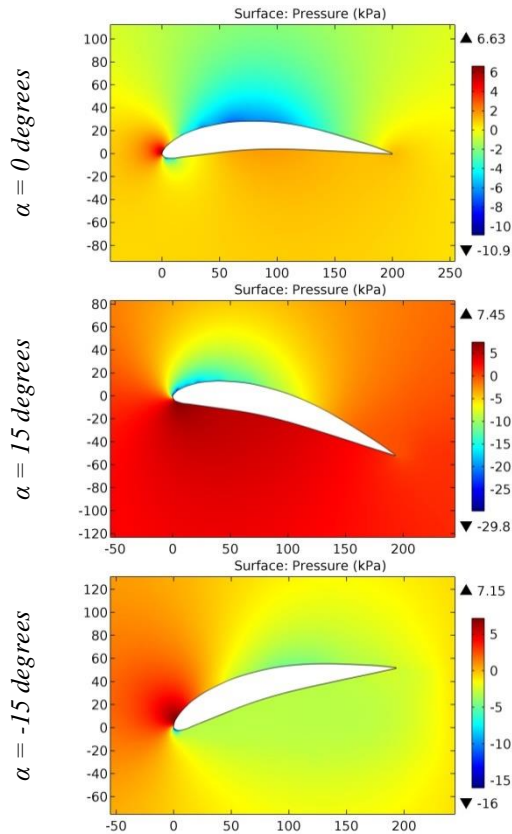**Figure 47. The pressure contours on the surfaces of the GOE 403 airfoil.**
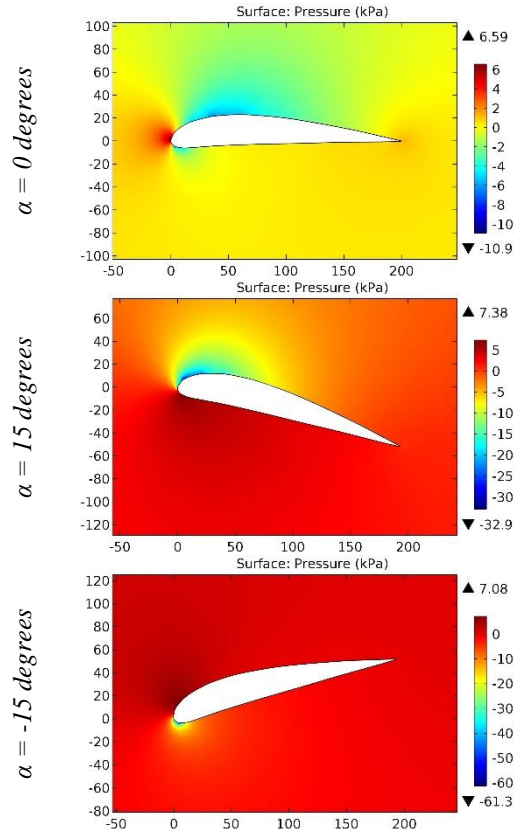
Figure 48. The pressure contours on the surfaces of the GOE 404 airfoil.
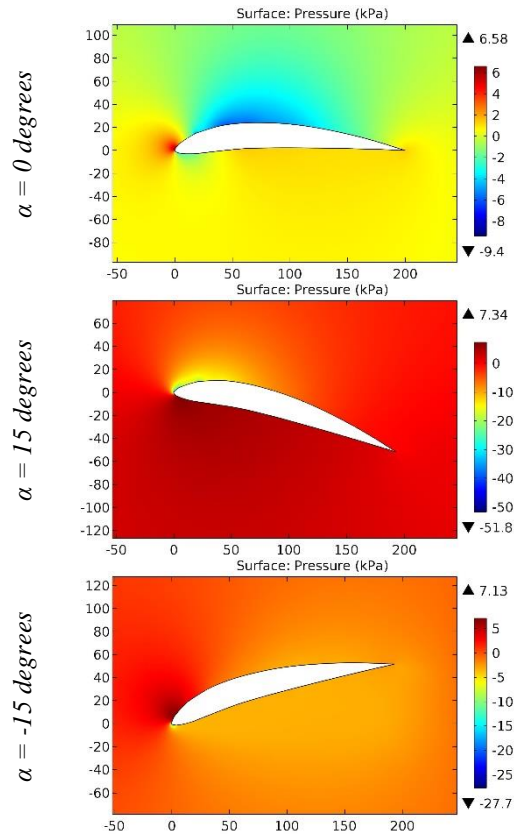
Figure 49. The pressure contours on the surfaces of the GOE 405 airfoil.

Figure 50. The pressure contours on the surfaces of the GOE 406 airfoil.
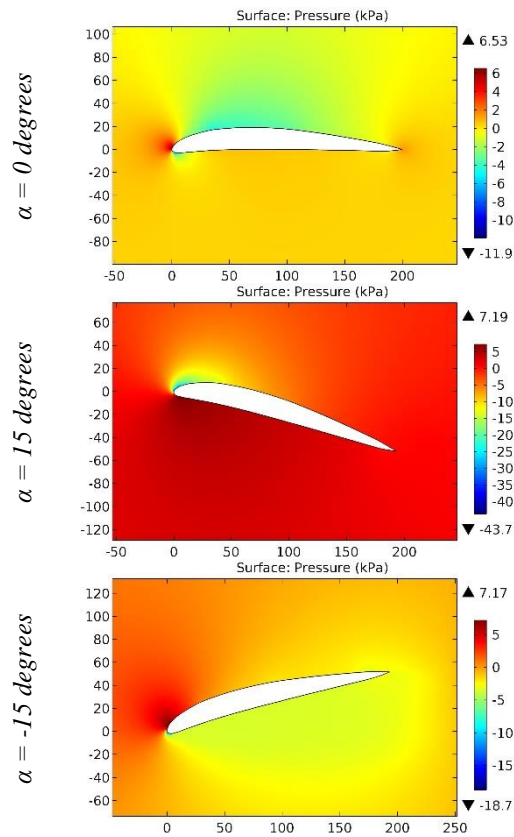
Figure 51. The pressure contours on the surfaces of the GOE 407 airfoil.

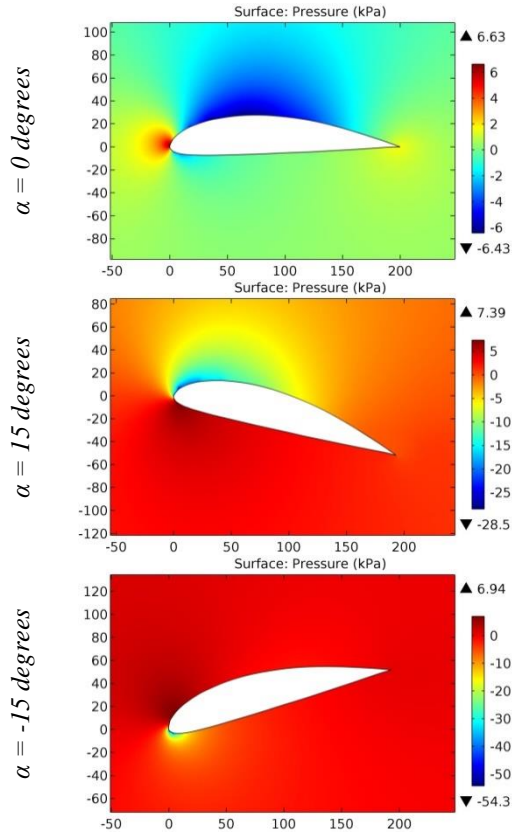**Figure 52. The pressure contours on the surfaces of the GOE 408 airfoil.**
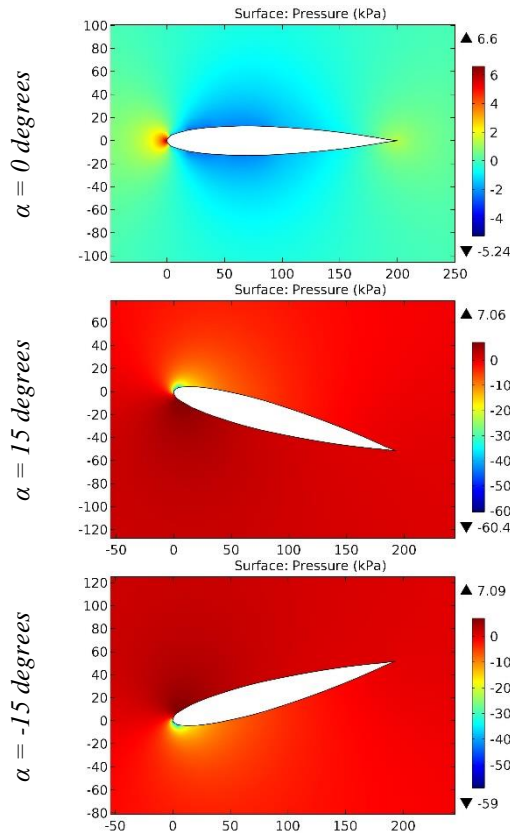
Figure 53. The pressure contours on the surfaces of the GOE 409 airfoil.
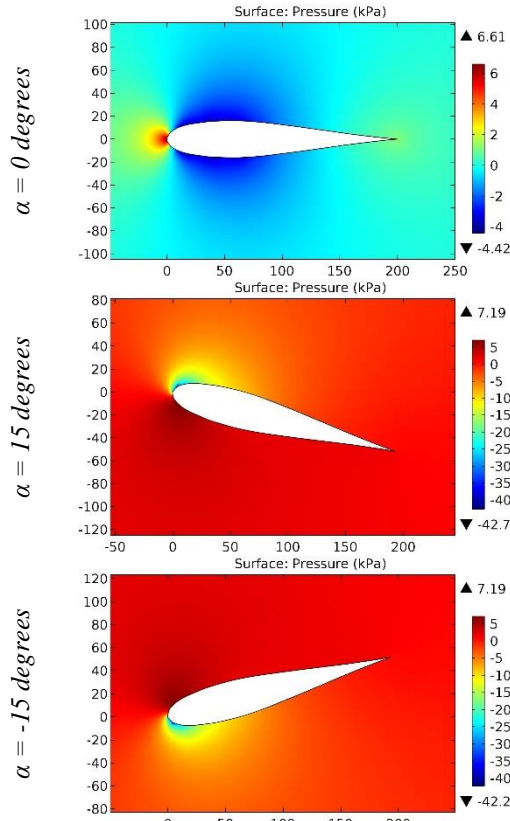
Figure 54. The pressure contours on the surfaces of the GOE 410 airfoil.
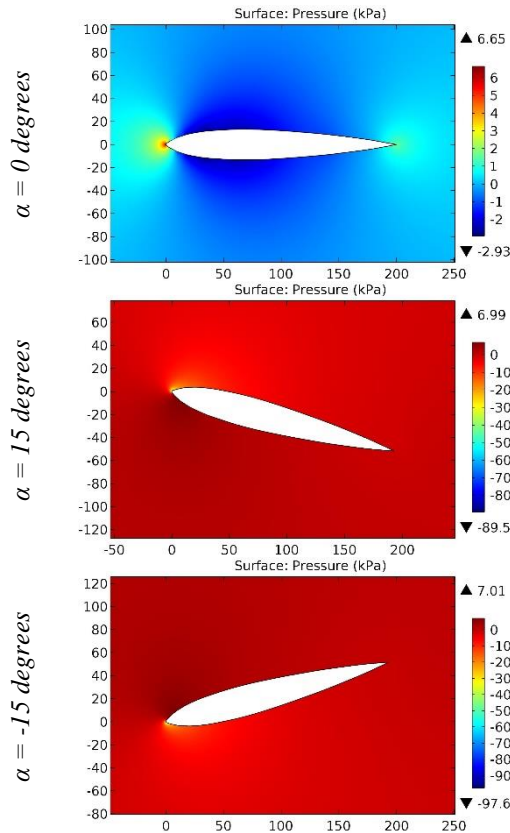
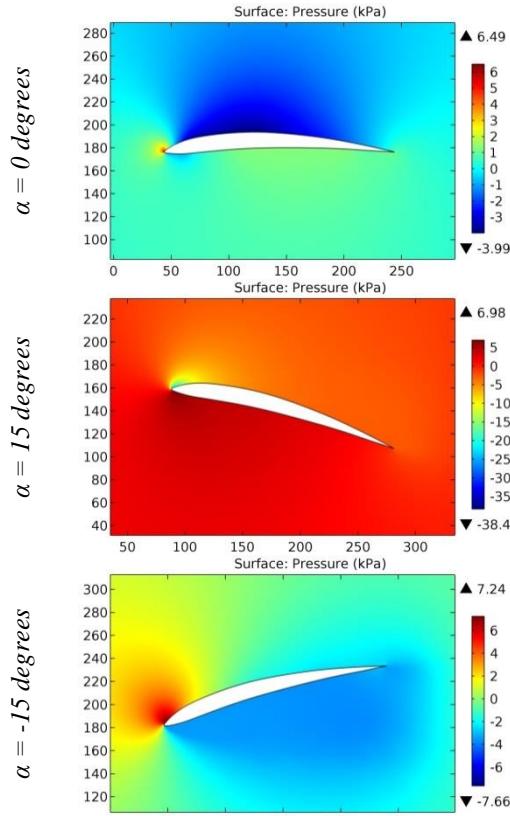**Figure 55. The pressure contours on the surfaces of the GOE 411 airfoil.**

Figure 56. The pressure contours on the surfaces of the GOE 412 airfoil.
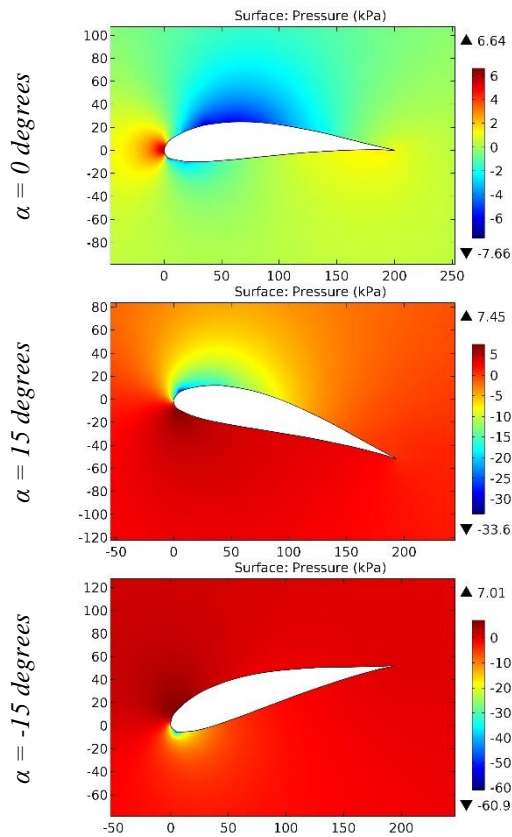
Figure 57. The pressure contours on the surfaces of the GOE 413 airfoil.

Figure 58. The pressure contours on the surfaces of the GOE 414 airfoil.
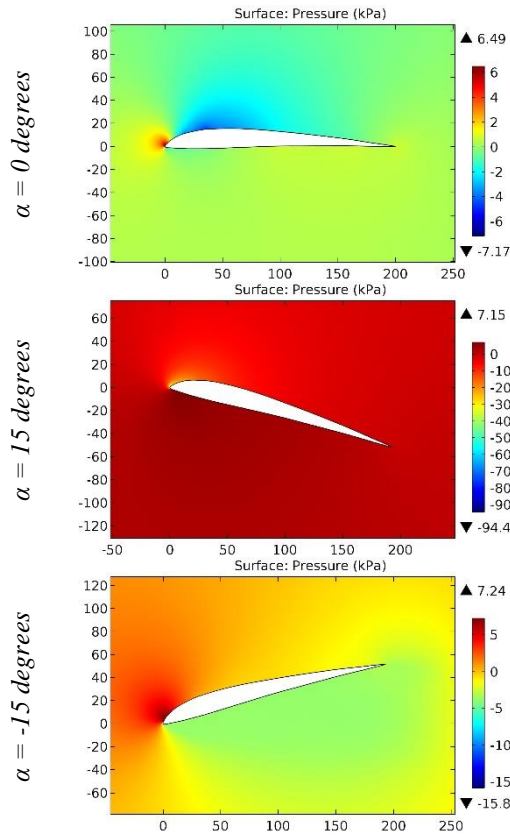
Figure 59. The pressure contours on the surfaces of the GOE 415 airfoil.

Figure 60. The pressure contours on the surfaces of the GOE 416A airfoil.
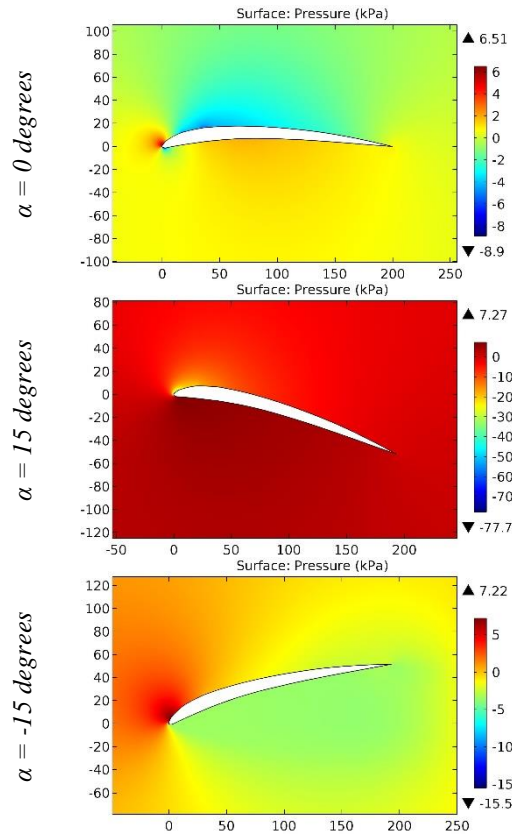
Figure 61. The pressure contours on the surfaces of the GOE 417 airfoil.

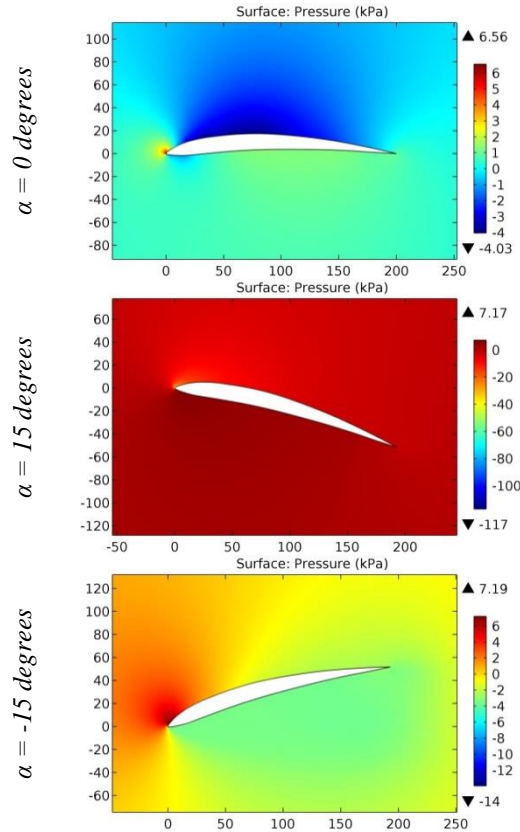**Figure 62. The pressure contours on the surfaces of the GOE 417A (GEW, PLATTE) airfoil.**
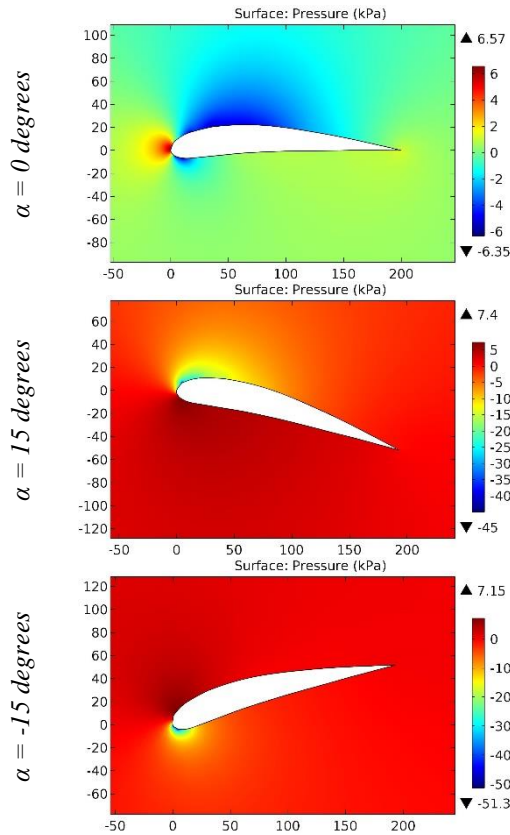
Figure 63. The pressure contours on the surfaces of the GOE 418 airfoil.

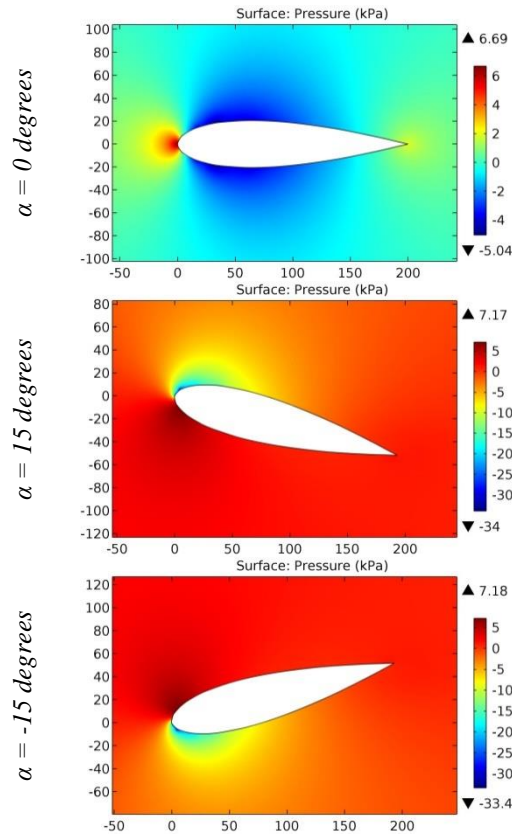**Figure 64. The pressure contours on the surfaces of the GOE 419 airfoil.**
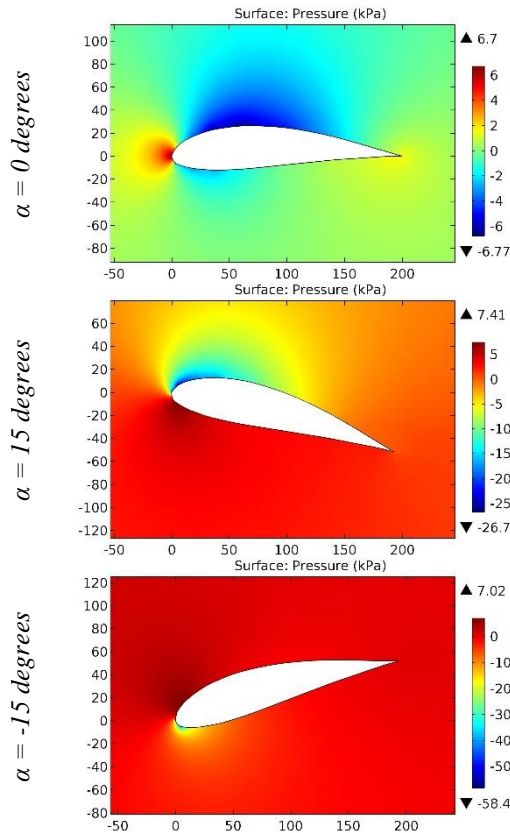
Figure 65. The pressure contours on the surfaces of the GOE 420 airfoil.

Figure 66. The pressure contours on the surfaces of the GOE 421 airfoil.
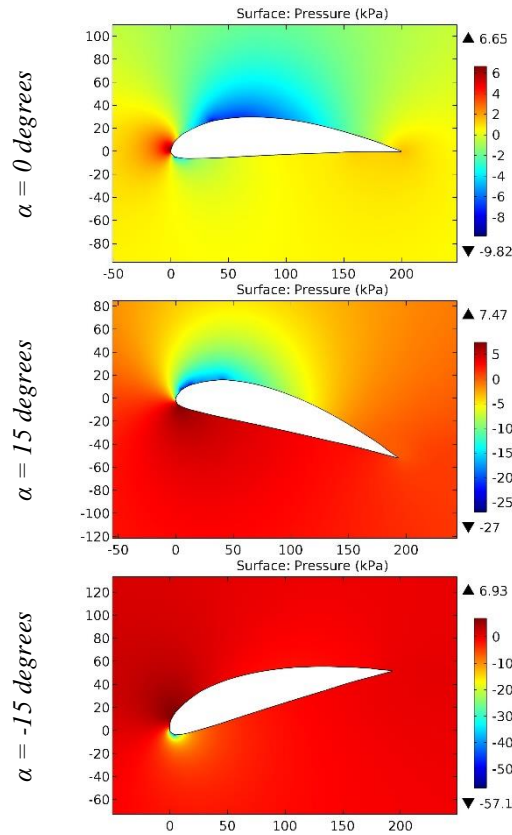
Figure 67. The pressure contours on the surfaces of the GOE 422 airfoil.

Figure 68. The pressure contours on the surfaces of the GOE 423 airfoil.
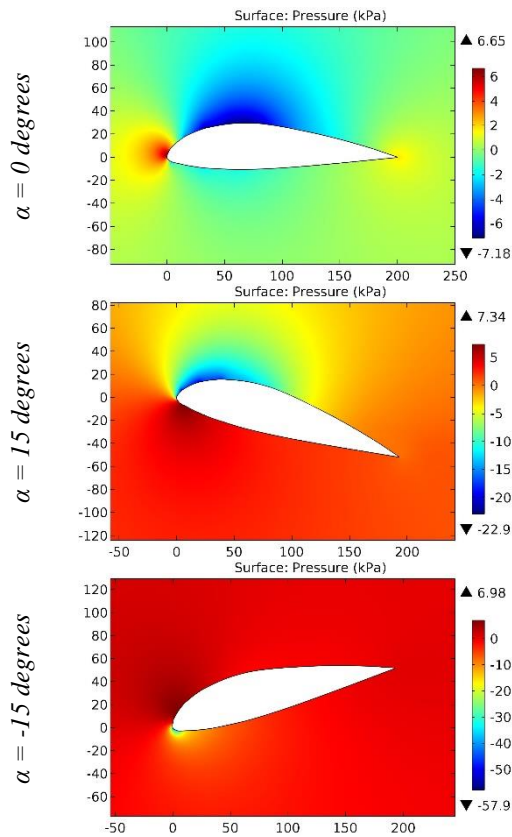
Figure 69. The pressure contours on the surfaces of the GOE 424 airfoil.

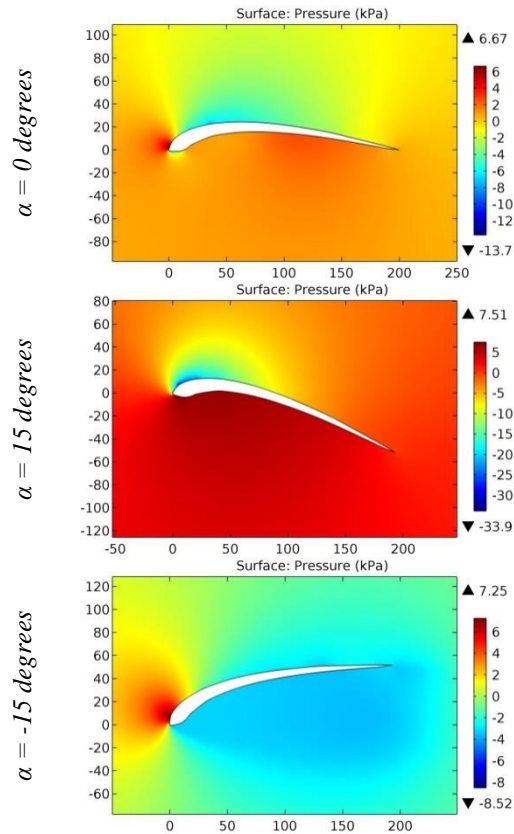**Figure 70. The pressure contours on the surfaces of the GOE 425 airfoil.**
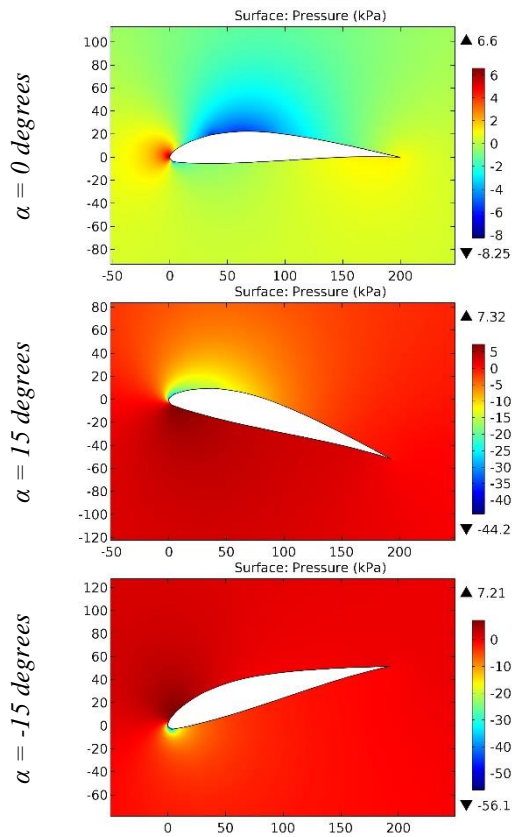
Figure 71. The pressure contours on the surfaces of the GOE 426 airfoil.

Figure 72. The pressure contours on the surfaces of the GOE 427 airfoil.
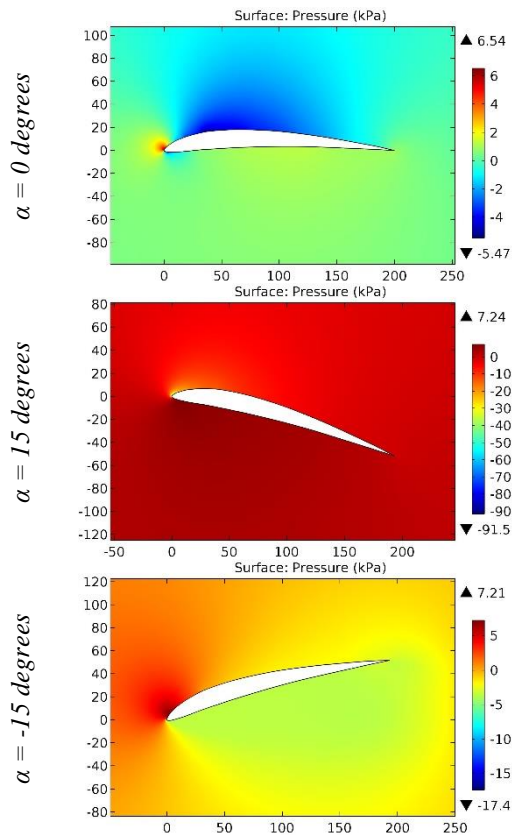
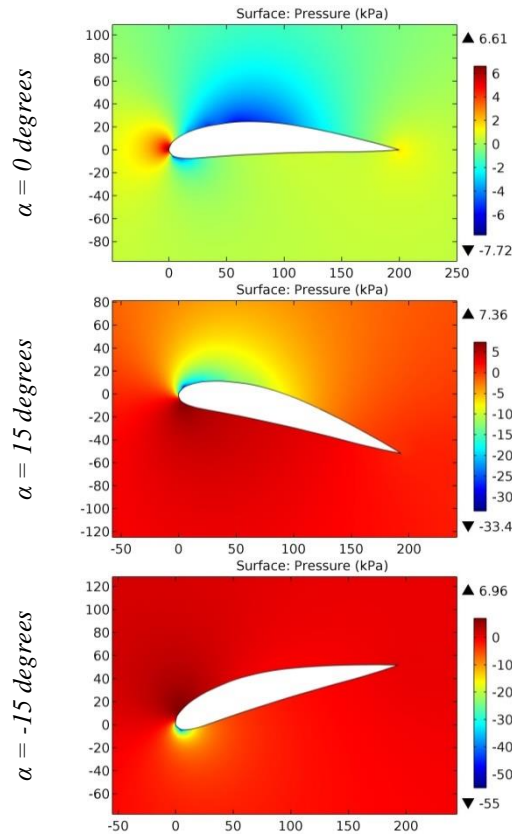**Figure 73. The pressure contours on the surfaces of the GOE 428 airfoil.**

Figure 74. The pressure contours on the surfaces of the GOE 429 airfoil.
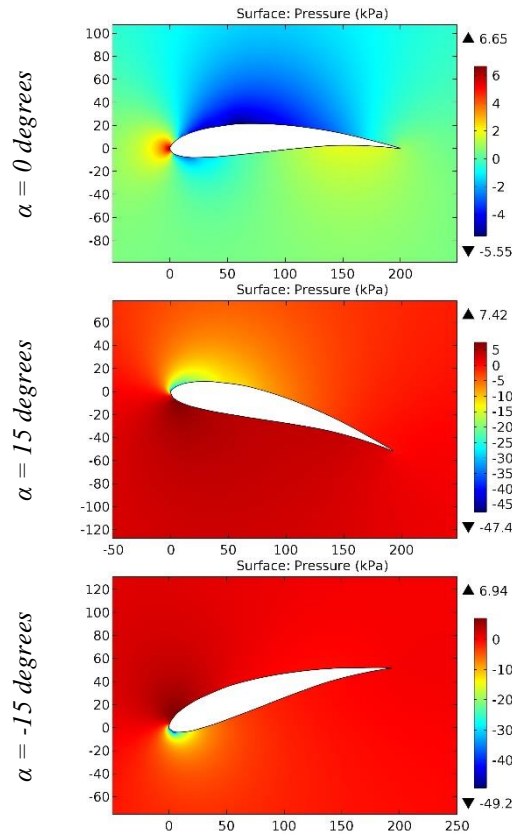
Figure 75. The pressure contours on the surfaces of the GOE 430 airfoil.

Figure 76. The pressure contours on the surfaces of the GOE 431 airfoil.
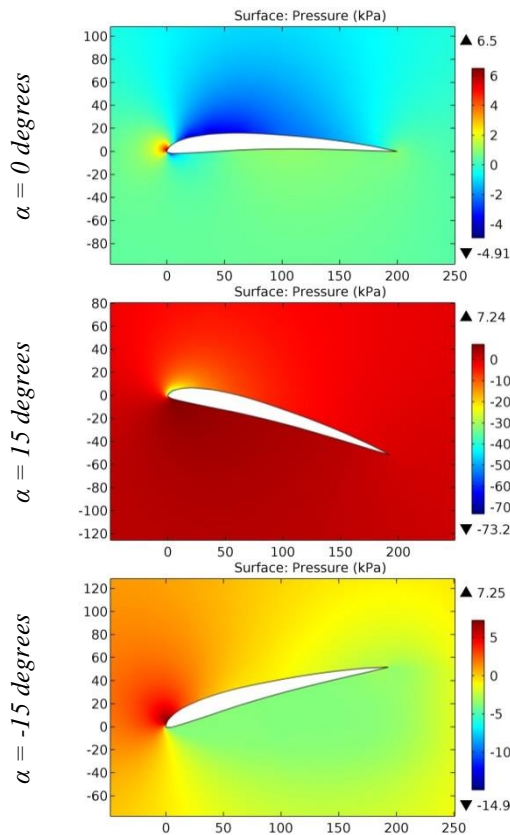
Figure 77. The pressure contours on the surfaces of the GOE 432 airfoil.

Figure 78. The pressure contours on the surfaces of the GOE 433 airfoil.
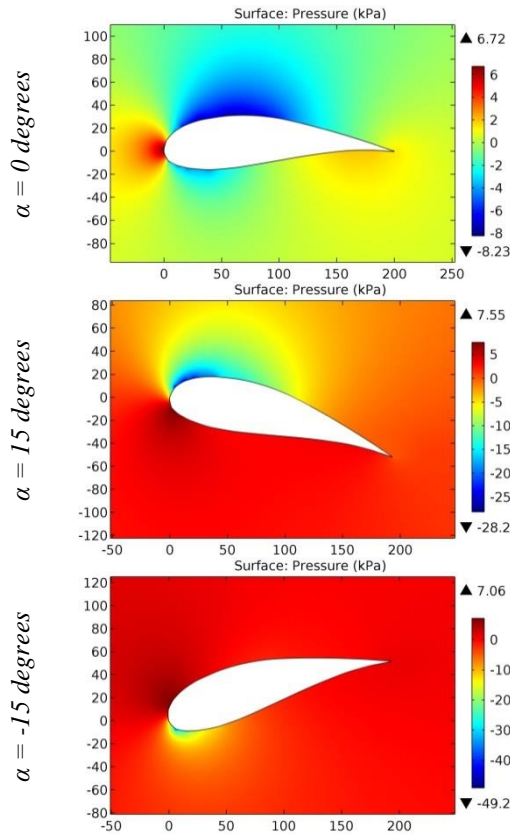
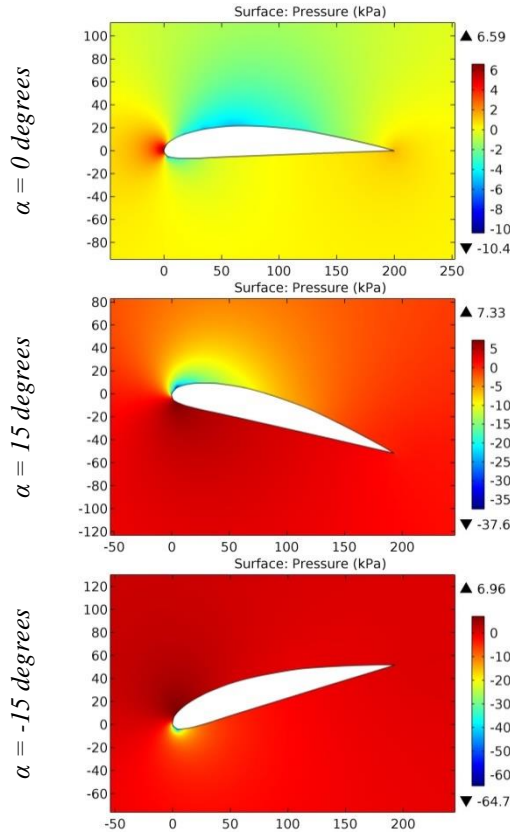**Figure 79. The pressure contours on the surfaces of the GOE 434 airfoil.**

Figure 80. The pressure contours on the surfaces of the GOE 435 airfoil.
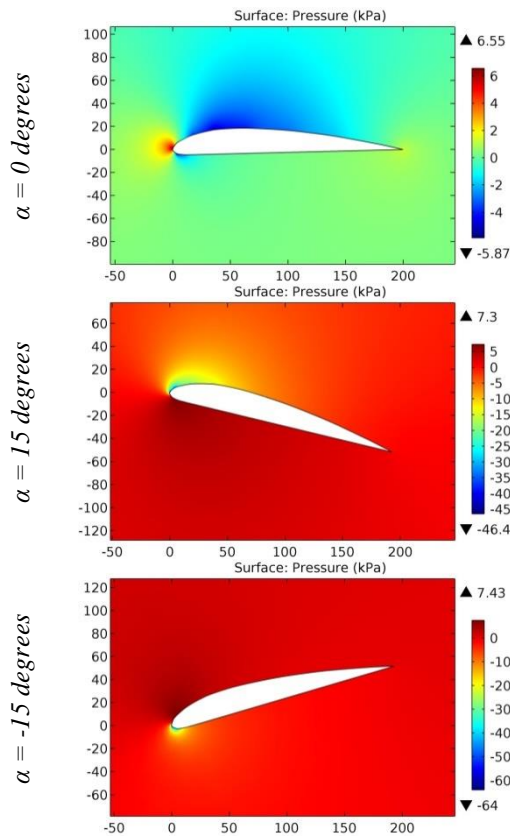
Figure 81. The pressure contours on the surfaces of the GOE 436 airfoil.

Figure 82. The pressure contours on the surfaces of the GOE 437 airfoil.
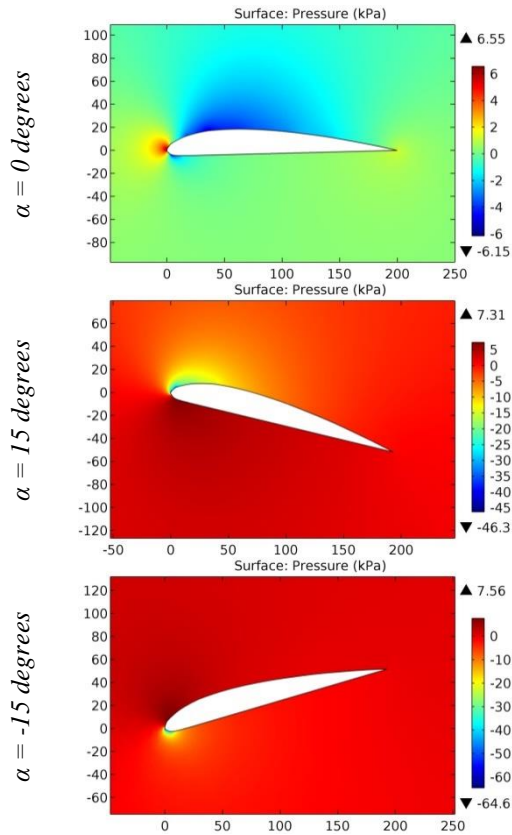
Figure 83. The pressure contours on the surfaces of the GOE 438 airfoil.

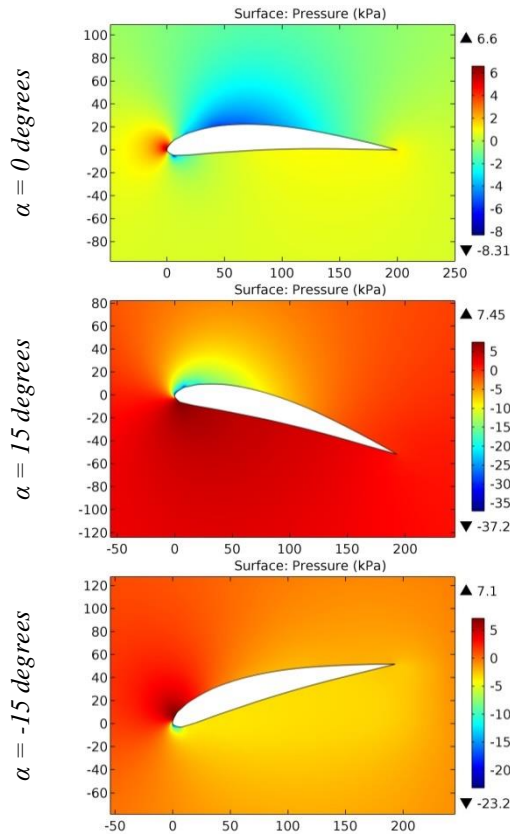**Figure 84. The pressure contours on the surfaces of the GOE 439 airfoil.**
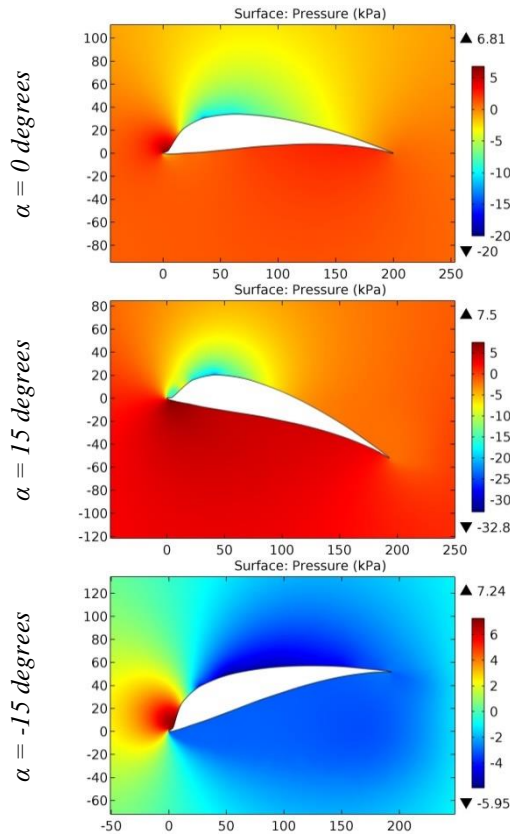
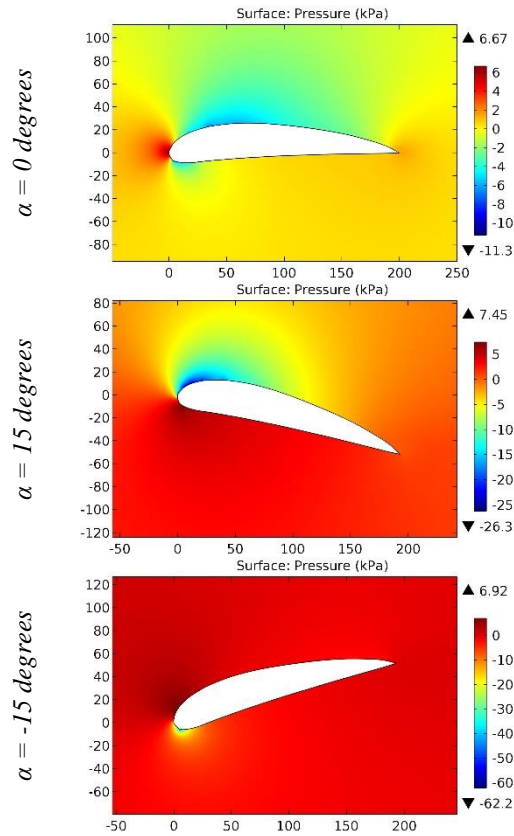**Figure 85. The pressure contours on the surfaces of the GOE 440 airfoil.**

Figure 86. The pressure contours on the surfaces of the GOE 441 airfoil.
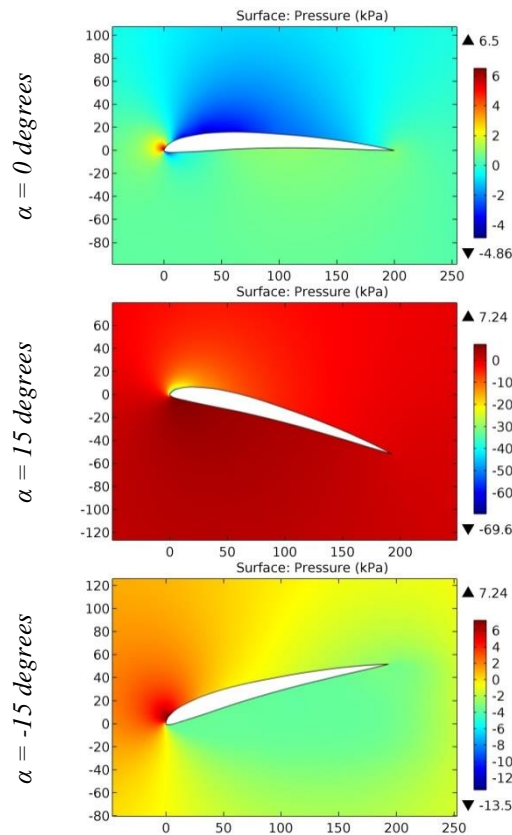
Figure 87. The pressure contours on the surfaces of the GOE 442 airfoil.

Figure 88. The pressure contours on the surfaces of the GOE 443 airfoil.
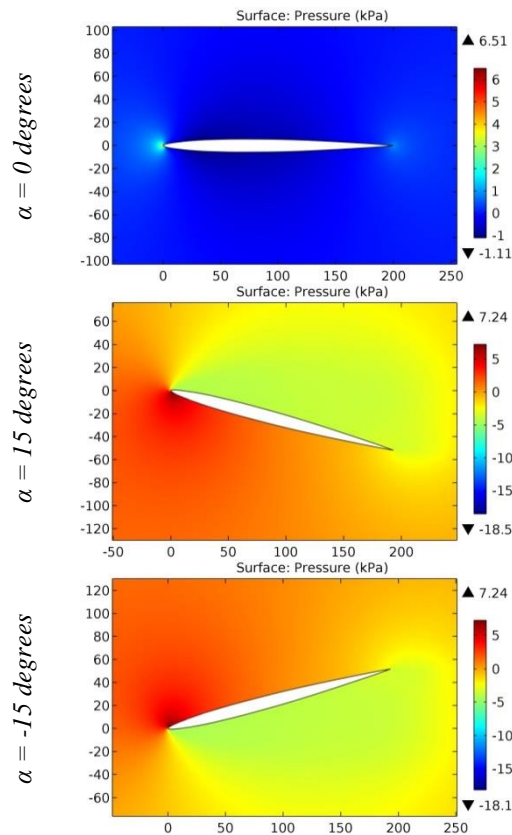
Figure 89. The pressure contours on the surfaces of the GOE 444 airfoil.

Figure 90. The pressure contours on the surfaces of the GOE 445 airfoil.
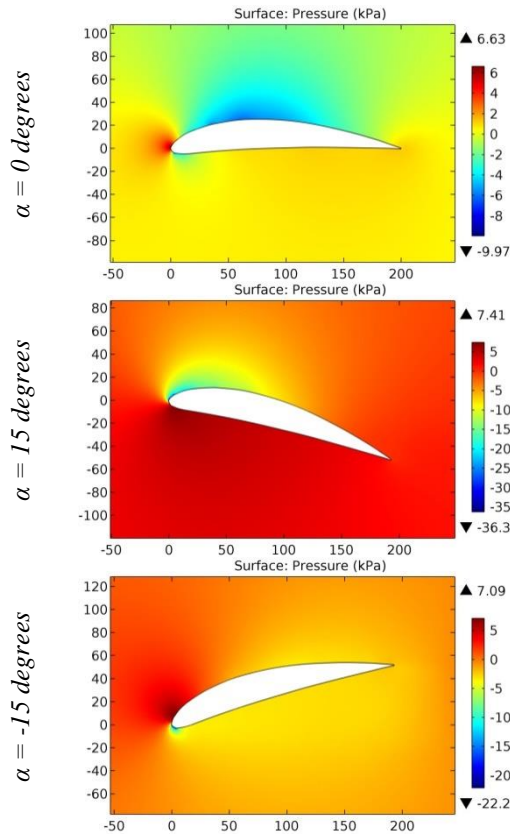
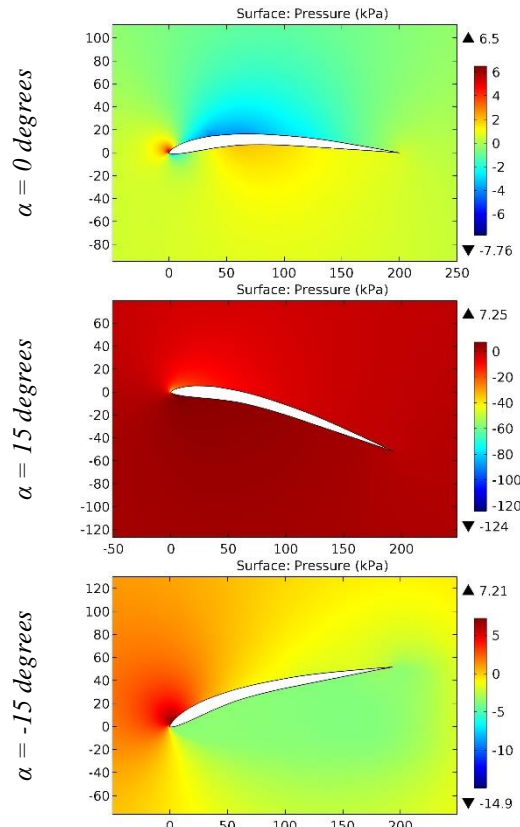**Figure 91. The pressure contours on the surfaces of the GOE 446 airfoil.**

Figure 92. The pressure contours on the surfaces of the GOE 447 airfoil.
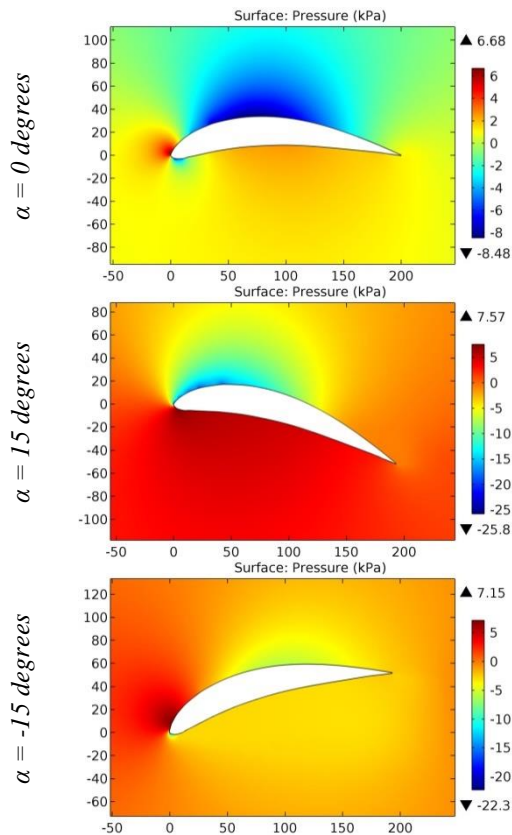
Figure 93. The pressure contours on the surfaces of the GOE 448 airfoil.

Figure 94. The pressure contours on the surfaces of the GOE 449 airfoil.
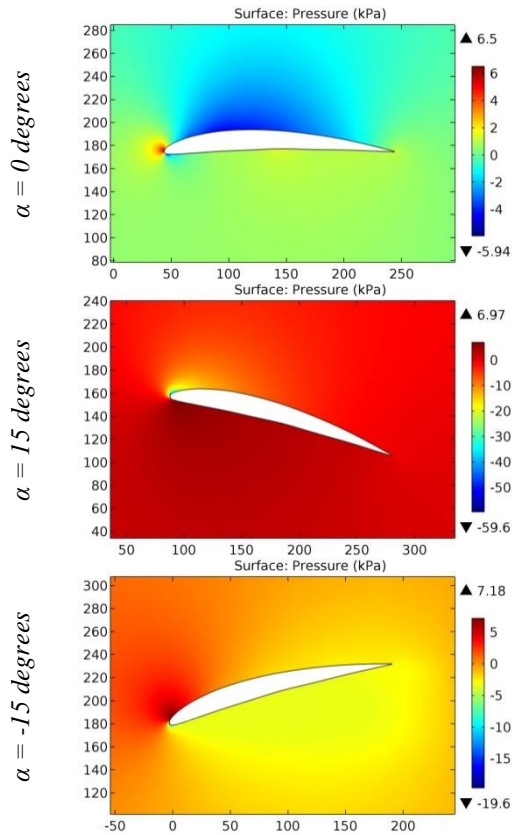
Figure 95. The pressure contours on the surfaces of the GOE 450 airfoil.

Figure 96. The pressure contours on the surfaces of the GOE 456 airfoil.
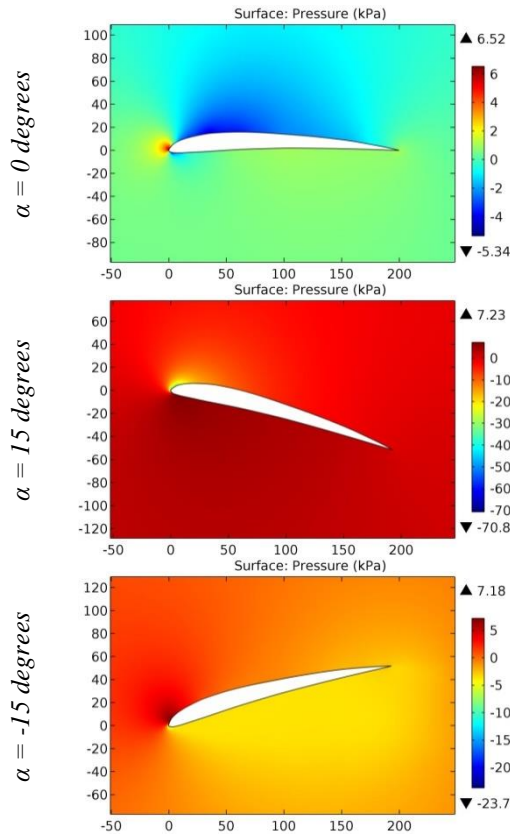
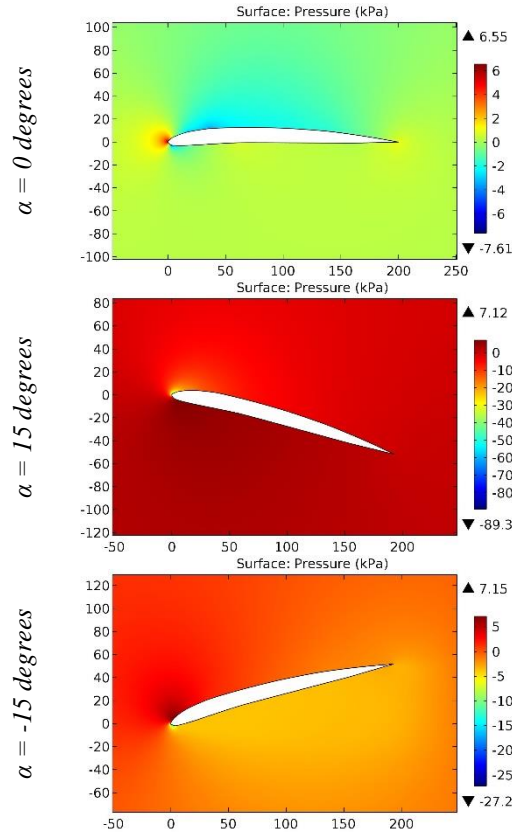**Figure 97. The pressure contours on the surfaces of the GOE 457 airfoil.**

Figure 98. The pressure contours on the surfaces of the GOE 458 airfoil.
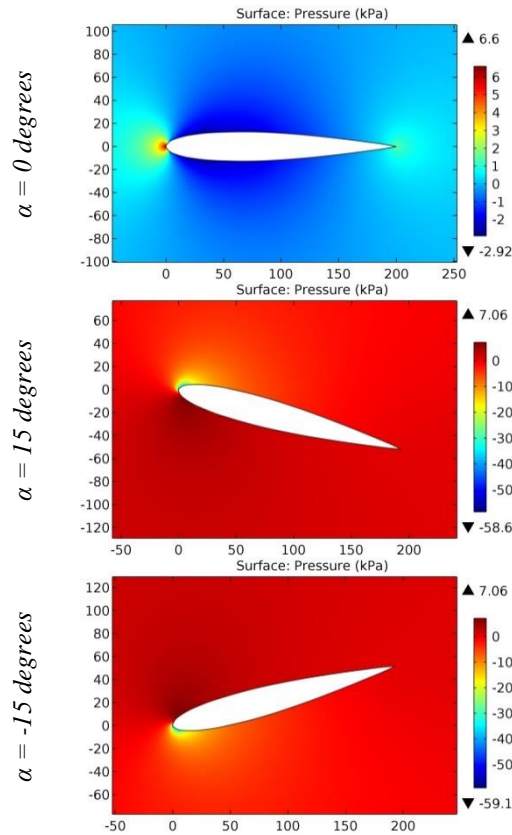
Figure 99. The pressure contours on the surfaces of the GOE 459 airfoil.
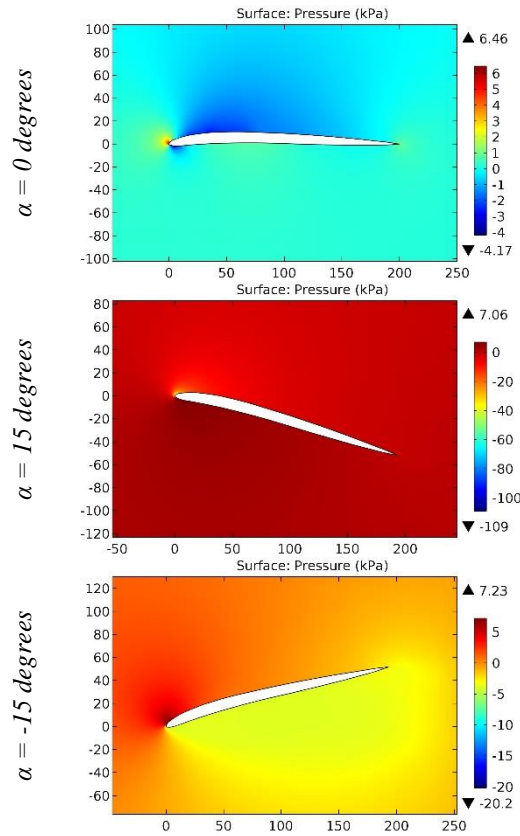
Figure 100. The pressure contours on the surfaces of the GOE 460 airfoil.
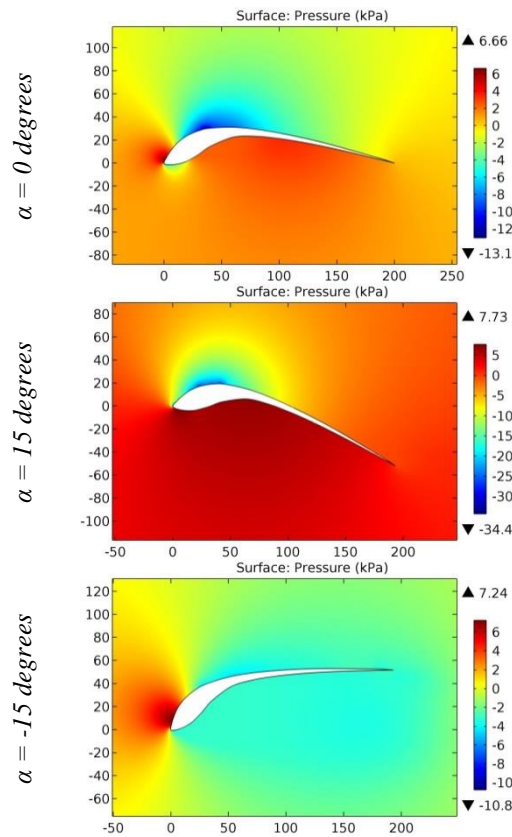
Figure 101. The pressure contours on the surfaces of the GOE 462 airfoil.

Figure 102. The pressure contours on the surfaces of the GOE 464 airfoil.
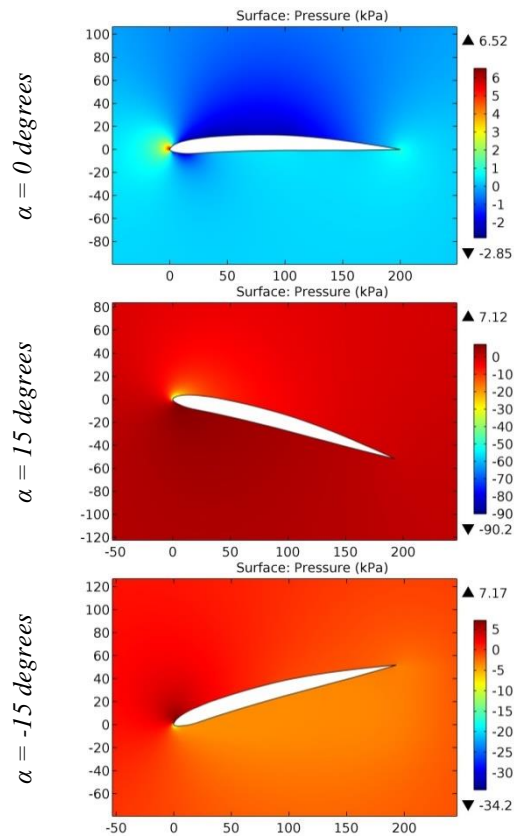
Figure 103. The pressure contours on the surfaces of the GOE 474 airfoil.

Figure 104. The pressure contours on the surfaces of the GOE 476 airfoil.
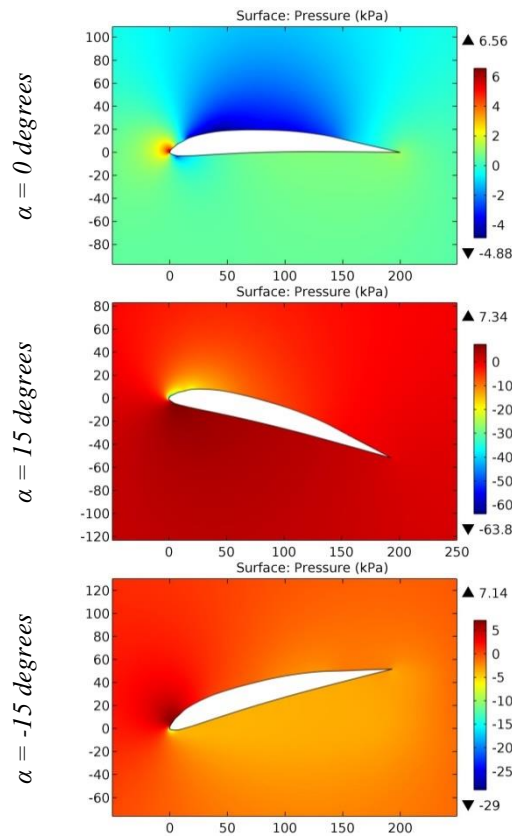
Figure 105. The pressure contours on the surfaces of the GOE 477 airfoil.

Figure 106. The pressure contours on the surfaces of the GOE 478 airfoil.
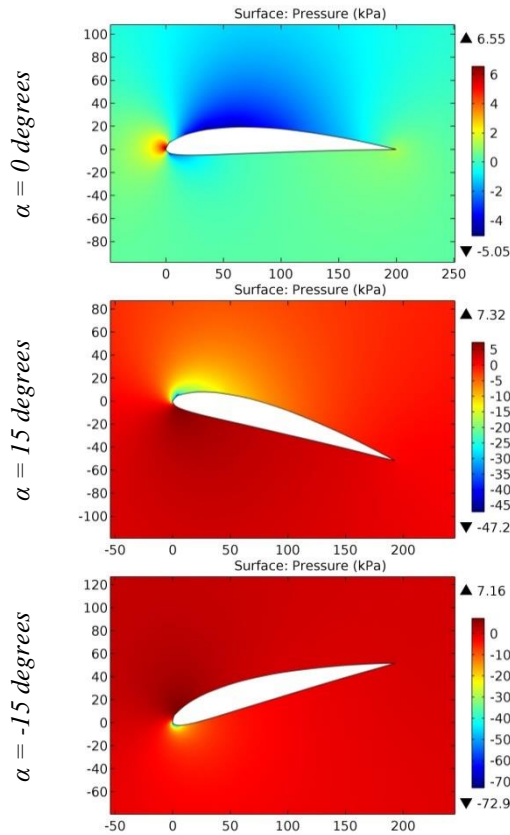
Figure 107. The pressure contours on the surfaces of the GOE 479 airfoil.
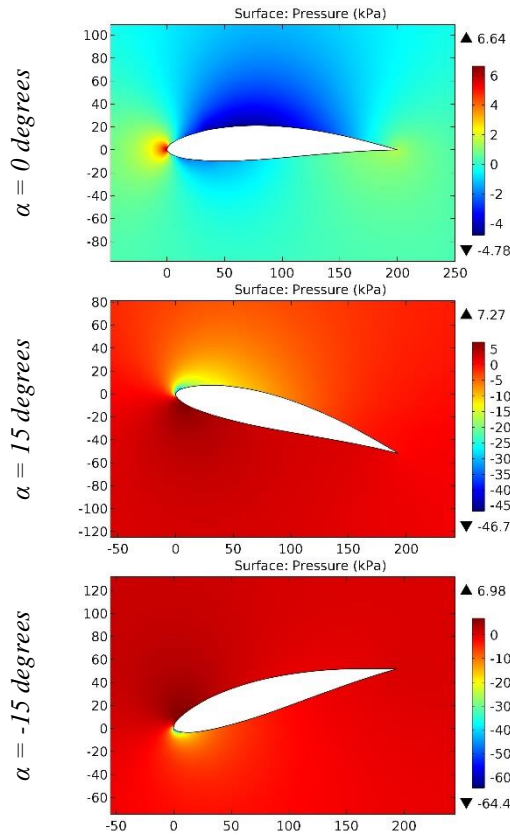
Figure 108. The pressure contours on the surfaces of the GOE 480 airfoil.
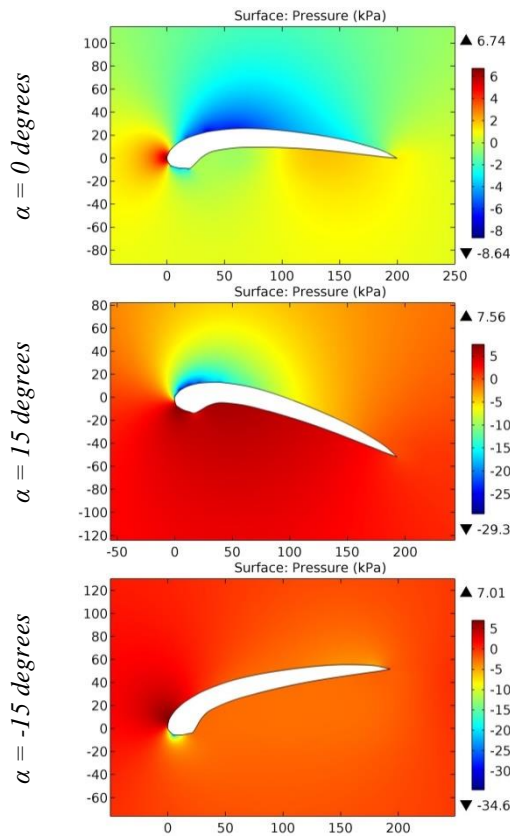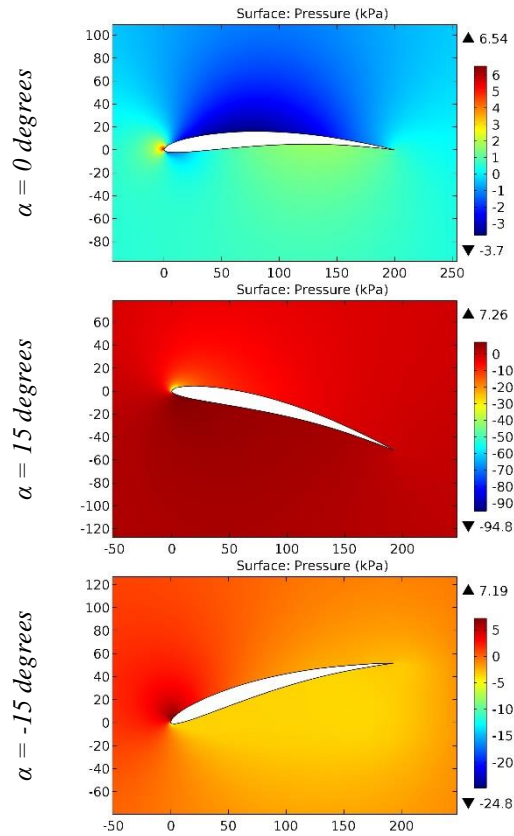

Figure 109. The pressure contours on the surfaces of the GOE 481 airfoil.

Figure 110. The pressure contours on the surfaces of the GOE 481A airfoil.
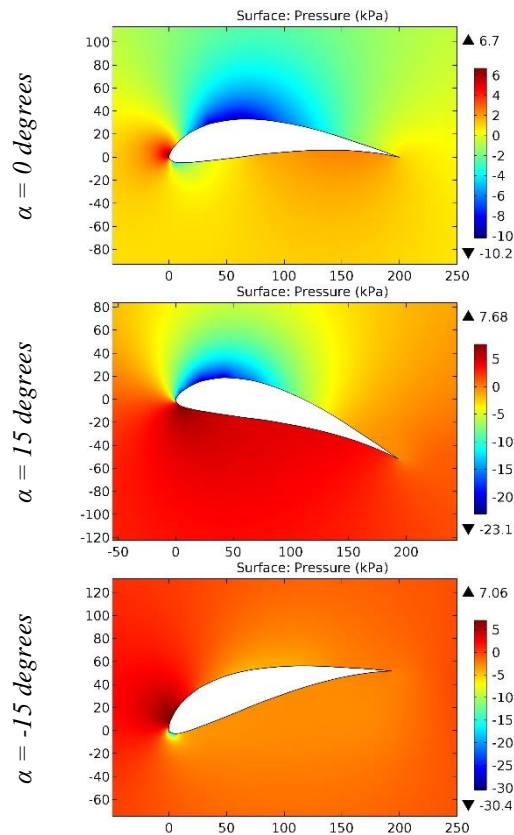
Figure 111. The pressure contours on the surfaces of the GOE 482 airfoil.

Figure 112. The pressure contours on the surfaces of the GOE 483 airfoil.
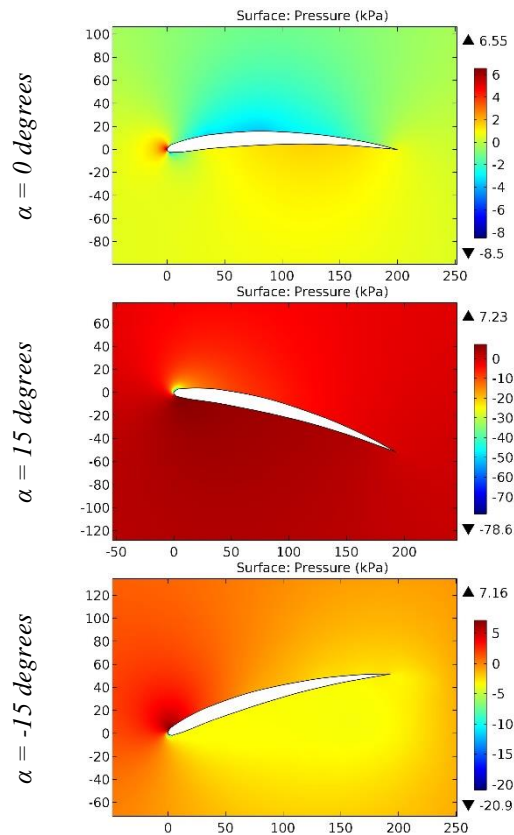
Figure 113. The pressure contours on the surfaces of the GOE 484 airfoil.

Figure 114. The pressure contours on the surfaces of the GOE 488 airfoil.
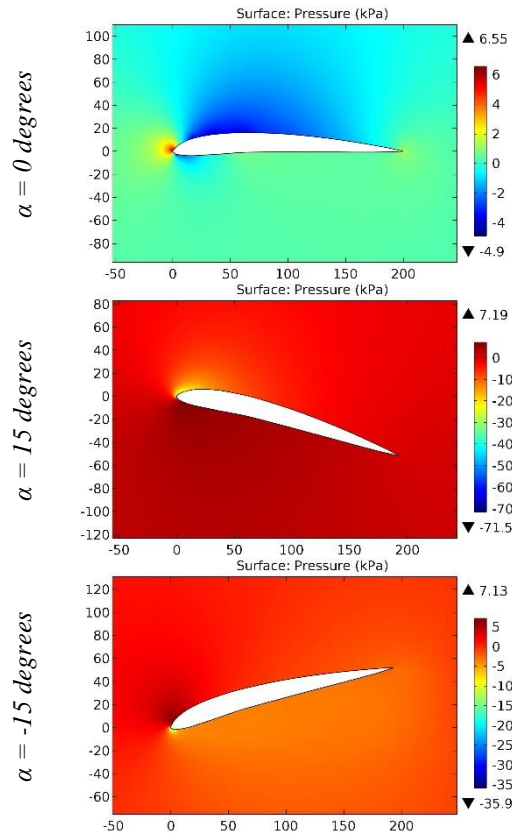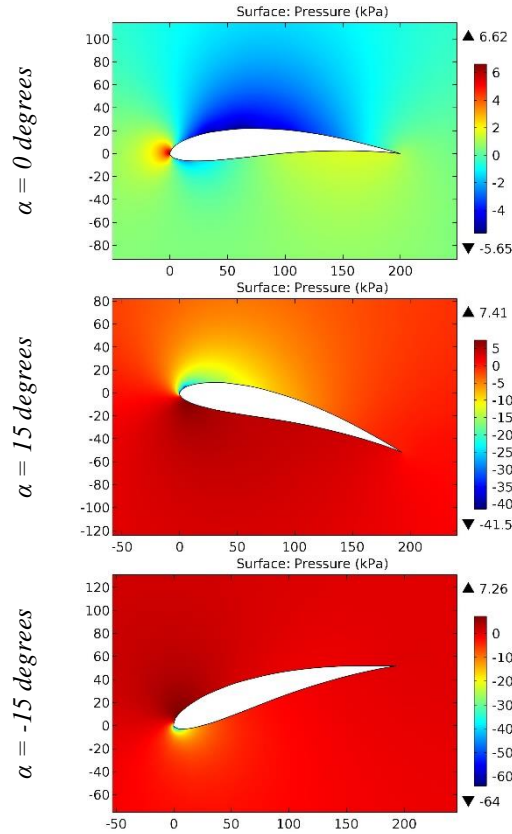

Figure 115. The pressure contours on the surfaces of the GOE 490 airfoil.

Figure 116. The pressure contours on the surfaces of the GOE 491 airfoil.
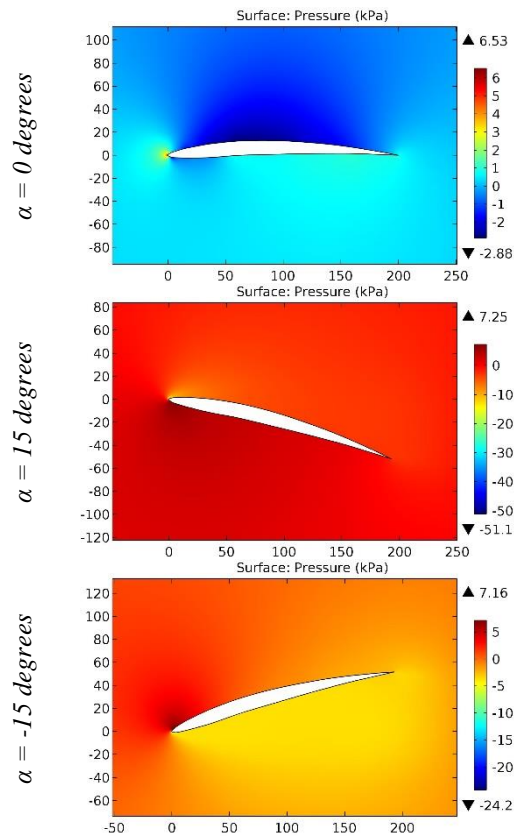
Figure 117. The pressure contours on the surfaces of the GOE 492 airfoil.

Figure 118. The pressure contours on the surfaces of the GOE 493 airfoil.
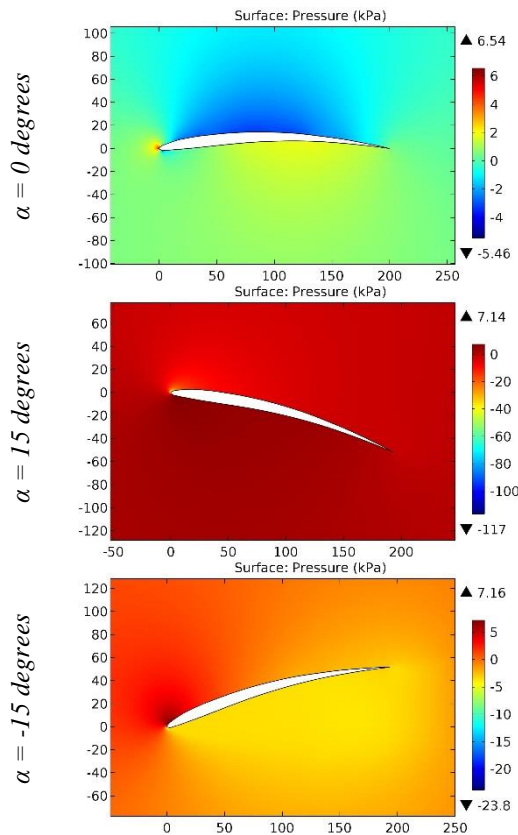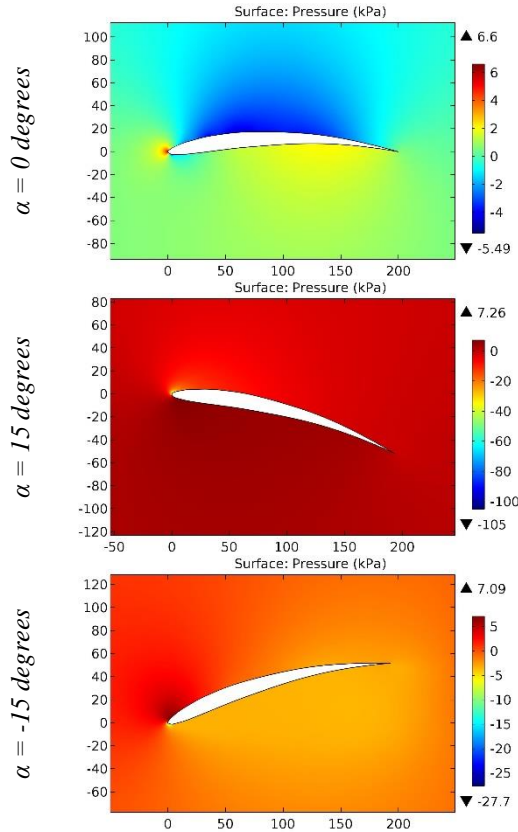
Figure 119. The pressure contours on the surfaces of the GOE 494 airfoil.

Figure 120. The pressure contours on the surfaces of the GOE 495 airfoil.
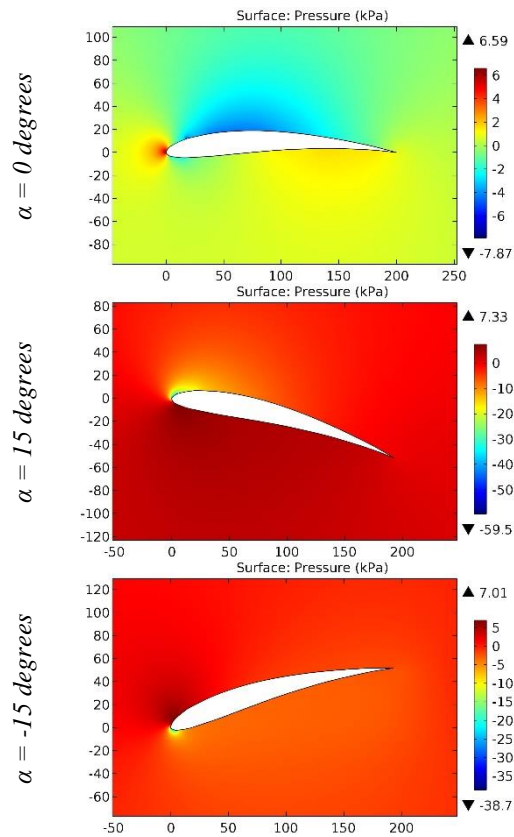
Figure 121. The pressure contours on the surfaces of the GOE 496 airfoil.

Figure 122. The pressure contours on the surfaces of the GOE 497 airfoil.
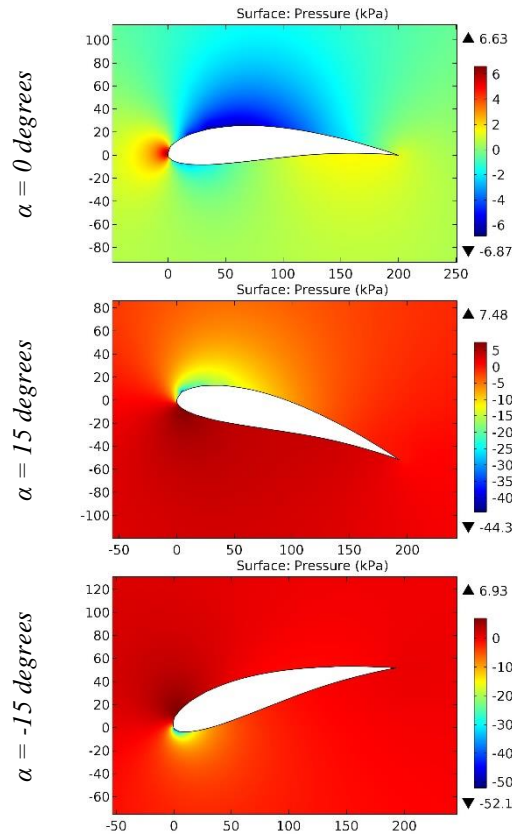
Figure 123. The pressure contours on the surfaces of the GOE 498 airfoil.

Figure 124. The pressure contours on the surfaces of the GOE 499 airfoil.
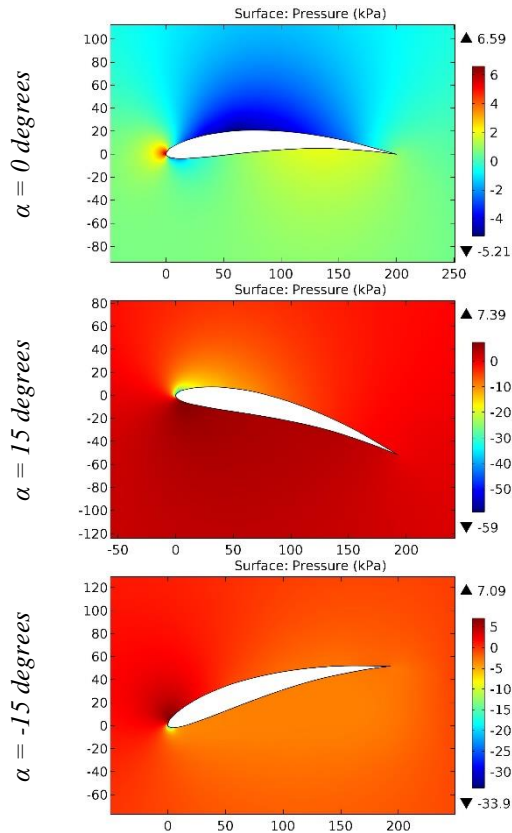
Figure 125. The pressure contours on the surfaces of the GOE 500 airfoil.
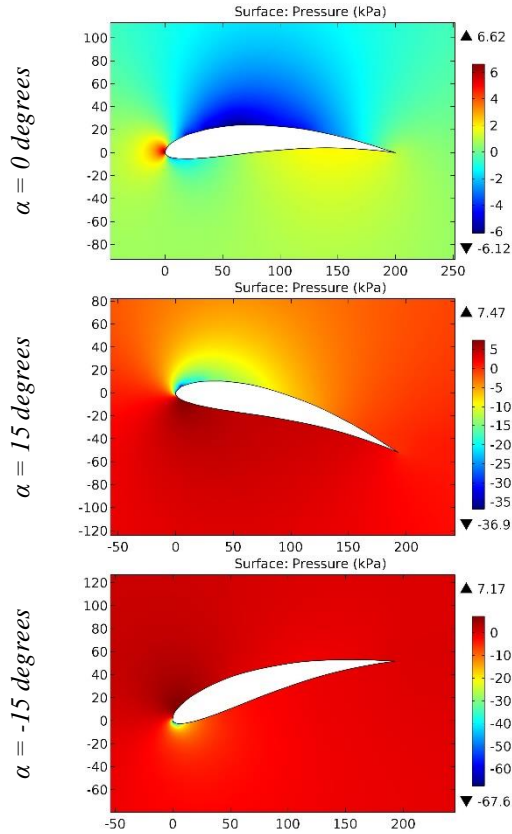
Figure 126. The pressure contours on the surfaces of the GOE 501 airfoil.
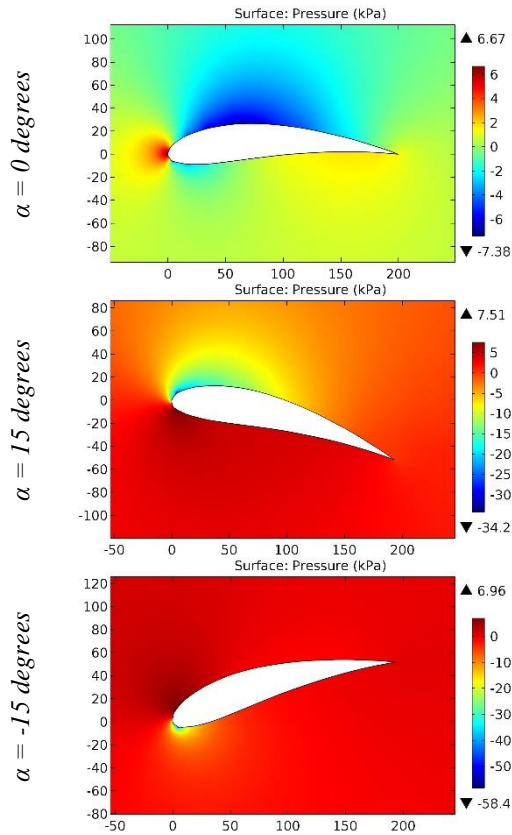
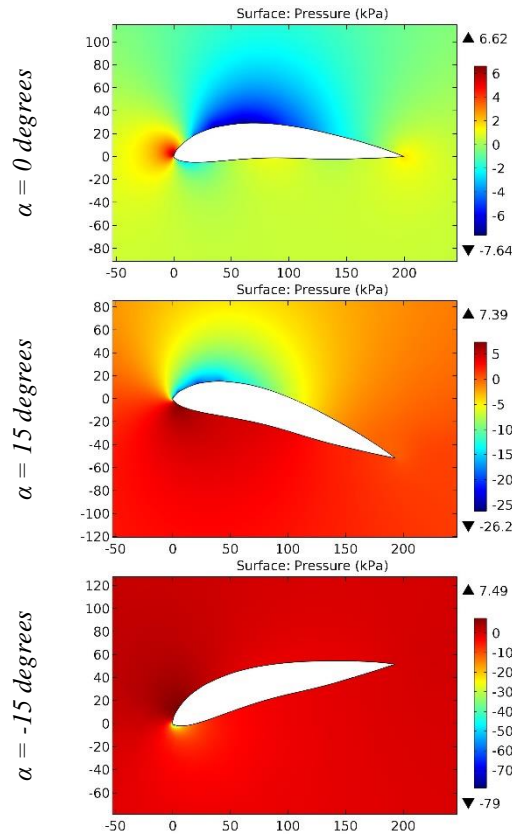**Figure 127. The pressure contours on the surfaces of the GOE 502 airfoil.**

Figure 128. The pressure contours on the surfaces of the GOE 503 airfoil.
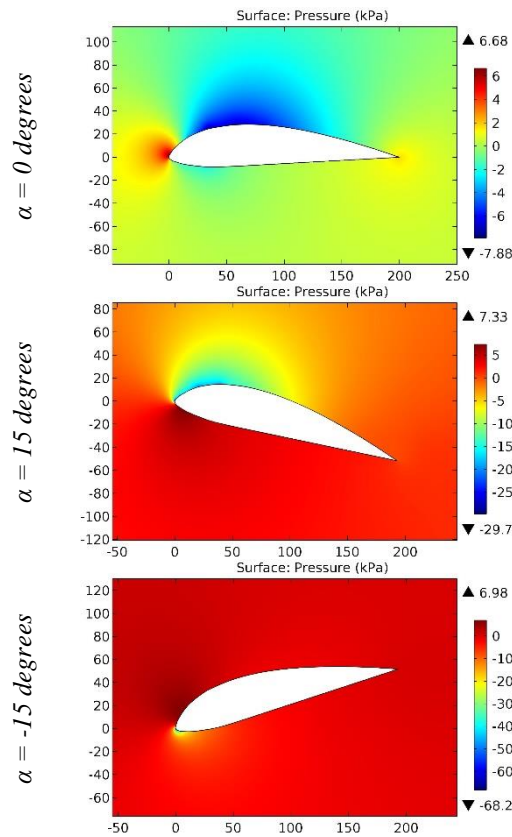
Figure 129. The pressure contours on the surfaces of the GOE 504 airfoil.

Figure 130. The pressure contours on the surfaces of the GOE 505 airfoil.
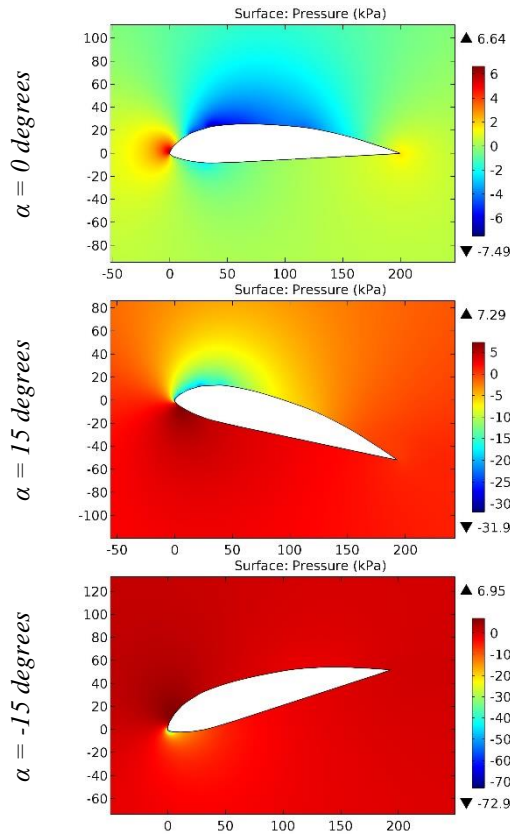
Figure 131. The pressure contours on the surfaces of the GOE 506 airfoil.

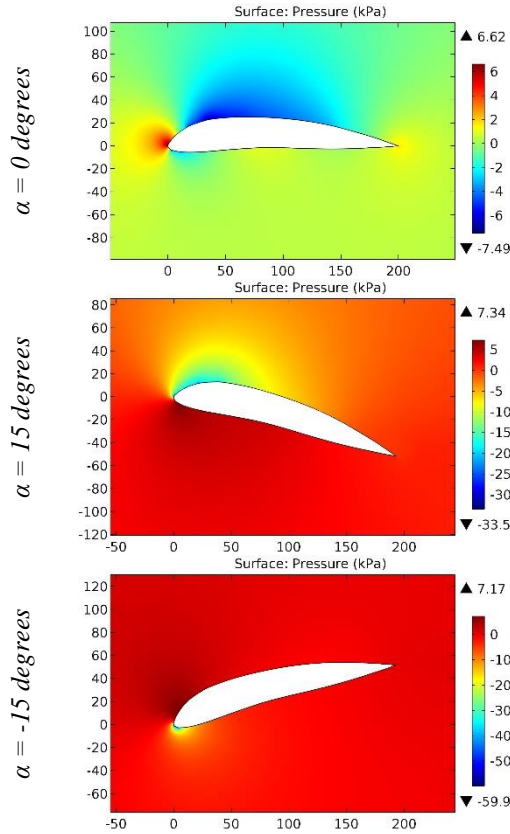Figure 132. The pressure contours on the surfaces of the GOE 507 airfoil.
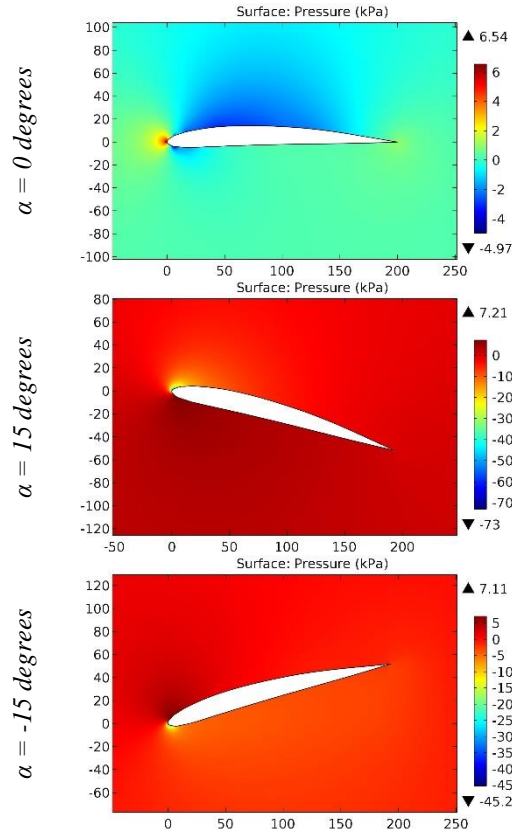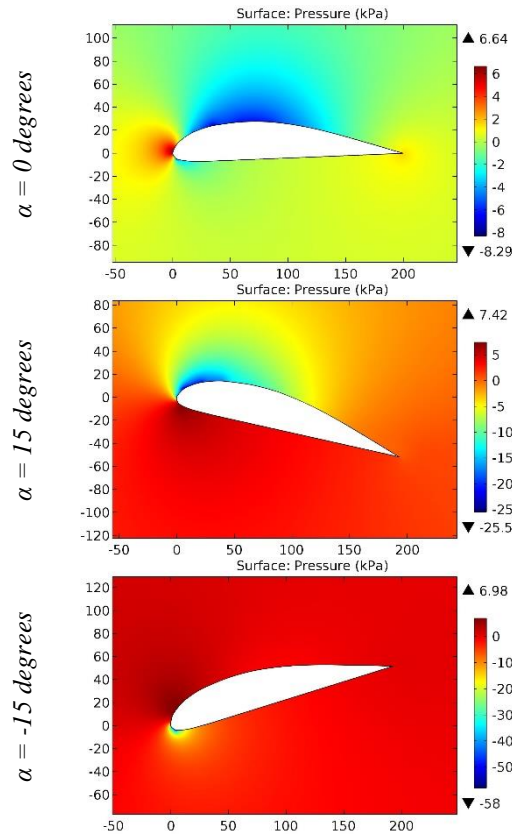
Figure 133. The pressure contours on the surfaces of the GOE 508 airfoil.

Figure 134. The pressure contours on the surfaces of the GOE 509 airfoil.
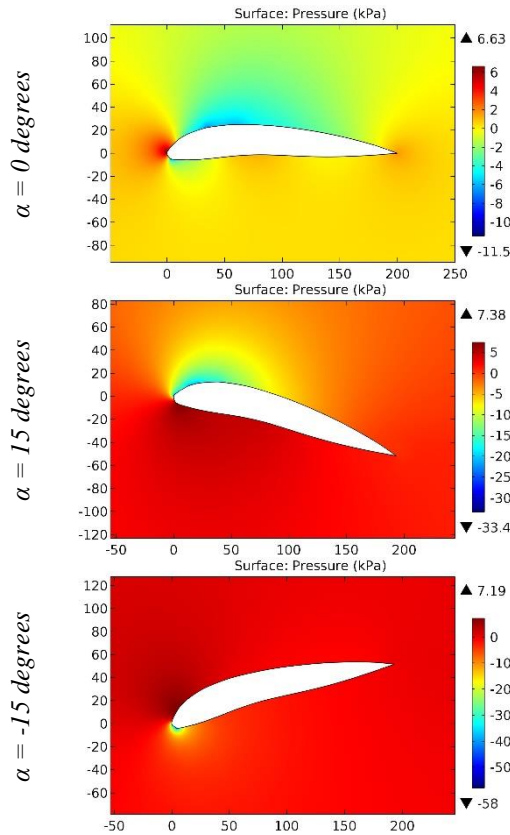
Figure 135. The pressure contours on the surfaces of the GOE 510 airfoil.

Figure 136. The pressure contours on the surfaces of the GOE 511 airfoil.
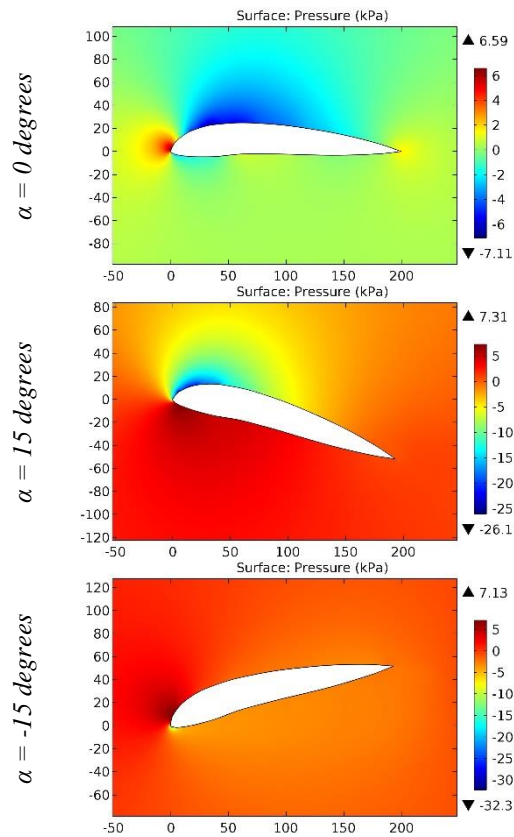
Figure 137. The pressure contours on the surfaces of the GOE 512 airfoil.

Figure 138. The pressure contours on the surfaces of the GOE 513 airfoil.
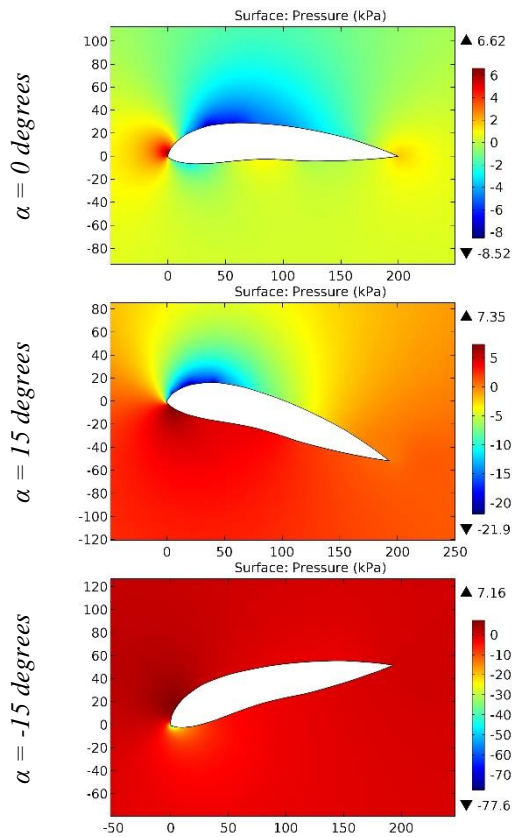
Figure 139. The pressure contours on the surfaces of the GOE 514 airfoil.
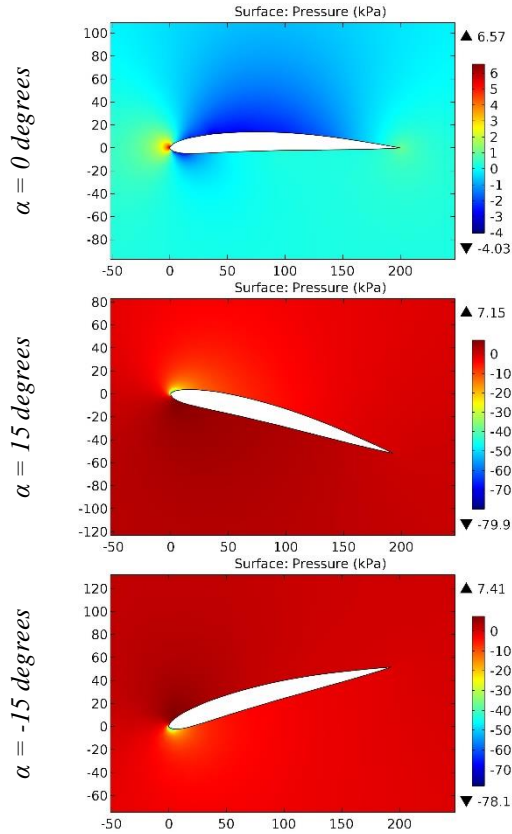
Figure 140. The pressure contours on the surfaces of the GOE 515 airfoil.
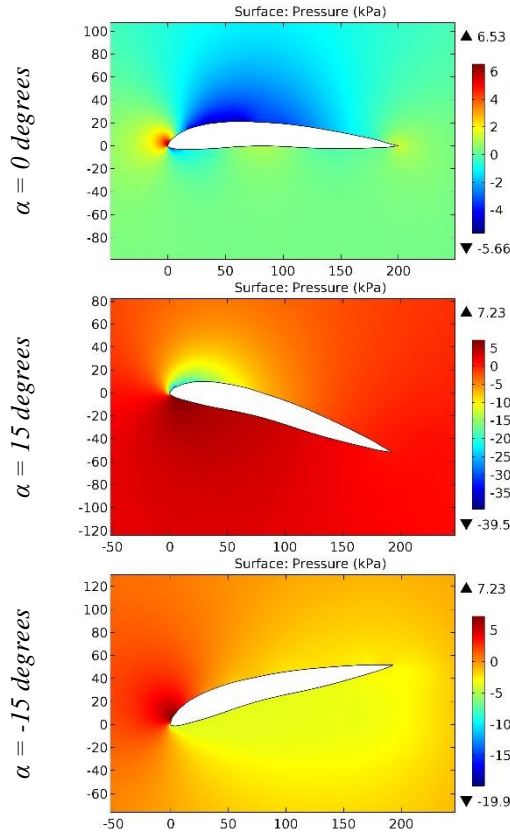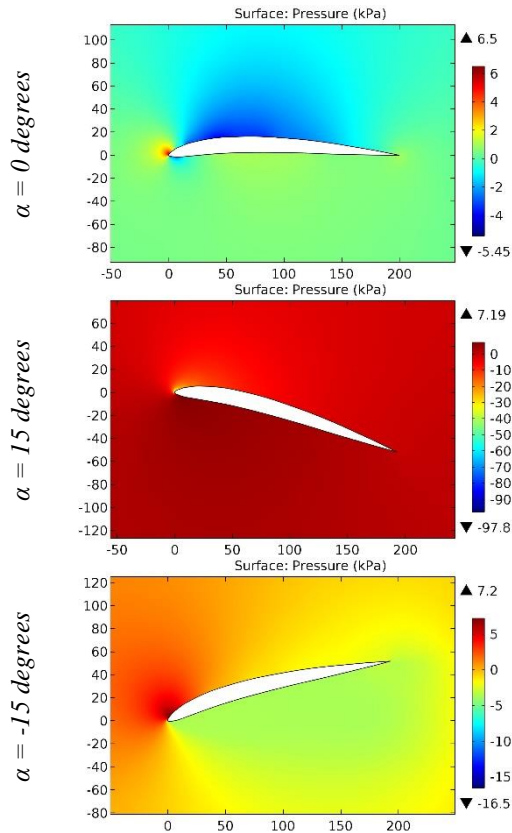

Figure 141. The pressure contours on the surfaces of the GOE 517 airfoil.
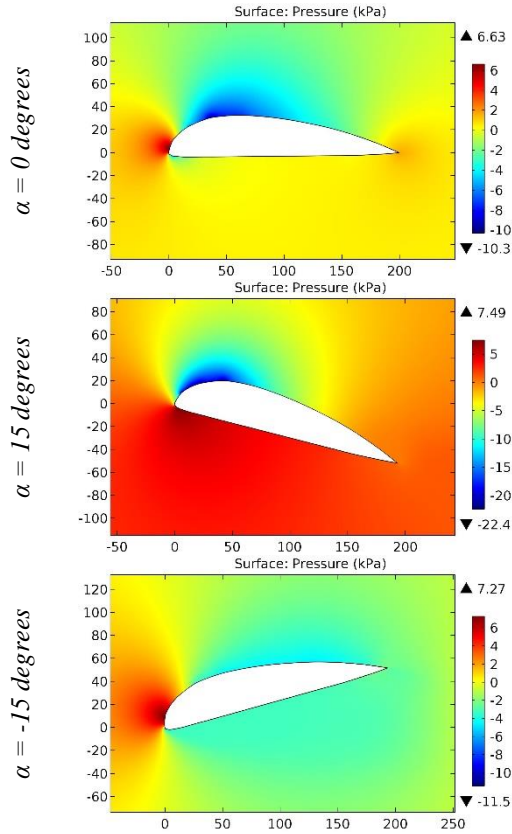
Figure 142. The pressure contours on the surfaces of the GOE 518 airfoil.
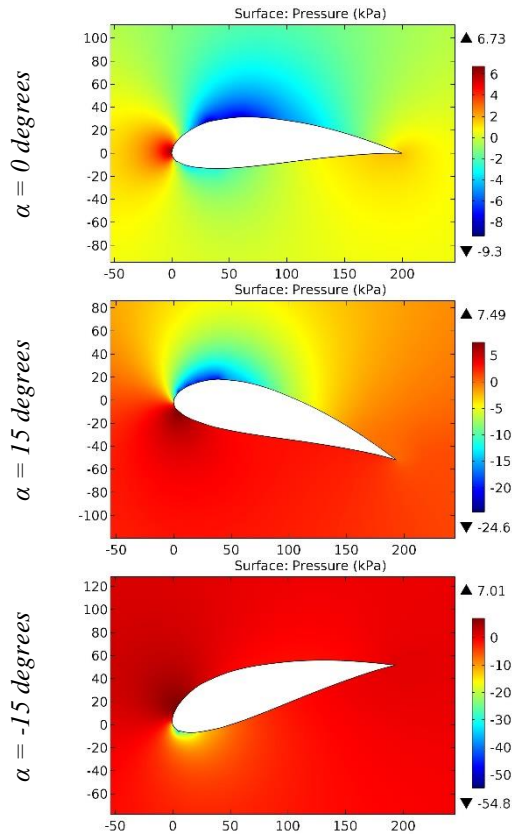
Figure 143. The pressure contours on the surfaces of the GOE 522 airfoil.

Figure 144. The pressure contours on the surfaces of the GOE 523 airfoil.
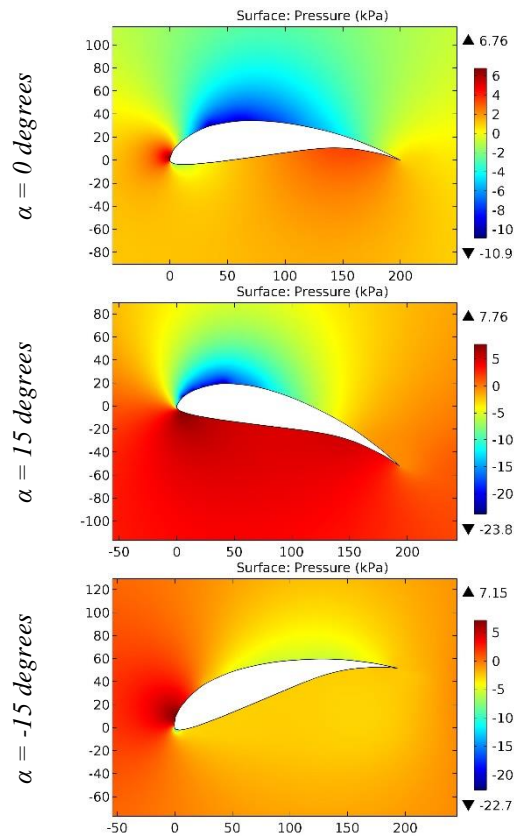
Figure 145. The pressure contours on the surfaces of the GOE 525 airfoil.
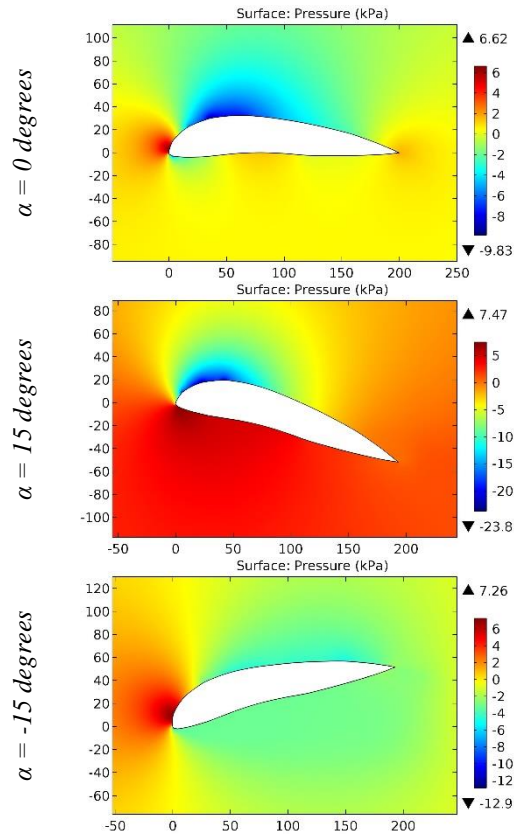
Clarivate
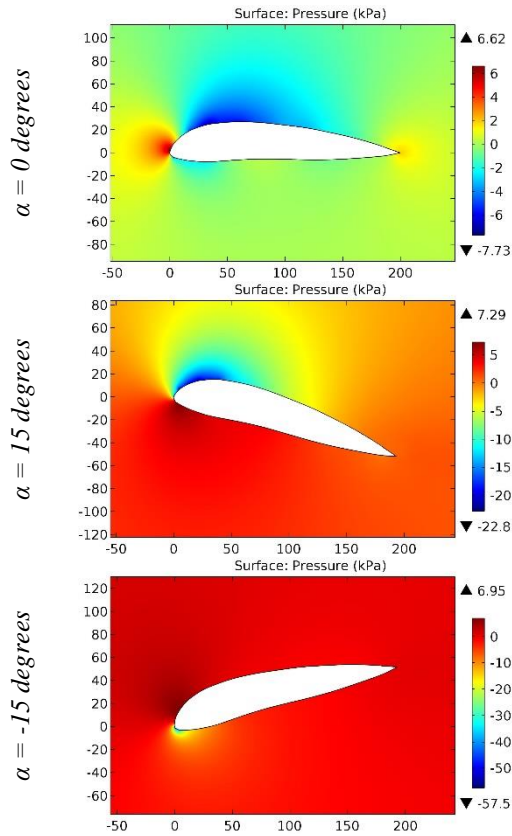Analytics **indexed**

Figure 146. The pressure contours on the surfaces of the GOE 526 airfoil.
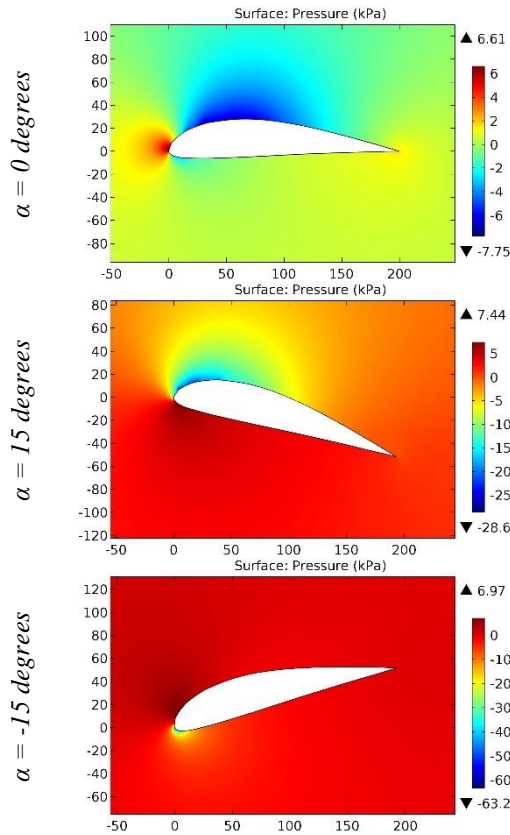
Figure 147. The pressure contours on the surfaces of the GOE 527 airfoil.
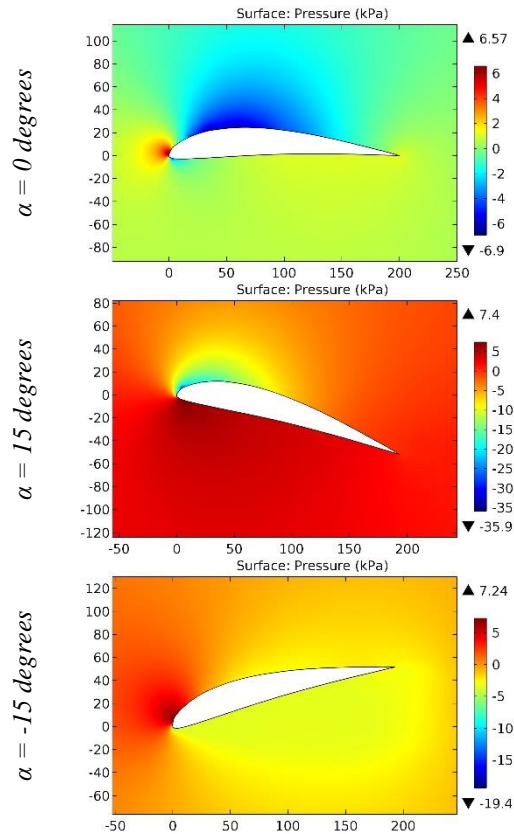
Figure 148. The pressure contours on the surfaces of the GOE 528 airfoil.

Conclusion

Based on the analysis of the computer simulation of the flight process of the airplane with the different airfoils of the wings of the GOE series, the following conclusions were made:

1. The good aerodynamic characteristics of the airplanes wings are determined by high lift and low drag. To create these airplane flight conditions, it is preferable to choose the asymmetrical subsonic airfoils, in comparison with the symmetrical subsonic airfoils.

2. The processing of the numerical values of pressures at the leading edge of the supersonic airfoils makes it possible to assert that the drag value depends on the maximum thickness.

References:

1. Anderson, J. D. (2010). *Fundamentals of Aerodynamics.* McGraw-Hill, Fifth edition.
2. Shevell, R. S. (1989). *Fundamentals of Flight.* Prentice Hall, Second edition.
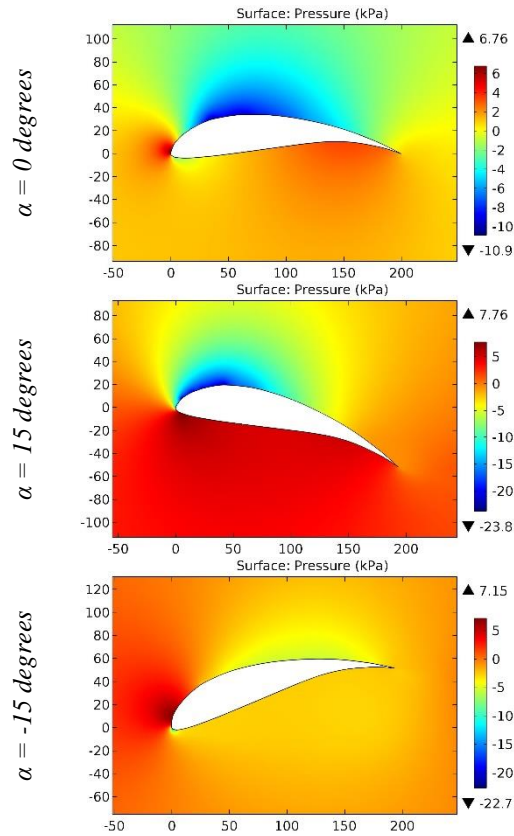3. Houghton, E. L., & Carpenter, P. W. (2003). *Aerodynamics for Engineering Students*. Fifth edition, Elsevier.
4. Lan, E. C. T., & Roskam, J. (2003). *Airplane Aerodynamics and Performance*. DAR Corp.
5. Sadraey, M. (2009). *Aircraft Performance Analysis.* VDM Verlag Dr. Müller.
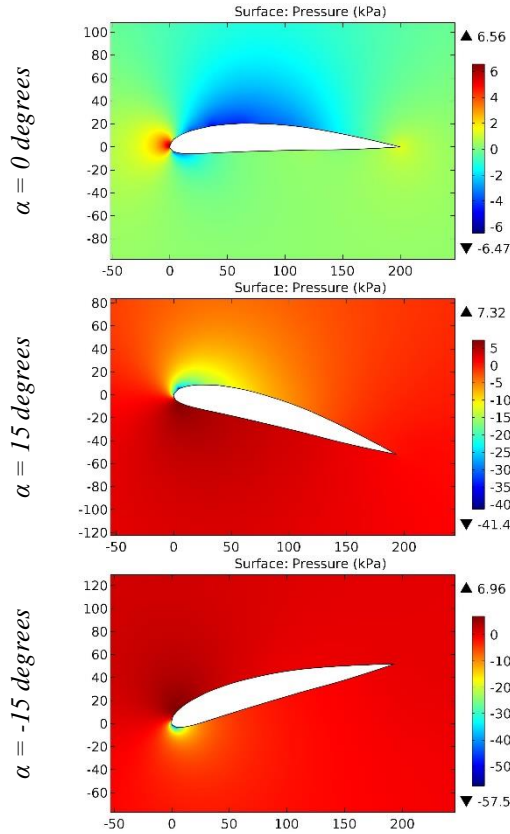6. Anderson, J. D. (1999). *Aircraft Performance and Design*. McGraw-Hill.
7. Roskam, J. (2007). *Airplane Flight Dynamics and Automatic Flight Control,* Part I. DAR Corp.
8. Etkin, B., & Reid, L. D. (1996). *Dynamics of Flight, Stability and Control*. Third Edition, Wiley.
9. Stevens, B. L., & Lewis, F. L. (2003). *Aircraft Control and Simulation*. Second Edition, Wiley.
10. Chemezov, D., et al. (2021). Pressure distribution on the surfaces of the NACA 0012 airfoil under conditions of changing the angle of attack. *ISJ Theoretical & Applied Science, 09 (101)*, 601-606.
11. Chemezov, D., et al. (2021). Stressed state of surfaces of the NACA 0012 airfoil at high angles

of attack. *ISJ Theoretical & Applied Science, 10 (102)*, 601-604.

12. Chemezov, D., et al. (2021). Reference data of pressure distribution on the surfaces of airfoils having the names beginning with the letter A (the first part). *ISJ Theoretical & Applied Science, 10 (102)*, 943-958.

13. Chemezov, D., et al. (2021). Reference data of pressure distribution on the surfaces of airfoils having the names beginning with the letter A (the second part). *ISJ Theoretical & Applied Science, 11 (103)*, 656-675.

14. Chemezov, D., et al. (2021). Reference data of pressure distribution on the surfaces of airfoils having the names beginning with the letter B. *ISJ Theoretical & Applied Science, 11 (103)*, 1001-1076.

15. Chemezov, D., et al. (2021). Reference data of pressure distribution on the surfaces of airfoils having the names beginning with the letter C. *ISJ Theoretical & Applied Science, 12 (104)*, 814-844.

16. Chemezov, D., et al. (2021). Reference data of pressure distribution on the surfaces of airfoils having the names beginning with the letter D. *ISJ Theoretical & Applied Science, 12 (104)*, 1244-1274.

17. Chemezov, D., et al. (2022). Reference data of pressure distribution on the surfaces of airfoils (hydrofoils) having the names beginning with the letter E (the first part). *ISJ Theoretical & Applied Science, 01 (105)*, 501-569.

18. Chemezov, D., et al. (2022). Reference data of pressure distribution on the surfaces of airfoils (hydrofoils) having the names beginning with the letter E (the second part). *ISJ Theoretical & Applied Science, 01 (105)*, 601-671.

19. Chemezov, D., et al. (2022). Reference data of pressure distribution on the surfaces of airfoils having the names beginning with the letter F. *ISJ Theoretical & Applied Science, 02 (106)*, 101-135.

Clarivate Analytics **indexed**